Supporting Information

Redox Neutral electrochemical Diazo Coupling: Controlled Synthesis of Olefins and Azines via modulating reaction conditions

Abinash Mohapatra[a], and Vikas Tyagi[a]*

[a]*Department of Chemistry and Biochemistry, Thapar Institute of Engineering and Technology, Patiala-147004, Punjab, India.* Email: vikas.tyagi@thapar.edu

Table of contents

1.0 General Information

Materials. All the reagents and solvents were used directly as received from the manufacturer without further purification.

Instrumentation. The electrochemical reaction was conducted on an OWON (P4305) instrument equipped with an undivided cell and magnetic stirrer. The ^{1}H NMR and ^{13}C NMR were recorded on 400, 500, or 700 MHz JEOL or Bruker Avance AV-III spectrometers in $CDCl_3$ using tetramethylsilane (TMS) as an internal reference. The chemical shift is represented by δ (ppm) and the coupling constant in *J* (Hz). Other abbreviations used in NMR follow-up experiments: b, broad; s, singlet; d, doublet; t, triplet; q, quartet; m, multiplet; td or dd, doublet of triplet and double doublet. HRMS data were measured using the Water QTOF mass spectrometer (XEVO G2 XS) in ESI(+ve) mode. Silica gel containing glass plates was used for Thin Layer Chromatography (TLC) to monitor the reaction progress. The column chromatography was performed using silica gel (60-120 mesh) as the stationary phase and ethyl acetate in hexane as the mobile phase. All the compounds were characterized using ^{1}H NMR, ^{13}C NMR, and HRMS data. Cyclic voltammograms were acquired using a VSP-300, Bio-Logic, France Potentiostat instrument.

2.0 Experimental Section

2.1General Procedure for the Synthesis of phenyl diazoesters[1]

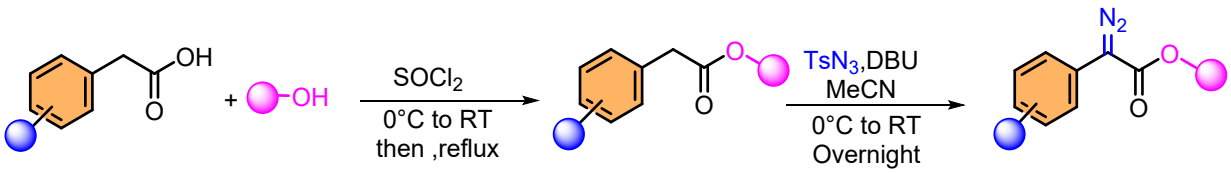

Scheme S1: Synthesis of aryl diazoesters.

Step I: To a stirred solution of phenylacetic acid (1.36 g, 10 mmol) in 15 mL of alcohol at 0 °C, thionyl chloride (1.45 mL, 20 mmol) was added dropwise over 10 minutes. After stirring the reaction mixture for 30 min, the solution was refluxed for 4-6 h. After the completion of the reaction, the ester was extracted with ethyl acetate and washed with 10 mL of saturated sodium bicarbonate solution, and dried over Na_2SO_4, followed by evaporation of the volatiles to obtain the corresponding esters.

Step-II: To a stirred solution of the ester (5 mmol, 1 equiv.) and *p*-tosyl azide (5.5 mmol, 1.1 equiv.) in 10 mL CH_3CN as a solvent at 0 °C, DBU (7 mmol, 1.4 equiv.) was added dropwise. The solution was stirred overnight while slowly warming up to room temperature. The reaction progress was monitored by TLC, and upon complete consumption of the reactants, the organic layer was washed with saturated aqueous NH_4Cl solution and extracted with DCE. The organic layer was dried over Na_2SO_4, and the solvent was removed in a vacuum. The crude product was purified by silica gel column chromatography using ethyl acetate (EtOAc) in hexane as the mobile phase, which provided the desired diazo compound.

2.2 General procedure for electrochemical Methods and Quantification.

All electrochemical reactions were performed in an undivided cell equipped with either platinum or carbon plate electrodes (immersed geometric surface area 1.5 cm^2 per electrode; interelectrode distance 1 cm). Electrolysis was conducted under constant current conditions (I = 5 mA), corresponding to a current density of 3.33 $mA \cdot cm^{-2}$, at room temperature under argon atmosphere for 6 h. Under these conditions, a total charge of 108 C was passed, corresponding to 11.2 F/mol relative to the theoretical $1e^-$ initiation required for 0.1 mmol of starting diazo. Whereas for the 0.1 mmol of starting diazo, the total charge passed Q = 2.23 F/mol Faradaic

efficiencies were calculated on a single electron basis using isolated yields and total charge passed.

2.3 General procedure for Optimization of Electrochemical Coupling of aryl diazoester 1a.

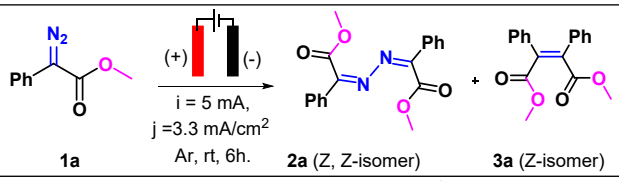

1a **2a** (Z, Z-isomer) **3a** (Z-isomer)

Entry	Solvent	Electrolyte	Anode (+)/Cathode (-)	Yield [%] [b] (2a)	*%de*(2a)[C]	Yield [%] [b] (3a)	*%de*(3a)[C]
1	MeCN	Bu_4NPF_6	Pt/Pt	31%	99	15%	90
2	MeCN	Bu_4NI	Pt/Pt	11%	89	0	0
3	MeCN	Bu_4NBr	Pt/Pt	78%	99	20%	97
4	MeCN	$Bu4NBF_4$	Pt/Pt	58%	78	13%	99
5	MeCN	Bu_4NBr	C/C	8%	80	70%	99
6	MeCN	Bu_4NI	C/C	12%	90	67%	98
7	MeCN	$Bu4NBF_4$	C/C	17%	86	57%	92
8	MeCN	Bu_4NPF_6	C/C	27%	92	48%	86
9	DCE	Bu_4NPF_6	**Pt/Pt**	**95%**	**86**	**0**	**0**
10	DCE	Bu_4NBr	Pt/Pt	90%	94	4%	0
11	DCE	Bu_4NI	Pt/Pt	25%	99	14%	99
12	DCE	$Bu4NBF_4$	Pt/Pt	62%	96	15%	50
13	DCE	Bu_4NPF_6	C/C	12%	62	66%	56
14	DCE	Bu_4NBr	**C/C**	**0**	**0**	**83%**	**99**
15	DCE	$Bu4NBF_4$	C/C	4%	65	13%	38
16	DCE	Bu_4NI	C/C	7%	98	64%	97
17	HFIP	Bu_4NPF_6	Pt/Pt	8%	79	3%	99
18	HFIP	Bu_4NBr	C/C	15%	30	32%	75
19	DCE	Bu_4NPF_6	Pt/Fe	36%	91	9%	99
20	DCE	Bu_4NPF_6	C/Pt	49%	89	23%	0
21	DCE	Bu_4NPF_6 *no current*	**Pt/Pt**	0	0	0	0
22	DCE	Bu_4NPF_6 Open Air	**Pt/Pt**	0	0	0	0
23	DCE	Bu_4NPF_6	**Pt/Pt (10mA)**	88%	75%	0	0
24	DCE	Bu_4NPF_6	**Pt/Pt (3mA)**	46%	80%	0	0
25	DCE	Bu_4NPF_6 0.2M	**Pt/Pt**	36%	79	0	0
26	DCE	Bu_4NPF_6 0.8M	**Pt/Pt**	93%	85	0	0

[a]All entries were carried out under identical constant-current conditions with **1a** (0.1 mmol,17.6 mg) in 2 mL of solvent containing 0.04 M electrolyte. Entries 1–4 were performed in acetonitrile (**MeCN**), entries **5–9** in 1,2-dichloroethane (**DCE**), unless otherwise noted. [b] Determined by HPLC, [c] Diastereomeric excess (% *de*) determined by HPLC.

Table S1. Optimization of solvent, electrolyte, and electrode combinations for the electrochemical reductive coupling of phenyl diazoester 1a.

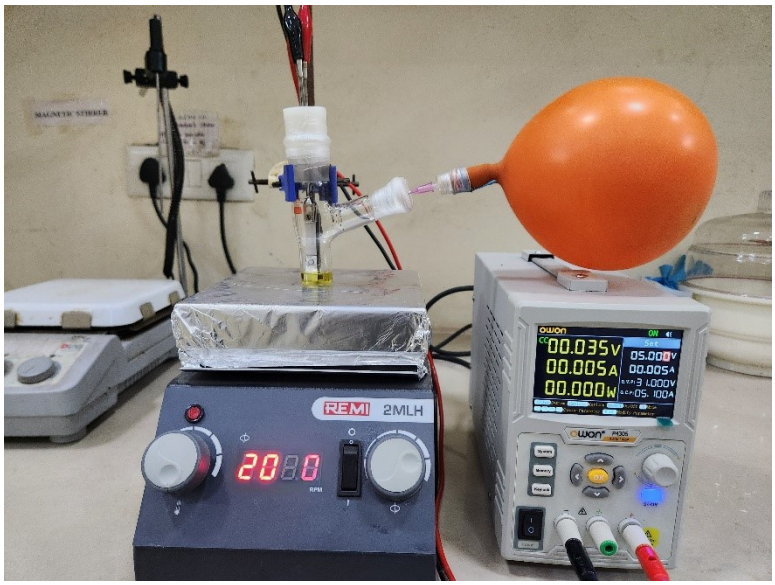

Figure S1. Reaction setup for the optimization study, showing the electrochemical cell after it was purged with argon to establish an inert atmosphere.

We began our investigation by screening reaction conditions for the electrochemical coupling of phenyl diazo-ester **1a** (**Table 1**, **entry 1**; see also Supporting Information, **Table S1**). In the initial experiment, 0.1 mmol of 1a was electrolysed in acetonitrile (MeCN) with 0.04 M nBu_4NPF_6 as supporting electrolyte, using Pt/Pt electrodes at a constant current of 5 mA, room temperature, and an inert atmosphere (**Table 1, entry 1**). Under these conditions, azine **2a** was obtained in 31 % yield together with 15 % olefin **3a**, both products exhibiting high diastereomeric excess. To improve conversion and chemoselectivity, we systematically varied the electrolyte, electrode material, and solvent. Replacing nBu_4NPF_6 by nBu_4NI markedly reduced the reaction efficiency, affording only 11 % azine and suppressing olefin formation (**entry 2**), indicating that iodide is poorly suited in polar media. In contrast, the use of nBu_4NBr enhanced the outcome, delivering 78 % azine and 20 % olefin (**entry 3**), while nBu_4NBF_4 gave an intermediate performance (58 % azine, **entry 4**). A pronounced electrode effect emerged when Pt/Pt was exchanged for C/C electrodes in MeCN. With otherwise identical conditions, carbon electrodes consistently shifted the selectivity toward olefin formation: nBu_4NBr (70 % olefin, **entry 5**), nBu_4NI (67 % olefin, **entry 6**), nBu_4NBF_4 (57 % olefin, **entry 7**), and nBu_4NPF_6 (48 % olefin, **entry 8**), with only trace azine detected. This trend underscores the strong influence of electrode material on the reaction pathway. Solvent screening revealed that

less-polar chlorinated solvents dramatically improve azine selectivity. In dichloroethane (DCE) with Pt/Pt electrodes, both nBu_4NPF_6 and nBu_4NBr afforded > 90 % azine (95 % and 90 %, respectively) with complete suppression of olefin (**entries 9**–**10**). By contrast, nBu_4NI and nBu_4NBF_4 in DCE gave lower azine yields (25–62 %) and minor amounts of olefin (**entries 11**–**12**). The electrode-dependent selectivity observed in MeCN persisted in DCE: switching to C/C electrodes inverted the product distribution, favoring olefin formation (nBu_4NPF_6 → 66 % **3a**, **entry 13**; nBu_4NBr → exclusive olefin **3a**, 83 % yield, **entry 14**). Similar inversions were obtained with nBu_4NBF_4 and nBu_4NI (**entries 15**–**16**), confirming that carbon electrodes preferentially promote the olefin pathway irrespective of the electrolyte. The highly polar protic solvent hexafluoroisopropanol (HFIP) proved detrimental, affording low yields and reduced stereocontrol (**entries 17–18**), likely because strong solvation and hydrogen-bonding interactions disrupt the productive radical-anion pathway. Finally, mixed electrode systems (Pt/Fe and C/Pt) delivered intermediate results (36–49 % azine, **entries 19–20),** Further, control experiments highlighted the crucial role of electrochemical activation and an inert atmosphere. In the absence of applied current, no formation of azine (**2a)** or olefin (**3a)** was observed, demonstrating that the transformation does not proceed in the absence of electricity (**entry 21**). Likewise, conducting the reaction under open-air conditions led to the rapid oxidation of (**1a)** to methyl 2-oxo-2-phenylacetate, with no formation of coupling products (**2a)** and (**3a)** (entry 22). Also, further increasing or decreasing the current for the 0.1mmol of 2a, the reaction yield drops (**entries 23–24**). Additional experiments at 0.02 M and 0.08 M nBu_4NPF_6 under otherwise identical conditions. At 0.02 M, the yield of azine (2a) decreased to 36 %, likely due to insufficient ionic conductivity and higher cell resistance. At 0.08 M, the yield remained comparable to that at 0.04 M, though the reaction showed slightly diminished reproducibility, possibly due to increased ion pairing affecting the double-layer structure (**entries 25–26**).

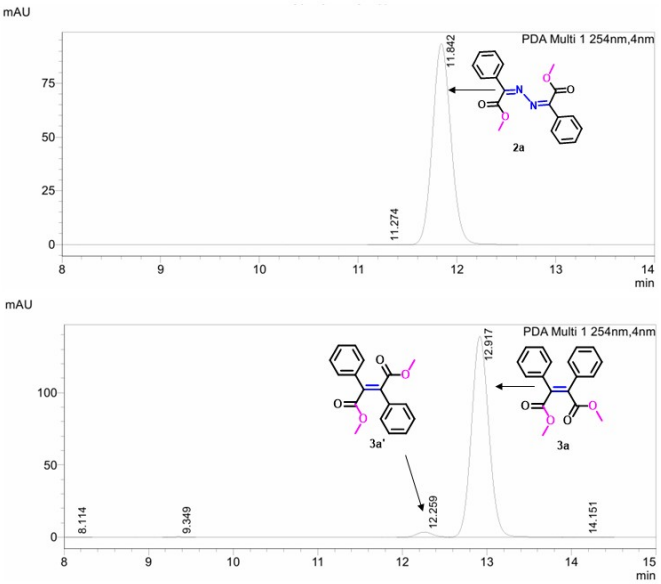

Figure S2: HPLC chromatogram of formation of 2a and 3a.

2.4 General procedure for the synthesis of azines (2a-2n).

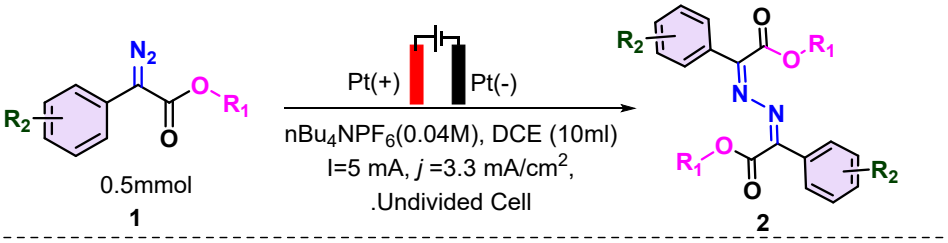

Synthesis of azines (**2a-2n**): An oven-dried 10 mL vial was configured as an undivided cell equipped with a Platinum anode and a Platinum cathode (immersed surface area of 1.5 cm^2 per electrode; interelectrode distance 1 cm). The vial was charged with phenyl diazo ester (1a) (0.5 mmol) and the supporting electrolyte nBu_4NBr (0.04 M, 128.9 mg) in DCE (10 mL). The reaction mixture was subjected to constant current electrolysis (I = 5 mA, j = 3.33 mA/cm^2) at room temperature under an argon atmosphere for 6 h (total charge passed Q = 2.23 F/mol), and the reaction progress was monitored by TLC. After the reaction was completed, the electrodes were washed with dilute HCl, and the reaction mixture was subjected to evaporation of volatiles under vacuum conditions. Then, the crude was taken in ethyl acetate and washed with a saturated aqueous NH_4Cl/NH_4F solution. The combined organic layer was extracted and dried over Na_2SO_4. After the solvent was evaporated using a rotary evaporator, the pure products (**2a-2n**) were obtained by column chromatography, using ethyl acetate in hexane as eluents and silica (60-120) as the stationary phase.

2.5 General procedure for the synthesis of olefines (3a-3m).

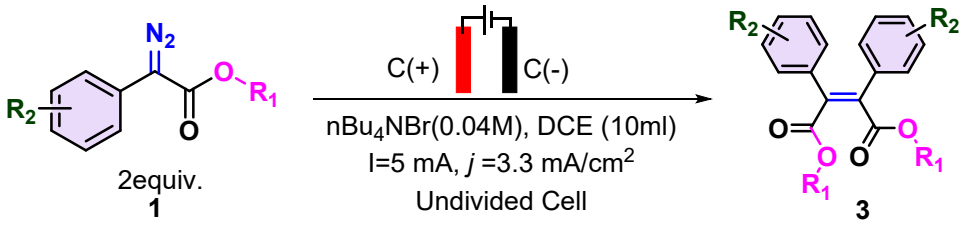

Synthesis of tetrasubstituted olefins (**3a–3n**): An oven-dried 10 mL vial was configured as an undivided cell equipped with a carbon anode and a carbon cathode (immersed surface area of 1.5 cm^2 per electrode; interelectrode distance 1 cm). The vial was charged with phenyl diazo ester (1a) (0.5 mmol) and the supporting electrolyte nBu_4NBr (0.04 M, 128.9 mg) in DCE (10 mL). The reaction mixture was subjected to constant current electrolysis (I = 5 mA, j = 3.33 mA/cm^2) at room temperature under an argon atmosphere for 6 h (total charge passed Q = 2.23 F/mol), and the reaction progress was monitored by TLC. After the reaction was completed, the reaction mixture was subjected to vacuum evaporation, then extracted with ethyl acetate and washed with a saturated aqueous NH_4Cl/NH_4F solution. The combined organic layer was dried with Na_2SO_4, followed by the evaporation of volatiles using a rotary evaporator. The pure products (**3a-3n**) were obtained using ethyl acetate in hexane as eluent by column chromatography on silica gel (60-120).

2.6 General Procedure for Cyclic Voltammetry (CV).

Cyclic voltammograms were obtained using a VSP-300 potentiostat (Bio-Logic, France) with a three-electrode cell to determine the redox potentials of all substrates.

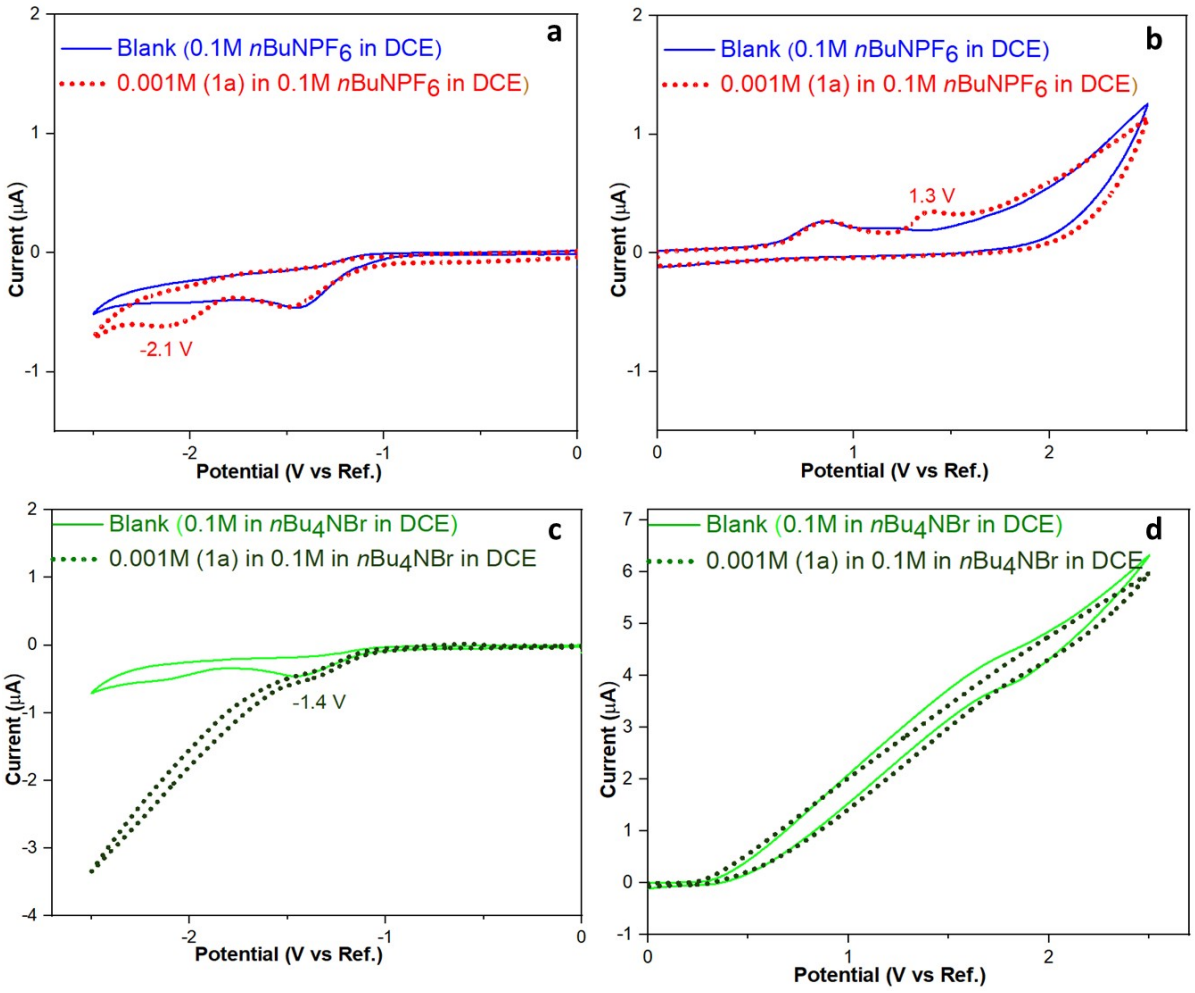

Figure S3: Cyclic voltammograms (IUPAC convention) of phenyl diazo ester **1a** recorded with a platinum disk or glassy carbon working electrode, a platinum wire counter electrode, and a non-aqueous Ag/Ag^+ reference electrode (Ag wire in MeCN/0.1 M nBu_4NClO_4/0.01 M $AgNO_3$). (**a**) Reduction Half under azine forming conditions (**b**) Reduction Half under azine forming conditions in 0.1 M nBu_4NPF_6 in DCE. (**c**) Reduction Half under olefin conditions (**d**) oxidation half under olefin conditions in 0.1 M nBu_4NBr in DCE.
0.1 M nBu_4NPF_6 in DCE (blank, blue) and 0.001 M 1a in 0.1 M nBu_4NPF_6 in DCE (red). 0.1 M nBu_4NBr in DCE (blank, light green) and 0.001 M 1a in 0.1 M nBu_4NBr in DCE (dark green). Scan rate: 0.05 V s^{-1}; initial potential: 0 V; first scan in the cathodic direction; room temperature. The cathodic peak potentials (E_p,c) of 1a are −2.1 V in DCE/nBu_4NPF_6 and −1.4 V in DCE/nBu_4NBr, and an anodic peak at +1.3 V is observed only in the presence of 1a in DCE/nBu_4NPF_6.

As depicted in (**Figure 1 in manuscript, and Figure S3)**, when a cyclic voltammetry experiment was set up, in the presence of 0.1 M nBu_4NPF_6 in DCE, recorded with a platinum disk working electrode and a non-aqueous Ag/Ag^+ reference electrode,[2] shows a pronounced irreversible cathodic wave with a peak potential at −2.1 V vs Ag/Ag^+, which might be

attributed to a one-electron reduction of (**1a**) to give the corresponding radical anion intermediate **(A)**. The radical anion intermediate **(A)** then decomposes rapidly, losing nitrogen to generate a carbanion (**B**), which subsequently couples with unreacted diazo to produce a hydrazone-radical intermediate(**C**). The cyclic voltammograms also display an anodic peak at +1.3 V vs Ag/Ag^+, which may correspond to intermediate (**C**). The appearance of this peak in DCE/nBu_4NPF_6 after extending the cathodic scan range suggests it may arise from an oxidation process involving a species generated during the preceding reduction, rather than from intermediate (C) directly. Overall, the findings from cyclic voltammetry studies strongly indicate that the conversion of anion radicals to azines occurs via a reductive dimerization pathway. Further, a cyclic voltammetry experiment was conducted under reaction conditions used for the selective synthesis of olefin products, i.e., phenyl diazo acetate (**1a**) in 0.1 M *n*Bu_4NBr in dichloroethane (DCE). In this medium, a cathodic peak is observed at −1.4 V vs Ag/Ag^+, which is not present in the blank electrolyte trace and is therefore assigned to the reduction of **1a** to radical anion (**A**). At more negative potentials, the current increases markedly, consistent with a follow-up chemical step and an overall EC-type process. On the reverse scan, only background anodic currents associated with the supporting electrolyte are observed. This sequence involves a cathodic reduction of phenyl diazo ester **(1a),** followed by an oxidation that regenerates it, thereby completing the electrochemical cycle.

3.0 General procedure for Cross-Coupling reaction.

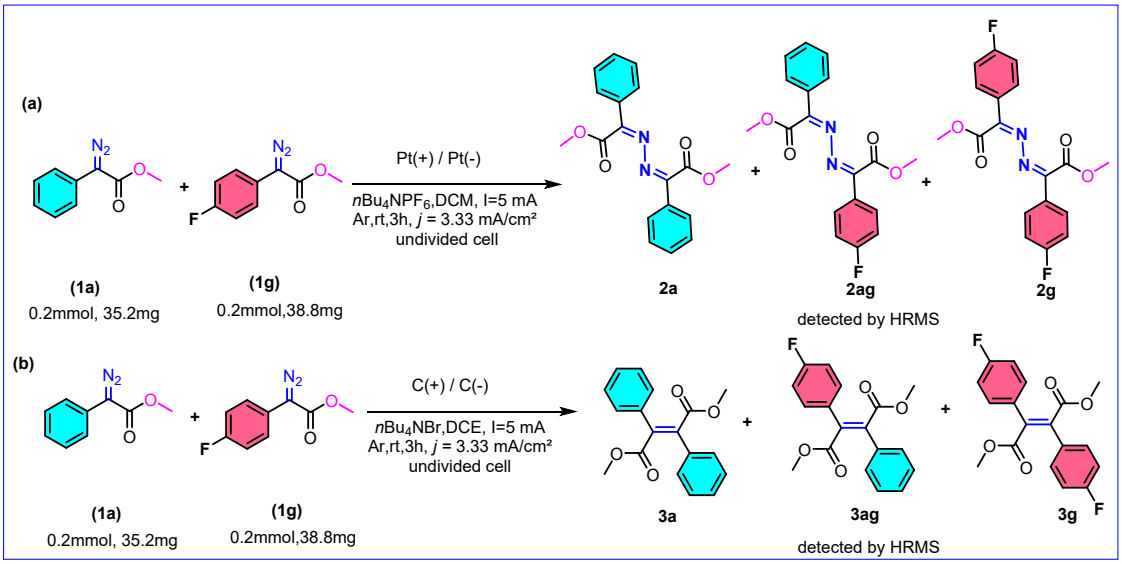

Scheme S1: (a) Cross-coupling of phenyl diazoesters, (**1a**) and (**1g**), for azine. (**b**) Cross-coupling of phenyl diazoesters, (**1a**) and (**1g**), for olefin.

We looked at how two different aryl diazo esters, (**1a**) and (**1g**), interacted with each other when the electrochemical conditions were set to either azine or olefin (Scheme **4a, b**). A constant current of 5 mA, an electrode immersed area of 1.5 cm^2 per electrode, and a current density of 3.33 $mA \cdot cm^{-2}$ were used in these tests. The electrochemical parameters stayed the same, but the solvent volume was doubled (4 mL) to make room for the combined substrate loading. The reaction went through both homo and cross coupling routes under these conditions, making a mix of azine and olefin products. were detected by HRMS, showed that the first spread of the product could be seen in the first 2 to 3 after electrolysis. After that, the relative rates mostly stayed the same, which makes sense. Since the reactions happened at the same time instead of one after the other. HRMS found that azine (**2ag)** and olefin (**3ag)** were cross-coupled, but they couldn't be separated because of competitive homocoupling and the way the products were statistically spread out. It was found that azine **2ag** had a peak at m/z 343.1101 (**Figure S1**) and olefin **3ag** had a peak at m/z 337.0855 (**Figure S2**). These results show that intermolecular cross-dimerization is possible within the current electrochemical framework, even though homo-coupling is still competitive in terms of kinetics.

3.1 HRMS Data of Cross-Coupling Reaction.

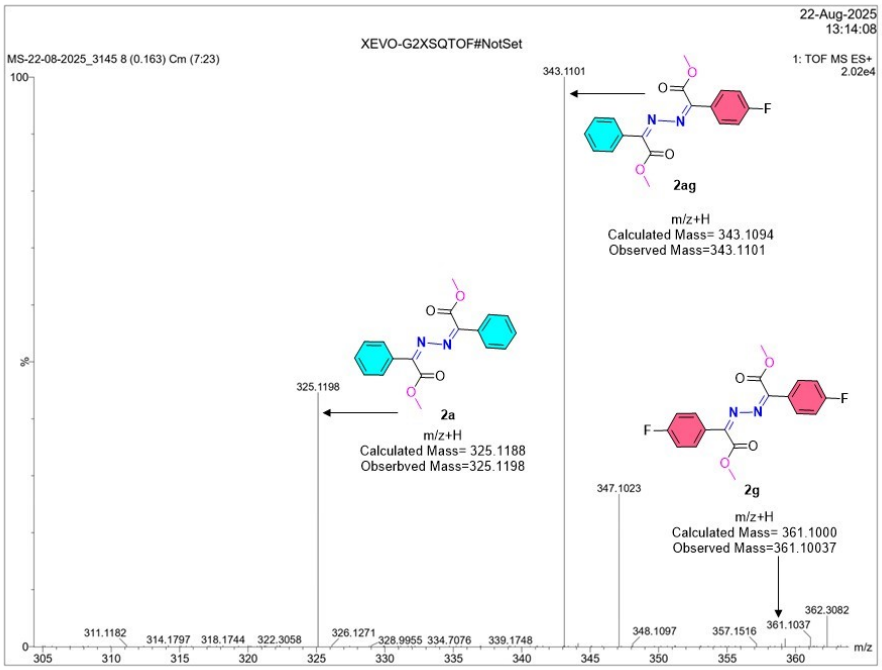

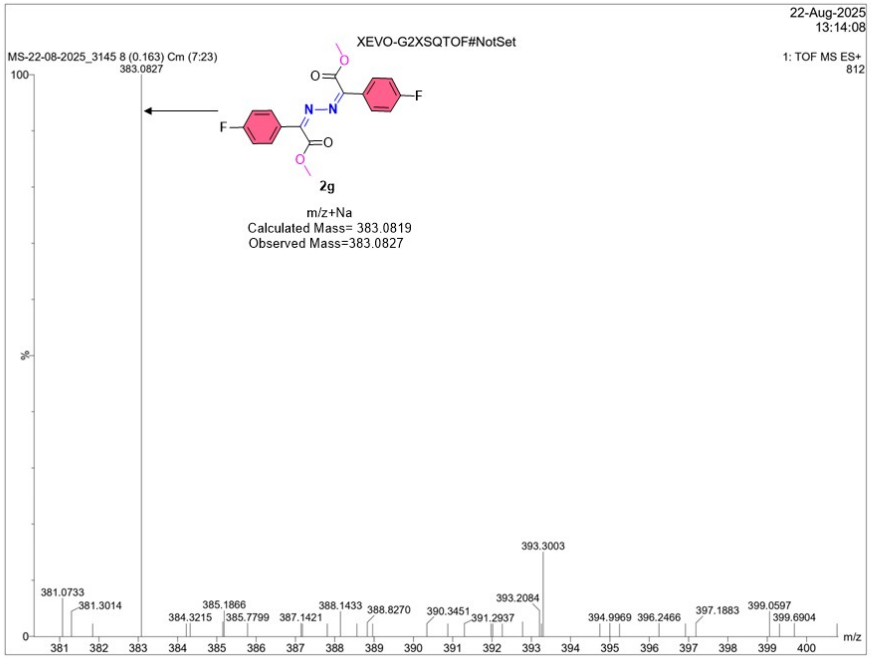

Figure S4. HR-MS Spectra of the Cross-Coupling reaction mixture of **(1a)** and **(1g)**

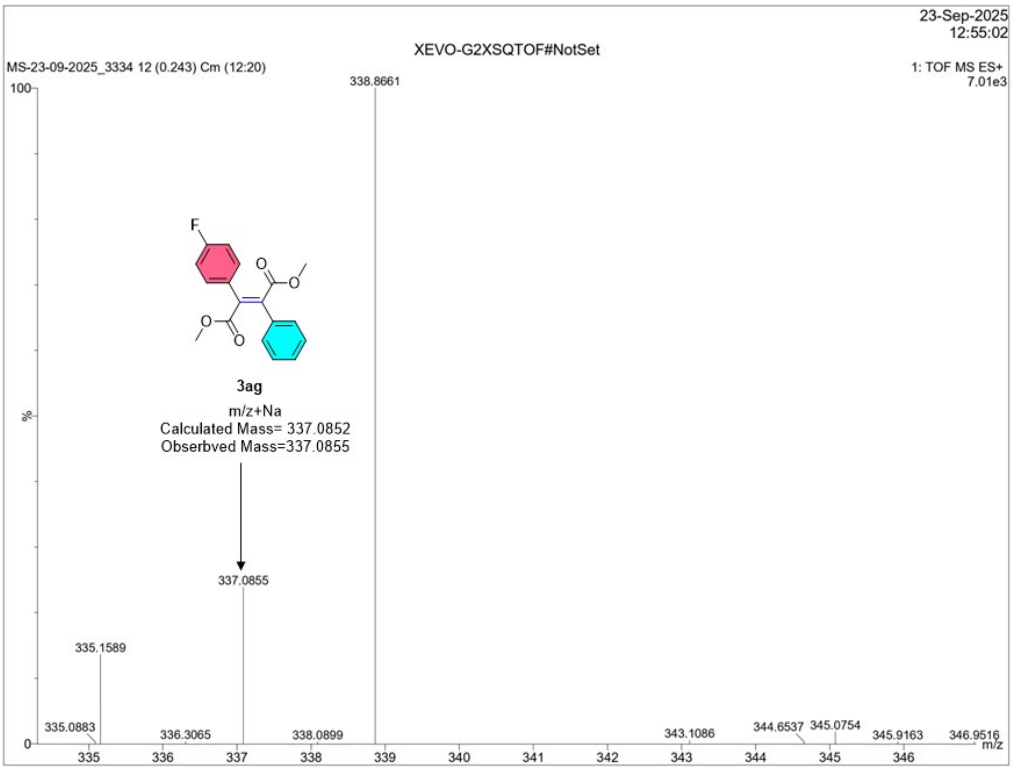

Figure S5. HR-MS Spectra of the cross-coupling reaction mixture of **(1a)** and **(1g)**

4.0 General procedure for control experiments

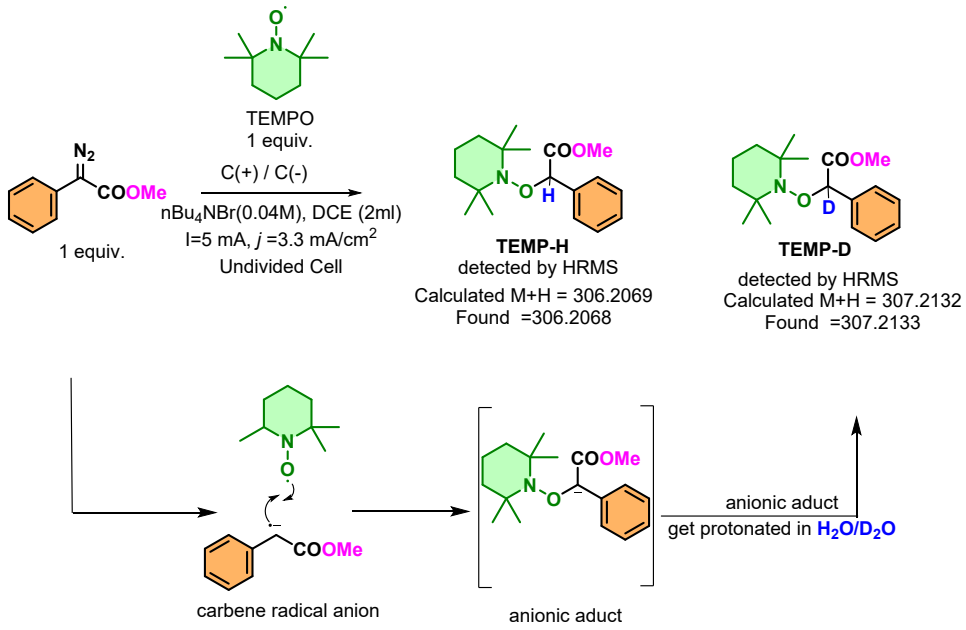

(I&II scheme 5) in olefinic conditions)

An oven-dry clean 10 mL vial equipped with a carbon electrode as an anode and a cathode set up as an undivided cell. The compound phenyl diazo ester (**1a)** (0.1 mmol,17.6mg), 2,2,6,6-tetramethyl-1-piperidinyloxy (TEMPO) (0.1 mmol, 15.6 mg), and supporting electrolyte nBu_4NBr 0.04M (25.8 mg) in DCE (2 mL), were electrolyzed under constant current conditions (5 mA at room temperature) in an argon atmosphere. After 1 h, the reaction mixture was quenched with H_2O/ D_2O and was immediately extracted with ethyl acetate and dried with Na_2SO_4. The solvent was evaporated using a rotary evaporator, and the sample was directly taken for HRMS analysis.

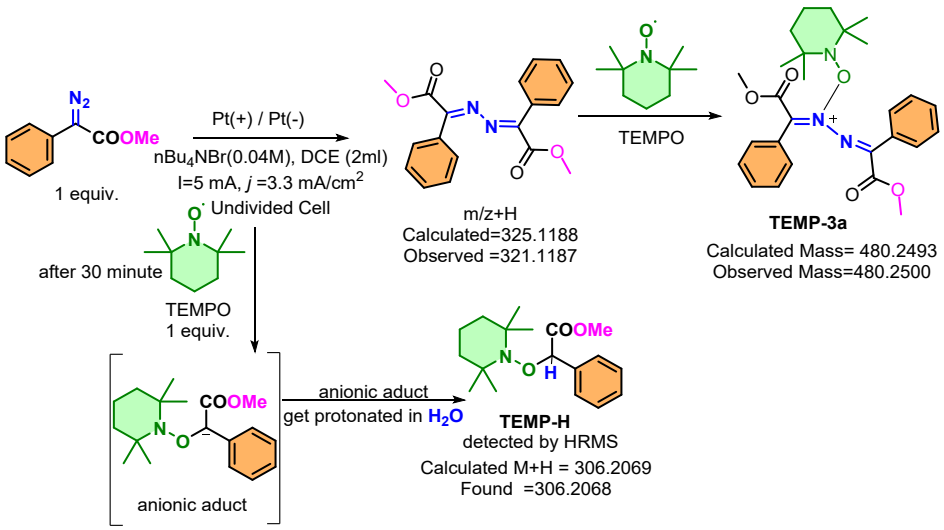

(III&IV scheme 5) in diazine condition)

An oven-dry clean 10 mL vial equipped with a carbon electrode as an anode and a cathode set up as an undivided cell. The compound phenyl diazo ester (**1a)** (0.1 mmol,17.6mg), 2,2,6,6-tetramethyl-1-piperidinyloxy (TEMPO) (0.1 mmol, 15.6 mg), and supporting electrolyte nBu_4NPF_6 0.04M (31.0 mg) in DCE (2 mL), were electrolyzed under constant current conditions (5 mA at room temperature) in an argon atmosphere. After 0.5 h, the TEMPO was added to the reaction, and after 1h, the reaction mixture was quenched with H_2O and immediately extracted with ethyl acetate and dried with Na_2SO_4. The solvent was evaporated using a rotary evaporator, and the sample was directly taken for HRMS analysis.

4.1 HRMS Data of Control Reaction.

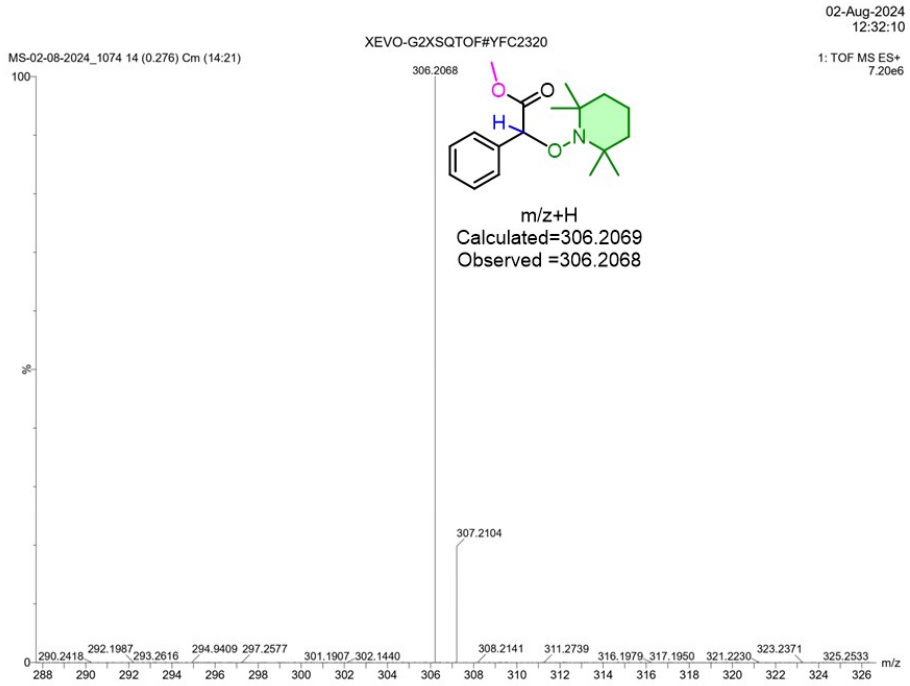

Figure S6. HR-MS Spectra of the reaction mixture of **(1a)** under the reaction conditions used for olefin synthesis. After 1 h, the reaction mixture was quenched with H_2O.

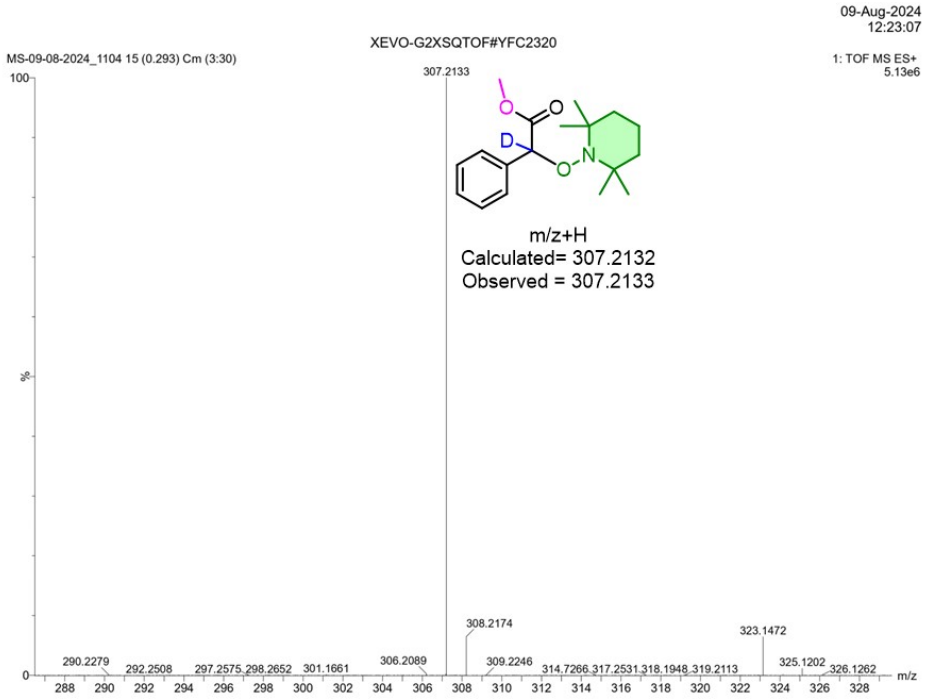

Figure S7. HR-MS Spectra of the reaction mixture of **(1a)** under the reaction conditions used for olefin synthesis. After 1 h, the reaction mixture was quenched with D_2O.

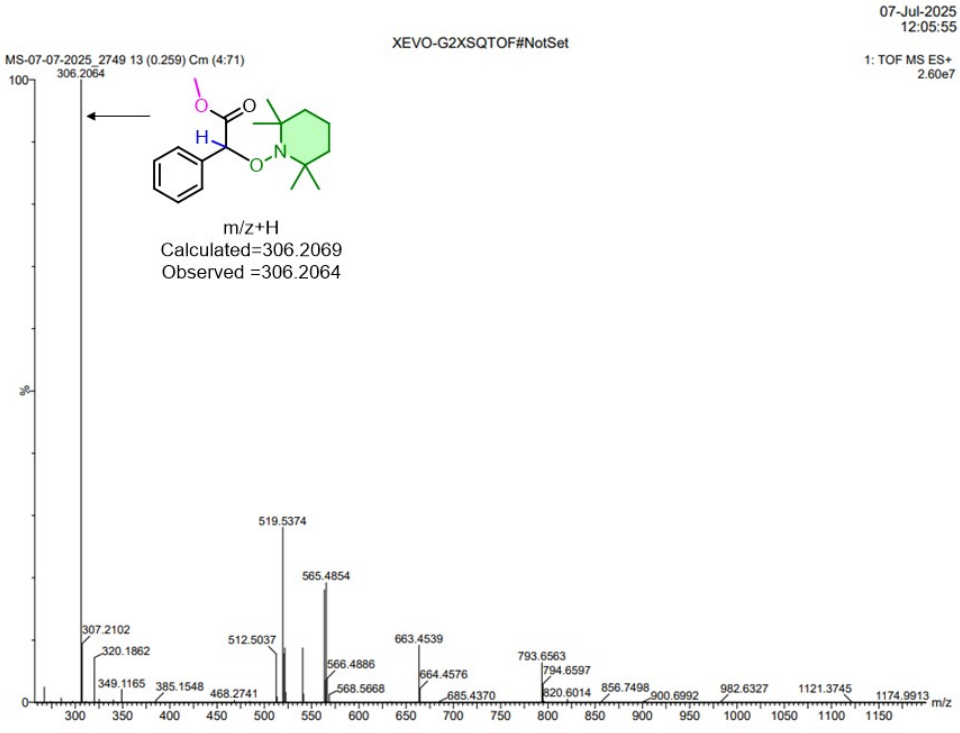

Figure S8. HR-MS Spectra of the reaction mixture of **(1a)** under the reaction conditions used for azine synthesis. After 1 h, the reaction mixture was quenched with H_2O.

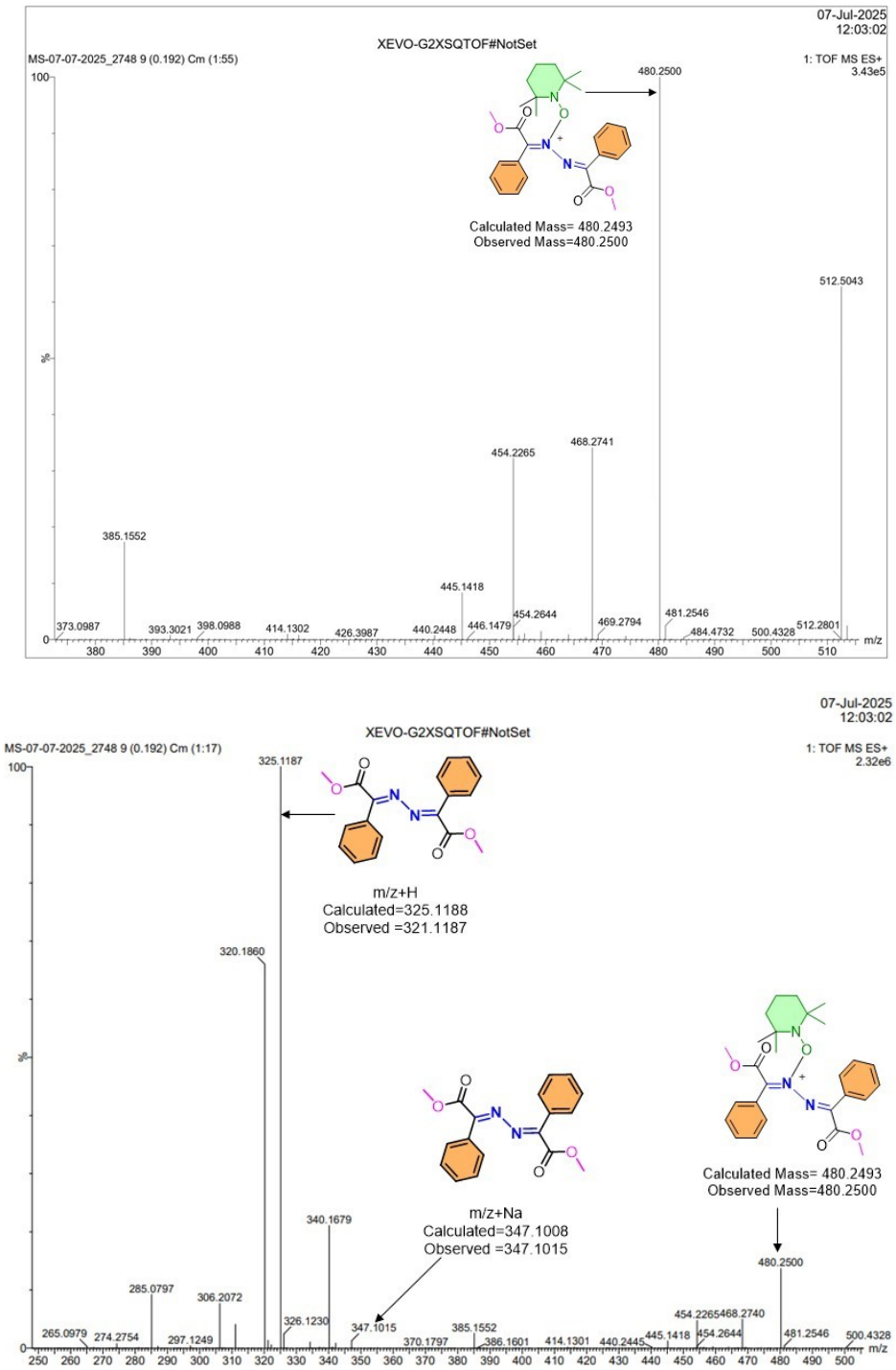

Figure S9. HR-MS Spectra of the reaction mixture of **(1a)** under the reaction conditions used for azine synthesis, TEMPO was added after 30 minutes from the initiation of the reaction, and the spectra were recorded after 10 minutes from the addition of TEMPO.

5.0 General procedure for Gram scale-up reaction.

Scale-up reaction of (2c).

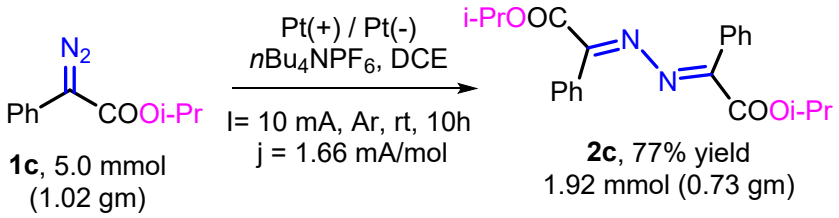

An oven-dry round-bottom flask equipped with a Platinum electrode as an anode and a Platinum cathode set up as an undivided cell. The compound phenyl diazo ester (**1c)** (5.0 mmol, 1.021g) and supporting electrolyte nBu$_4$NPF$_6$ (0.04 M, 1.549 g) in DCE (100 mL) were electrolyzed under constant current conditions (10 mA at room temperature), and the reaction was monitored using TLC. After the reaction was completed, the solution was extracted with 30 mL of ethyl acetate. The combined organic layer was dried with Na_2SO_4 and filtered. The solvent was removed with a rotatory evaporator. The pure products **2c** were obtained in 77% yield (0.73g, 1.92 mmol) by column chromatography using ethyl acetate in hexane as eluent and silica gel as a mobile phase.

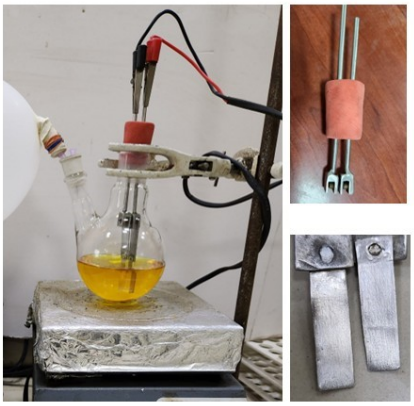

Figure S10. Reaction setup for the scale-up study for 2c.

Scale-up reaction of (3b).

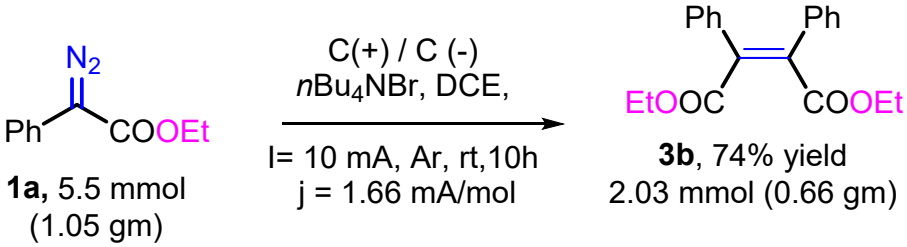

An oven-dry round-bottom flask equipped with a carbon electrode as an anode and a carbon cathode set up as an undivided cell. The compound phenyl diazo ester (**1b)** (5.5 mmol, 1.046g) and supporting electrolyte nBu$_4$NBr (0.04 M, 1.289 g) in DCE (100 mL) were electrolyzed under constant current conditions (10 mA at room temperature), and the reaction was monitored using TLC. After the reaction was completed, the solution was extracted with 30

mL of ethyl acetate. The combined organic layer was dried with Na_2SO_4 and filtered. The solvent was removed with a rotatory evaporator. The pure products **3b** were obtained in 74% yield (0.66g, 2.03 mmol) by column chromatography using ethyl acetate in hexane as eluent and silica gel as a mobile phase.

6.0 Computational Calculation Details.

Computational analysis was undertaken to elucidate the intrinsic factors governing stereo selectivity across both the olefin and azine. Because the electrode, electrolyte, and solvent primarily facilitate electron transfer and stabilize charged intermediates along the reaction coordinate, the calculations were focused on evaluating the inherent stabilities and stereochemical preferences of the neutral products formed after the electrochemical steps, without explicitly modeling the electrode electrolyte interface or the redox events, as commonly adopted in product level mechanistic studies of electrochemical transformations.

The geometries of the relevant isomeric products (2a), (2a′), (3a), and (3a′) were optimized using density functional theory (DFT) with the hybrid B3LYP functional and the 6-311G** basis set.[3-5] Dispersion interactions were treated using Grimme's empirical correction, which is essential for accurately describing noncovalent effects such as π–π stacking and dispersive stabilization in conjugated organic systems.[6] All geometry optimizations and vibrational frequency calculations were performed at 298.15 K using Gaussian16, enabling thermal corrections to be included and confirming that all optimized structures correspond to true minima on the potential energy surface.[7] Single-point energy refinements were subsequently carried out on the optimized geometries using the domain-based local pair natural orbital coupled-cluster method with perturbative triples, DLPNO-CCSD(T).[8] These calculations employed TightPNO and TightSCF convergence criteria,[9] the RI-JCOSX approximation, and the def2-TZVPP basis set together with the corresponding def2/J and def2-TZVPP/C auxiliary basis sets,[10] as implemented in ORCA (version 5.0.3).[11] This multilevel DFT/DLPNO-CCSD(T) protocol has been shown to reliably reproduce relative energies of closely related organic isomers within chemical accuracy.

The calculated free-energy differences reveal a consistent intrinsic thermodynamic bias that rationalizes the experimentally observed selectivity across both reaction manifolds. For the azine products, isomer (**2a′**) is predicted to be less stable than (**2a**) by 3.3 kcal/mol, a free-energy difference that corresponds to a strongly selective population bias at ambient

temperature and is widely accepted as sufficient to account for stereochemical outcomes in organic reactions.[81] Likewise, for the olefinic coupling products, the Z-isomer (**3a**) is calculated to be more stable than the corresponding *E*-isomer (**3a′**) by 3.6 kcal/mol. These energetic preferences arise from a balance of electronic and noncovalent interactions, including favorable π–π stacking and dispersion effects that are selectively accessible in the preferred geometries and outweigh steric congestion, consistent with established mechanistic paradigms for conjugated olefins. Taken together, the computational results provide a unified thermodynamic framework for understanding the selectivity observed for both azine formation and C–C bond formation, highlighting the dominant role of intrinsic molecular stabilization in shaping the reaction outcome.

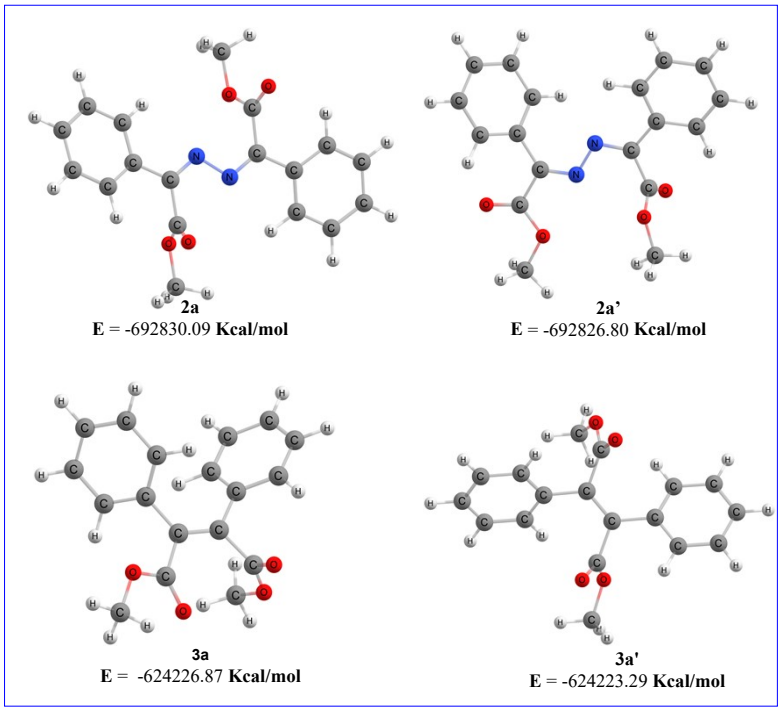

Figure S11. Optimized geometries and the corresponding electronic Energy of **2a, 2a'**,**3a**, and **3a'**.

2a

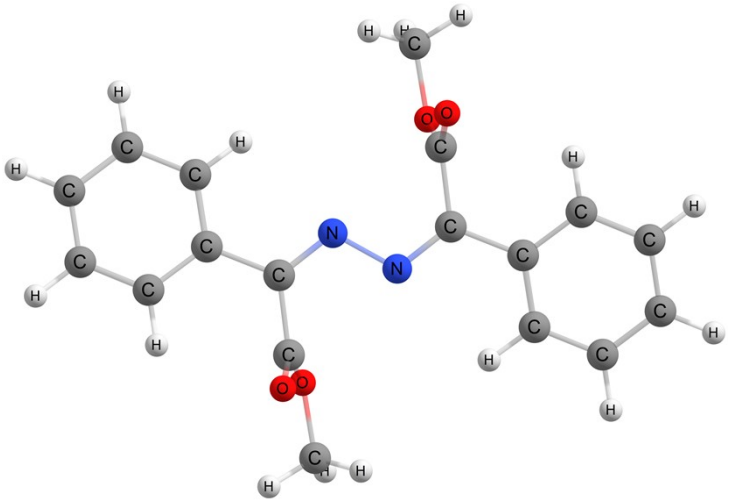

Coordinates

C	6.032846000	-3.284594000	-0.245180000
C	4.643786000	-3.320452000	-0.307132000
C	3.894338000	-2.167883000	-0.036015000
C	4.563384000	-0.979168000	0.296896000
C	5.947868000	-0.950330000	0.359207000
C	6.688019000	-2.102927000	0.088795000
H	6.602974000	-4.179875000	-0.462829000
H	4.141610000	-4.236100000	-0.591897000
H	3.974198000	-0.096890000	0.508131000
H	6.455891000	-0.029650000	0.621409000
H	7.770335000	-2.077214000	0.138570000
C	2.427831000	-2.189833000	-0.093220000
C	1.726521000	-3.529162000	-0.204056000
C	0.532996000	-5.173219000	0.972688000

H	0.232540000	-5.341951000	2.003479000
H	-0.338875000	-5.092142000	0.322400000
H	1.171400000	-5.982707000	0.616723000
O	1.646945000	-4.160401000	-1.225622000
O	1.257375000	-3.927740000	0.984414000
C	-0.275150000	-0.187296000	-0.194759000
C	0.432511000	1.151905000	-0.255389000
C	1.535884000	2.797722000	1.003980000
H	1.759316000	2.967970000	2.053918000
H	2.453443000	2.715730000	0.420055000
H	0.925602000	3.606664000	0.600608000
C	-1.741873000	-0.209239000	-0.246115000
C	-2.433771000	-1.397501000	0.038145000
C	-2.469158000	0.942895000	-0.573586000
C	-3.819073000	-1.426320000	-0.002044000
H	-1.861866000	-2.279441000	0.293653000
C	-3.858998000	0.907056000	-0.614461000
H	-1.947249000	1.858153000	-0.821774000
C	-4.537139000	-0.274157000	-0.328124000
H	-4.345145000	-2.346643000	0.223217000
H	-4.411422000	1.801989000	-0.874976000
H	-5.620174000	-0.299853000	-0.358477000
O	0.812534000	1.552234000	0.963932000
O	0.587453000	1.781652000	-1.269196000

N	0.387614000	-1.286775000	-0.123726000
N	1.761686000	-1.090289000	-0.072996000

2a'

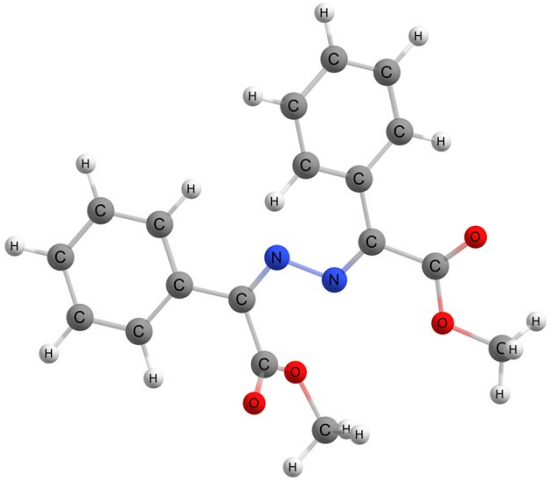

Coordinates:

C	1.006660000	-6.144978000	0.324863000
C	1.044497000	-4.759533000	0.435623000
C	-0.082659000	-3.993200000	0.108799000
C	-1.250523000	-4.640791000	-0.327951000
C	-1.280929000	-6.022151000	-0.438001000
C	-0.153070000	-6.778729000	-0.112801000
H	1.881461000	-6.729349000	0.583695000
H	1.942153000	-4.273042000	0.796107000
H	-2.114168000	-4.038875000	-0.578038000
H	-2.183454000	-6.515012000	-0.779777000
H	-0.180855000	-7.858607000	-0.200415000
C	-0.050982000	-2.533729000	0.216754000

C	1.255457000	-1.841967000	0.558105000
C	3.018215000	-0.567986000	-0.321751000
H	3.396717000	-0.326108000	-1.311466000
H	2.722837000	0.336548000	0.211102000
H	3.765270000	-1.108277000	0.260362000
O	1.686396000	-1.746140000	1.677413000
O	1.856330000	-1.390009000	-0.546613000
C	-1.913603000	0.282904000	0.089288000
C	-1.615690000	1.764919000	0.127214000
C	0.025915000	3.430371000	0.256055000
H	1.111030000	3.468279000	0.313480000
H	-0.332367000	3.948834000	-0.634618000
H	-0.423214000	3.889808000	1.137733000
C	-3.332481000	-0.126816000	-0.006382000
C	-3.831796000	-1.154838000	0.805523000
C	-4.195835000	0.501166000	-0.913599000
C	-5.161363000	-1.545609000	0.708406000
H	-3.176061000	-1.637281000	1.515885000
C	-5.520036000	0.092599000	-1.022343000
H	-3.829566000	1.309018000	-1.530849000
C	-6.007456000	-0.928835000	-0.211026000
H	-5.536928000	-2.333612000	1.350610000
H	-6.174062000	0.579874000	-1.735824000
H	-7.043135000	-1.238737000	-0.289964000

O	-0.303843000	2.032871000	0.192912000
O	-2.470883000	2.618147000	0.102106000
N	-0.882064000	-0.484815000	0.166926000
N	-1.128967000	-1.843413000	0.060959000

3a

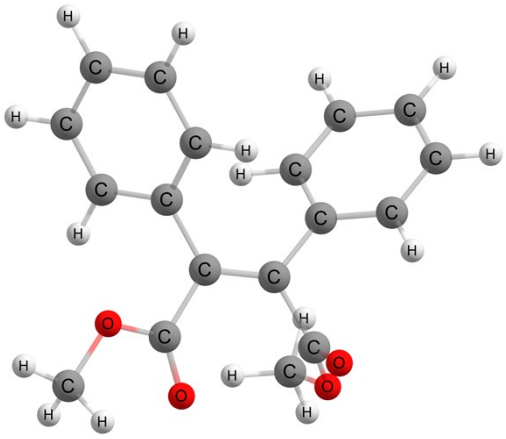

Coordinates:

C	-0.417349000	0.817228000	0.158487000
C	0.797279000	0.256981000	0.069906000
C	-1.704354000	0.082920000	0.092347000
C	-2.749653000	0.418236000	0.952871000
C	-1.905379000	-0.915400000	-0.864169000
C	-3.960257000	-0.255797000	0.878762000
H	-2.605033000	1.198848000	1.689664000
C	-3.119212000	-1.575561000	-0.943482000
H	-1.103995000	-1.168336000	-1.546881000
C	-4.148024000	-1.252918000	-0.067012000
H	-4.759890000	0.004521000	1.559811000
H	-3.263684000	-2.343228000	-1.692557000

H	-5.095479000	-1.772609000	-0.127927000
C	1.042369000	-1.205923000	0.046471000
C	0.490161000	-2.028641000	1.024874000
C	1.827854000	-1.776119000	-0.952829000
C	0.706521000	-3.397644000	0.995470000
H	-0.112236000	-1.586670000	1.808889000
C	2.037272000	-3.145885000	-0.988027000
H	2.272972000	-1.141453000	-1.710213000
C	1.476000000	-3.960259000	-0.013598000
H	0.275098000	-4.025989000	1.763844000
H	2.642861000	-3.578064000	-1.774134000
H	1.643551000	-5.029196000	-0.036977000
C	-0.595980000	2.295000000	0.440676000
O	-0.964484000	3.084664000	-0.567945000
C	-0.855273000	2.603353000	-1.904069000
H	0.173790000	2.315339000	-2.116617000
H	-1.532473000	1.764628000	-2.074435000
H	-1.143310000	3.436048000	-2.539258000
O	-0.547352000	2.709117000	1.561897000
C	1.975857000	1.177580000	0.034162000
O	1.922590000	2.325552000	-0.326290000
O	3.098362000	0.589331000	0.443654000
C	4.254016000	1.426676000	0.457790000
H	4.106211000	2.256240000	1.147710000

H	5.072957000	0.793921000	0.785142000
H	4.444658000	1.823724000	-0.538374000

3a'

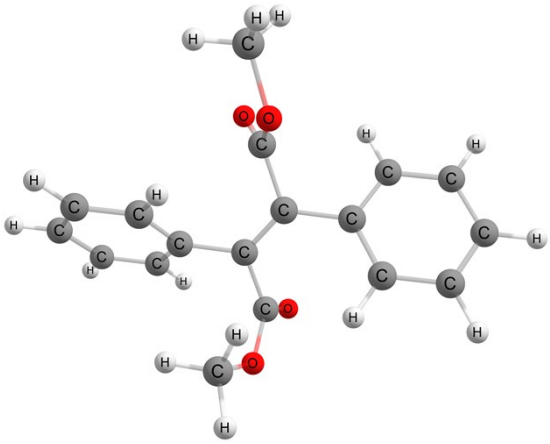

Coordinates:

C	-0.445627000	-0.563688000	-0.214415000
C	0.540401000	0.338041000	-0.173797000
C	-1.891271000	-0.239501000	-0.204395000
C	-2.758735000	-0.943032000	-1.040009000
C	-2.413995000	0.727951000	0.654364000
C	-4.116322000	-0.661435000	-1.038144000
H	-2.361986000	-1.700736000	-1.705485000
C	-3.771357000	1.005815000	0.655618000
H	-1.754706000	1.246418000	1.340893000
C	-4.625778000	0.314613000	-0.193241000
H	-4.777057000	-1.205537000	-1.700129000
H	-4.165115000	1.756890000	1.328019000
H	-5.685958000	0.531135000	-0.190250000

C	1.986483000	0.031910000	-0.120352000
C	2.488454000	-1.026284000	0.635448000
C	2.879593000	0.830433000	-0.836608000
C	3.848016000	-1.293339000	0.656645000
H	1.818198000	-1.641763000	1.222194000
C	4.237913000	0.560869000	-0.817161000
H	2.502217000	1.654404000	-1.431414000
C	4.726260000	-0.503213000	-0.071187000
H	4.222024000	-2.118968000	1.247620000
H	4.916291000	1.181030000	-1.388217000
H	5.787601000	-0.713251000	-0.053918000
C	-0.142229000	-2.034826000	-0.364303000
O	-0.427345000	-2.835883000	0.678386000
C	-0.930873000	-2.298115000	1.897080000
H	-0.398700000	-1.389740000	2.184670000
H	-1.995736000	-2.082436000	1.809389000
H	-0.770623000	-3.066710000	2.648194000
O	0.280472000	-2.505357000	-1.376672000
C	0.213912000	1.804737000	-0.253727000
O	-0.231106000	2.356145000	-1.219103000
O	0.529630000	2.436035000	0.884209000
C	0.296017000	3.844341000	0.878228000
H	-0.759088000	4.049793000	0.699487000
H	0.598664000	4.199954000	1.858043000

H 0.885587000 4.320345000 0.096067000

7.0 Crystallographic Data

A suitable crystal was selected. A Single crystal of all 4 structures was collected. A suitable crystal was selected and mounted on a nylon loop on a SuperNova, Dual, Cu at home/near, Pilatus 200K diffractometer. The crystal was kept at 100.2(4) for ska-meaze-2_auto **(2a)** , at 100.01(10) K for SKA-172-S2-4Br_auto **(3j)** , at 111.44(10) K SKA-172-S1-4 Br **(3j')** cooled with liquid nitrogen. Using Olex2[12], the structure was solved with the SHELXT[13] structure solution program using Intrinsic Phasing and refined with the SHELXL[14] refinement package using Least Squares minimisation.

Identification code	**ska-meaze-2_auto**
Empirical Formula	C18 H16 N2 O4
Formula weight	324.33
Temperature/K	100.2(4)
Crystal system	monoclinic
Space group	$P2_1/c$
a/ Å	8.8787(5)
b/ Å	11.4494(7)
c/ Å	8.0683(5)
α/°	90
β/°	102.012(6)
γ/°	90
Volume/ Å3	802.23(8)
Z	2
ρ_{calc}g/cm^3	1.343
μ/mm^{-1}	0.096

F000	340.0
Crystal size/mm^3	0.18 × 0.16 × 0.14
Radiation	Mo Kα (λ = 0.71073)
Theta (max)	61.778
R(reflections)	9469
Data/restraints / parameters	2099/0/110
GOF on F2	1.090
R1, wR2 c [I > 2σ(I)]	0.0512, 0.1359

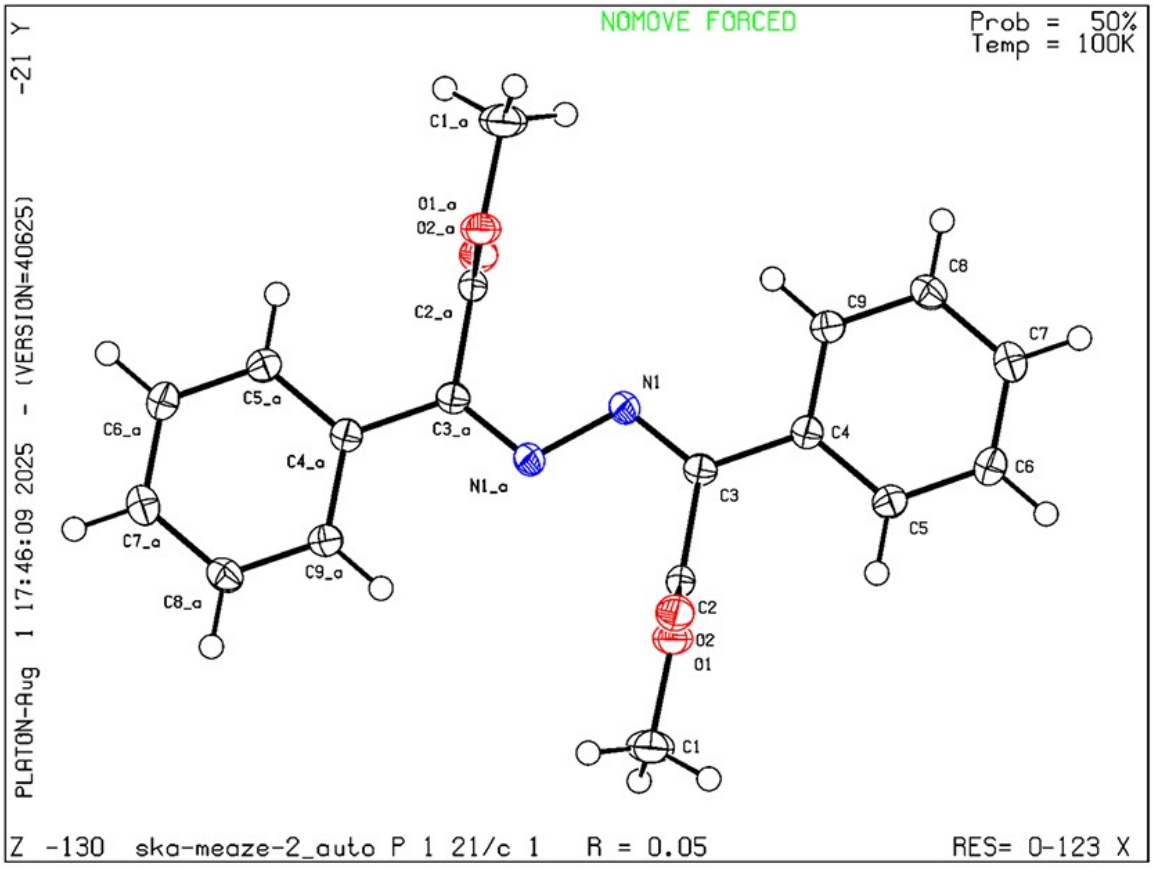

Figure S12. Solid-state structure of SKA-172-S2-4Br_auto **(2a)** with thermal ellipsoids at 50% probability level. oxygen = red, hydrogen = white spere, carbon = black ellipsoid, nitrogen = blue (CCDC 2493473).

Identification code	**SKA-172-S2-4Br_auto**	**SKA-172-S1-4 Br**
Empirical Formula	$C_{18}H_{14}Br_2O_4$	$C_{18}H_{14}Br_2O_4$

Formula weight	454.11	454.11
Temperature/K	100.01(10)	111.44(10)
Crystal system	triclinic	monoclinic
Space group	P-1	$P2_1/n$
a/ Å	11.5931(4)	5.9647(2)
b/ Å	11.8651(4)	18.3812(7)
c/ Å	13.9114(4)	8.0674(3)
α/°	73.921(3)	90
β/°	82.098(3)	93.059(3)
γ/°	72.791(3)	90
Volume/ Å3	1753.17(11)	883.24(6)
Z	4	2
ρ_{calc}g/cm^3	1.720	1.708
μ/mm^{-1}	4.642	4.607
F000	896.0	448.0
Crystal size/mm^3	0.22 × 0.18 × 0.16	0.2 × 0.18 × 0.16
Radiation	Mo Kα (λ = 0.71073)	Mo Kα (λ = 0.71073)
Theta (max)	61.624	59.51
R(reflections)	32420	9222
Data/restraints / parameters	8721/0/437	1985/0/110
GOF on F2	1.021	1.052
R1, wR2 c [I > 2σ(I)]	0.0388, 0.0743	0.0244, 0.0598

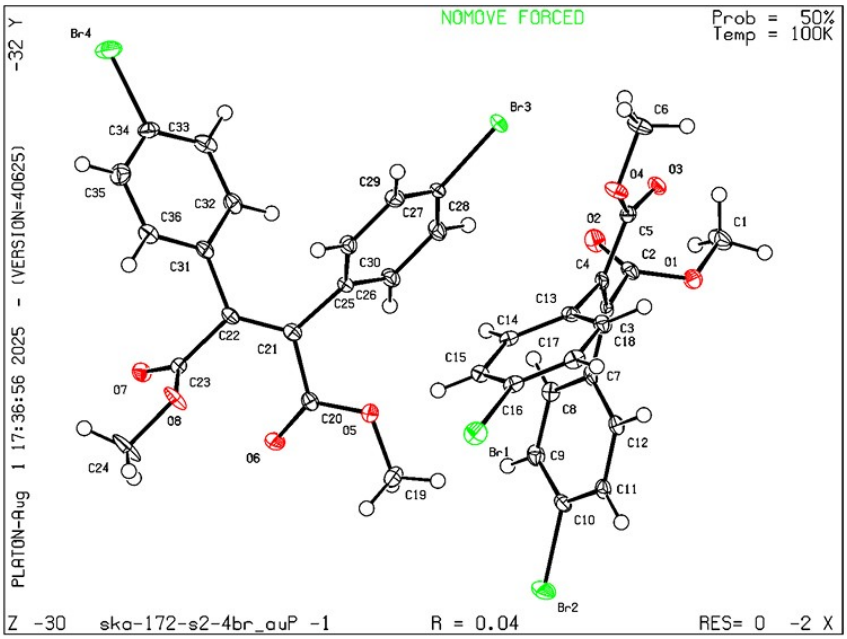

Figure S13. Solid-state structure of SKA-172-S2-4Br_auto **(3j)** with thermal ellipsoids at 50% probability level. oxygen = red, hydrogen = white spere, carbon = black ellipsoid, bromine = green (CCDC 2493474).

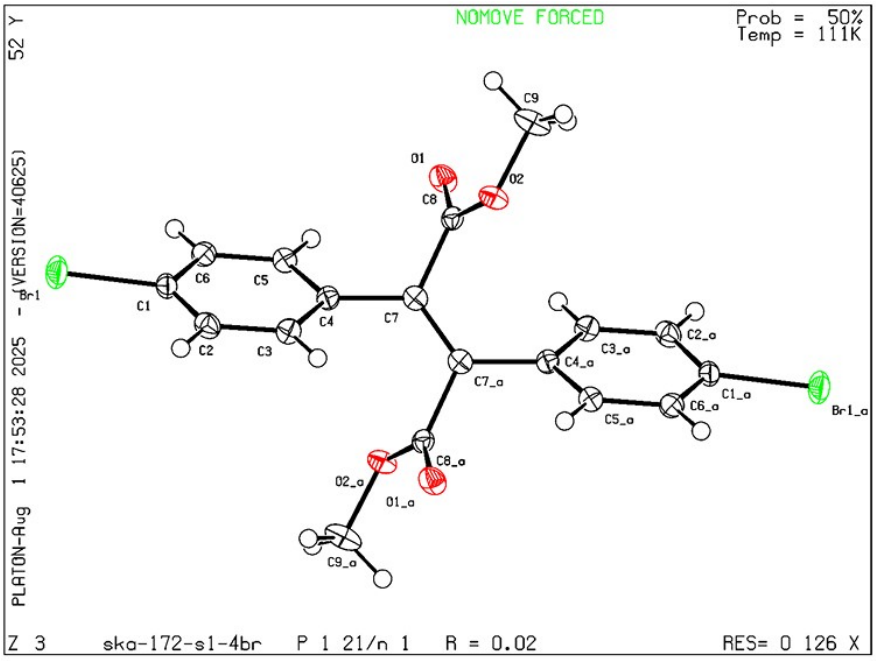

Figure S14. Solid-state structure of SKA-172-S1-4Br **(3j')** with thermal ellipsoids at 50% probability level. oxygen = red, hydrogen = white spere, carbon = black ellipsoid, bromine = green (CCDC 2493475).

8.0 References.

1. (a) Jana, S.; Yang, Z.; Li, F.; Empel, C.; Ho, J.; Koenigs, R. M. Photochemical Carbene Transfer Reactions of Diazoalkanes with Arenes. *Angew. Chem., Int. Ed.* **2020**, *59*, 5562–566.
   (b) Jana, S.; Yang, Z.; Pei, C.; Xu, X.; Koenigs, R. M. Visible-Light-Mediated Carbene Transfer Reactions with Diazo Compounds. *Chem. Sci.* **2019**, *10*, 10129–10134.
   (c) Keipour, H.; Ollevier, T. Iron-Catalyzed Carbene Transfer Reactions of Diazo Compounds. *Org. Lett.* **2017**, *19*, 5736–5739.
2. S. Singh, S. Rath, S. Bera, D. Maiti and S. Sen, *Cell Rep Phys Sci*, 2024, **5**, 101944.
3. Becke, A. D. Density-Functional Thermochemistry. III. The Role of Exact Exchange. *J. Chem. Phys.* **1993**, *98*, 5648–5652.
4. Lee, C.; Yang, W.; Parr, R. G. Development of the Colle–Salvetti Correlation-Energy Formula into a Functional of the Electron Density. *Phys. Rev. B* .**1988**, *37*, 785–789.
5. Krishnan, R.; Binkley, J. S.; Seeger, R.; Pople, J. A. Self-Consistent Molecular Orbital Methods. XX. A Basis Set for Correlated Wave Functions. *J. Chem. Phys.* **1980**, *72*, 650–654.
6. Grimme, S.; Antony, J.; Ehrlich, S.; Krieg, H. A Consistent and Accurate *Ab Initio* Parametrization of Density Functional Dispersion Correction (DFT-D) for the 94 Elements H–Pu. *J. Chem. Phys.* **2010**, *132*, 154104.
7. Frisch, M. J.; Trucks, G. W.; Schlegel, H. B.; Scuseria, G. E.; Robb, M. A.; Cheeseman, J. R.; Scalmani, G.; Barone, V.; Petersson, G. A.; Nakatsuji, H.; Li, X.; Caricato, M.; Marenich, A. V.; Bloino, J.; Janesko, B. G.; Gomperts, R.; Mennucci, B.; Hratchian, H. P.; Ortiz, J. V.; Izmaylov, A. F.; Sonnenberg, J. L.; Williams-Young, D.; Ding, F.; Lipparini, F.; Egidi, F.; Goings, J.; Peng, B.; Petrone, A.; Henderson, T.; Ranasinghe, D.; Zakrzewski, V. G.; Gao, J.; Rega, N.; Zheng, G.; Liang, W.; Hada, M.; Ehara, M.; Toyota, K.; Fukuda, R.; Hasegawa, J.; Ishida, M.; Nakajima, T.; Honda, Y.; Kitao, O.; Nakai, H.; Vreven, T.; Throssell, K.; Montgomery, J. A., Jr.; Peralta, J. E.; Ogliaro, F.; Bearpark, M. J.; Heyd, J. J.; Brothers, E. N.; Kudin, K. N.; Staroverov, V. N.; Keith, T. A.; Kobayashi, R.; Normand,

J.; Raghavachari, K.; Rendell, A. P.; Burant, J. C.; Iyengar, S. S.; Tomasi, J.; Cossi, M.; Millam, J. M.; Klene, M.; Adamo, C.; Cammi, R.; Ochterski, J. W.; Martin, R. L.; Morokuma, K.; Farkas, O.; Foresman, J. B.; Fox, D. J. *Gaussian 16*, Revision C.01; Gaussian, Inc.: Wallingford, CT, 2016.

8. a) Riplinger, C.; Neese, F. An Efficient and near Linear Scaling Pair Natural Orbital Based Local Coupled Cluster Method. *J. Chem. Phys.* **2013**, *138*, 034106. b) Riplinger, C.; Sandhoefer, B.; Hansen, A.; Neese, F. Natural Triple Excitations in Local Coupled Cluster Calculations with Pair Natural Orbitals. *J. Chem. Phys.* **2013**, *139*, 134101.c)Riplinger, C.; Pinski, P.; Becker, U.; Valeev, E. F.; Neese, F. Sparse Maps—A Systematic Infrastructure for Reduced-Scaling Electronic Structure Methods. II. Linear Scaling Domain Based Pair Natural Orbital Coupled Cluster Theory. *J. Chem. Phys.* **2016**, *144*, 024109.
9. Neese, F.; Wennmohs, F.; Hansen, A.; Becker, U. Efficient, Approximate and Parallel Hartree–Fock and Hybrid DFT Calculations. A "Chain-of-Spheres" Algorithm for the Hartree–Fock Exchange. *Chem. Phys.* **2009**, *356*, 98–109.
10. a) Weigend, F.; Ahlrichs, R. Balanced Basis Sets of Split Valence, Triple Zeta Valence and Quadruple Zeta Valence Quality for H to Rn: Design and Assessment of Accuracy. *Phys. Chem. Chem. Phys.* **2005**, *7*, 3297–3305. b) Weigend, F. Accurate Coulomb-Fitting Basis Sets for H to Rn. *Phys. Chem. Chem. Phys.* **2006**, *8*, 1057–1065.
11. Neese, F.; Wennmohs, F.; Becker, U.; Riplinger, C. The ORCA Quantum Chemistry Program Package. *J. Chem. Phys.* **2020**, *152*, 224108.
12. Dolomanov, O. V.; Bourhis, L. J.; Gildea, R. J.; Howard, J. A. K.; Puschmann, H. OLEX2: A Complete Structure Solution, Refinement and Analysis Program. *J. Appl. Crystallogr.* **2009**, *42*, 339–341.
13. Sheldrick, G. M. SHELXT—Integrated Space-Group and Crystal-Structure Determination. *Acta Crystallogr. A* **2015**, *71*, 3–8.
14. Sheldrick, G. M. Crystal Structure Refinement with SHELXL. *Acta Crystallogr. C* **2015**, *71*, 3–8.

9.0 NMR Data

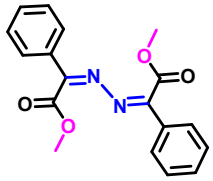

dimethyl 2,2'-(hydrazine-1,2-diylidene)(2Z,2'Z)-bis(2-phenylacetate)(2a)

Purification by column chromatography (mobile phase: EtOAc/Hexane 1:20), (63.3mg, 78% yield) as a yellow solid.**^{1}H NMR (700 MHz, $CDCl_3$)** δ 7.78 (q, *J* = 7.7 Hz, 4H), 7.51 (d, *J* = 11.9 Hz, 2H), 7.44 (d, *J* = 15.8 Hz, 4H), 4.00 (s, 6H).**^{13}C NMR (175 MHz, $CDCl_3$)** δ 165.76, 162.39, 132.16, 131.10, 128.86, 127.71, 52.22.**HRMS (ESI)** m/z calcd. for $C_{18}H_{16}N_2O_4$ ([M + H]+): 325.1188, found: 325.1190.

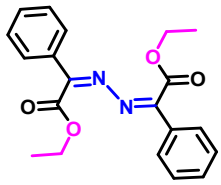

diethyl 2,2'-(hydrazine-1,2-diylidene)(2Z,2'Z)-bis(2-phenylacetate) (2b)

Purification by column chromatography (mobile phase: EtOAc/Hexane 1:20), (69.5mg, 79% yield) as a yellow solid.**^{1}H NMR (500 MHz, $CDCl_3$)** δ 7.45 – 7.42 (m, 3H), 7.30 – 7.26 (m, 2H), 7.26 – 7.19 (m, 4H), 4.23 (q, *J* = 7.1 Hz, 4H), 1.25 (t, *J* = 7.1 Hz, 6H).**^{13}C NMR (125 MHz, $CDCl_3$)** δ 169.28, 162.94, 136.70, 131.19, 128.18, 127.86, 58.53, 14.00.**HRMS (ESI)** m/z calcd. for $C_{20}H_{20}N_2O_4$ ([M + H]+): 381.1814, found: 381.1805.

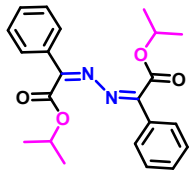

diisopropyl 2,2'-(hydrazine-1,2-diylidene)(2Z,2'Z)-bis(2-phenylacetate) (2c)

Purification by column chromatography (mobile phase: EtOAc/Hexane 1:20), (78mg, 82% yield) as a yellow solid.**^{1}H NMR (500 MHz, $CDCl_3$)** δ 7.80 (d, *J* = 7.1 Hz, 4H), 7.52 – 7.43 (m, 4H), 7.42 (d, *J* = 7.2 Hz, 3H), 5.42 (hept, *J* = 6.3 Hz, 2H), 1.42 (s, 6H), 1.40 (s, 6H).**^{13}C NMR (125 MHz, $CDCl_3$)** δ 165.04, 162.15, 131.96, 131.64, 128.88, 128.03, 69.93, 22.14. **HRMS (ESI)** m/z calcd. for $C_{22}H_{24}N_2O_4$ ([M + H]+): 381.1814, found: 381.1805.

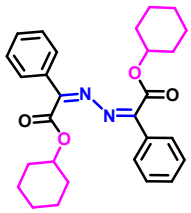

dicyclohexyl 2,2'-(hydrazine-1,2-diylidene)(2Z,2'Z)-bis(2-phenylacetate) (2d)

Purification by column chromatography (mobile phase: EtOAc/Hexane 1:20), (97.8mg, 85% yield) as a yellow solid.**^{1}H NMR (700 MHz, $CDCl_3$)** δ 7.16 (q, *J* = 7.4 Hz, 6H), 7.09 (d, *J* = 6.1 Hz, 4H), 4.94 (tt, *J* = 9.0, 3.9 Hz, 2H), 1.89 (d, *J* = 8.6 Hz, 4H), 1.65 (dd, *J* = 9.4, 4.3 Hz, 4H), 1.51 (dt, *J* = 9.0, 4.7 Hz, 2H), 1.47 – 1.40 (m, 4H), 1.35 (dt, *J* = 13.9, 10.3 Hz, 4H), 1.28 – 1.17 (m, 3H).**^{13}C NMR (175 MHz, $CDCl_3$)** δ 171.81, 166.36, 147.80, 142.07, 140.07, 138.73, 130.59, 129.31, 124.08, 123.72, 58.59, 23.73, 19.56, 13.50.**HRMS (ESI)** m/z calcd. for $C_{22}H_{24}N_2O_4$ ([M + H]+): 461.2440, found: 461.2444.

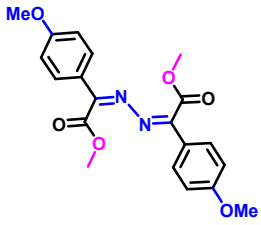

dimethyl 2,2'-(hydrazine-1,2-diylidene)(2Z,2'Z)-bis(2-(4-methoxyphenyl)acetate) (2f)

Purification by column chromatography (mobile phase: EtOAc/Hexane 1:20), (82.5mg, 86% yield) as a yellow solid.**^{1}H NMR (500 MHz, $CDCl_3$)** δ 7.71 (d, *J* = 6.8 Hz, 4H), 6.93 (d, *J* = 9.0 Hz, 4H), 3.99 (s, 6H), 3.86 (s, 6H).**^{13}C NMR (125 MHz, $CDCl_3$)** δ 166.36, 162.80, 131.34, 129.84, 123.95, 114.42, 55.57, 52.14.**HRMS (ESI)** m/z calcd. for $C_{20}H_{20}N_2O_6$ ([M + H]+): 385.1400, found: 385.1392.

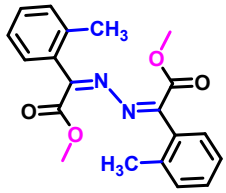

dimethyl 2,2'-(hydrazine-1,2-diylidene)(2Z,2'Z)-bis(2-(o-tolyl)acetate)(2g)

Purification by column chromatography (mobile phase: EtOAc/Hexane 1:20), (69.5mg, 79% yield) as a yellow solid **^{1}H NMR (500 MHz,)** δ 7.12 – 6.99 (m, 4H), 6.96 (d, *J* = 5.8 Hz, 4H), 3.80 (s, 6H), 2.22 (s, 6H).**^{13}C NMR (125 MHz, $CDCl_3$)** δ 165.04, 162.15, 131.96, 131.64,

128.88, 128.03, 52.20, 22.14.**HRMS (ESI)** m/z calcd. for $C_{20}H_{21}N_2O_4$ ([M + H]+): 353.1501, found: 353.1509.

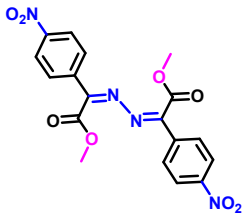

dimethyl 2,2'-(hydrazine-1,2-diylidene)(2Z,2'Z)-bis(2-(4-nitrophenyl)acetate) (2h)

Purification by column chromatography (mobile phase: EtOAc/Hexane 1:20), (74.5mg, 72% yield) as a yellow solid **^{1}H NMR (400 MHz,** δ 8.36 (d, *J* = 9.0 Hz, 1H), 8.26 (d, *J* = 9.1 Hz, 1H), 4.02 (s, 2H).**^{13}C NMR (175 MHz, $CDCl_3$)** δ 165.88, 162.51, 138.89, 134.47, 129.82, 128.30, 77.34, 77.16, 76.98, 52.90. **HRMS (ESI)** m/z calcd. for $C_{18}H_{14}N_4O_8$ ([M + Na]+): 415.0890, found: 415.0894.

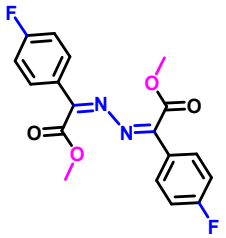

dimethyl 2,2'-(hydrazine-1,2-diylidene)(2Z,2'Z)-bis(2-(4-fluorophenyl)acetate) (2i)

Purification by column chromatography (mobile phase: EtOAc/Hexane 1:20), (68.5mg, 76% yield) as a yellow solid.^{1}H NMR (500 MHz, $CDCl_3$) δ 7.77 (dd, *J* = 9.0, 5.3 Hz, 1H), 7.16 – 7.11 (m, 1H), 4.00 (s, 2H).^{13}C NMR (125 MHz, $CDCl_3$) δ 166.19, 165.49, 164.17, 161.27,130.25 (d, $^3J_{C-F}$ = 9.0 Hz),127.34 (d, $^3J_{C-F}$ = 2.8 Hz),116.29, 116.11, 52.30.HRMS (ESI) m/z calcd. for $C_{18}H_{14}F_2N_2O_4$ ([M + H]+): 361.1000, found: 361.1003.

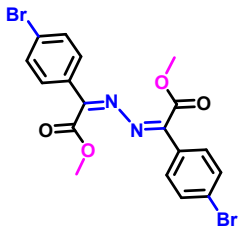

dimethyl 2,2'-(hydrazine-1,2-diylidene)(2Z,2'Z)-bis(2-(4-bromophenyl)acetate)(2j)

Purification by column chromatography (mobile phase: EtOAc/Hexane 1:20), (97.5mg, 81% yield) as a yellow solid. **^{1}H NMR (500 MHz, $CDCl_3$)** δ 7.52 (d, *J* = 8.6 Hz, 2H), 7.28 (s, 1H),

3.56 (s, 4H). **^{13}C NMR (125 MHz, $CDCl_3$)** δ 163.66, 161.68, 138.11, 131.71, 130.25, 115.72, 52.95.**HRMS (ESI)** m/z calcd. for $C_{18}H_{14}Br_2N_2O_4$ ([M + H]+): 482.9378, found: 482.9380.

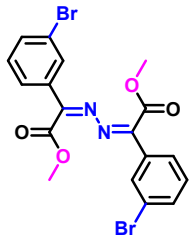

dimethyl 2,2'-(hydrazine-1,2-diylidene)(2Z,2'Z)-bis(2-(3-bromophenyl)acetate) (2k)

Purification by column chromatography (mobile phase: EtOAc/Hexane 1:20), (93.8mg, 81% yield) as a yellow solid. **^{1}H NMR (500 MHz, $CDCl_3$)** δ 7.58 (t, *J* = 1.7 Hz, 2H), 7.53 (ddd, *J* = 8.0, 2.0, 1.1 Hz, 2H), 7.34 (ddd, *J* = 7.7, 1.7, 1.1 Hz, 2H), 7.28 (d, *J* = 7.9 Hz, 2H), 3.59 (s, 6H).**^{13}C NMR (125 MHz, $CDCl_3$)** δ 164.00, 161.64, 137.15, 136.86, 132.07, 130.94, 130.01, 126.70, 122.52, 52.52.**HRMS (ESI)** m/z calcd. for $C_{18}H_{14}Br_2N_2O_4$ ([M + H]+): 482.9378, found: 482.9380.

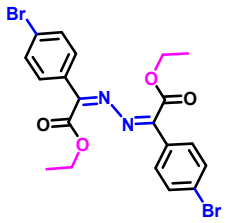

diethyl 2,2'-(hydrazine-1,2-diylidene)(2Z,2'Z)-bis(2-(4-bromophenyl)acetate) (2l)

Purification by column chromatography (mobile phase: EtOAc/Hexane 1:20), (107.3mg, 84% yield) as a yellow solid.**^{1}H NMR (500 MHz, $CDCl_3$)** δ 7.64 (d, *J* = 8.9 Hz, 4H), 7.57 (d, *J* = 8.9 Hz, 4H), 4.48 (q, *J* = 7.2 Hz, 4H), 1.41 (t, *J* = 7.1 Hz, 6H).**^{13}C NMR (125 MHz, $CDCl_3$)** δ 164.87, 161.40, 132.32, 130.32, 129.47, 127.07, 62.02, 14.58. **HRMS (ESI)** m/z calcd. for $C_{20}H_{18}Br_2N_2O_4$ ([M + H]+): 510.9691, found: 510.9695.

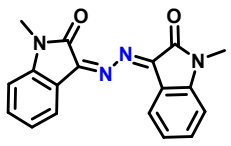

(3Z,3'E)-3,3'-(hydrazine-1,2-diylidene)bis(1-methylindolin-2-one) (2q)

Purification by column chromatography (mobile phase: EtOAc/Hexane 3:10),(33.6 mg, 65% yield) as a yellow solid **^{1}H NMR (500 MHz, $CDCl_3$)** δ 7.50 (d, *J* = 8.1 Hz, 1H), 7.27 (td, *J* =

7.7, 1.2 Hz, 1H), 7.08 (td, *J* = 7.5, 0.9 Hz, 1H), 6.85 (dt, *J* = 7.9, 0.9 Hz, 1H), 3.27 (s, 3H).**^{13}C NMR (125 MHz, $CDCl_3$)** δ 161.94, 141.15, 128.94, 128.09, 122.62, 121.56, 118.67, 108.34, 25.44.**HRMS (ESI)** m/z calcd. for $C_{18}H_{15}N_2O_4$ ([M + H]+): 319.1195, found: 319.1193.

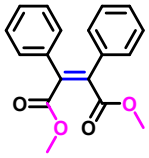

Dimethyl 2,3-Diphenylmaleate (3a)

Purification by column chromatography (mobile phase: EtOAc/Hexane 1:2023.), (57.8 mg, 76% yield) as a white solid. **^{1}H NMR (400 MHz, $CDCl_3$)** δ 7.41 – 7.38 (m, 6H), 7.37 (dd, *J* = 3.0, 2.0 Hz, 4H), 3.54 (s, 6H).**^{13}C NMR (100 MHz, $CDCl_3$)** δ 168.48, 137.58, 135.38, 128.86, 128.52, 127.98, 52.28. **HRMS (ESI)** m/z calcd. for $C_{18}H_{16}O_4$ ([M + Na]+): 319.0946, found: 319.0945.

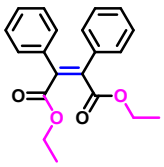

diethyl 2,3-diphenylmaleate (3b)

Purification by column chromatography (mobile phase: EtOAc/Hexane 1:20), (65 mg, 80% yield) as a white solid. **^{1}H NMR (500 MHz, $CDCl_3$)** δ 7.21 – 7.14 (m, 6H), 7.12 – 7.08 (m, 4H), 4.30 (q, *J* = 7.1 Hz, 4H), 1.30 (t, *J* = 7.1 Hz, 6H).**^{13}C NMR (125 MHz, CDCl3)** δ 167.96, 138.66, 134.66, 129.70, 128.19, 128.06, 61.69, 14.02.**HRMS (ESI)** m/z calcd. for $C_{20}H_{20}O_4$ ([M + H]+): 325.1440, found: 325.1433.

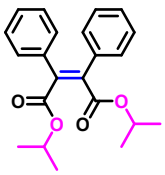

diisopropyl 2,3-diphenylmaleate (3c)

Purification by column chromatography (mobile phase: EtOAc/Hexane 1:20), (69.5mg, 79% yield) as a white solid.**^{1}H NMR (500 MHz, $CDCl_3$)** δ 7.48 (d, *J* = 7.4 Hz, 4H), 7.40 – 7.35 (m, 4H), 7.17 (t, *J* = 7.4 Hz, 2H), 5.21 (hept, *J* = 6.3 Hz, 2H), 1.33 (d, *J* = 6.3 Hz, 12H).**^{13}C ^{13}C NMR (125 MHz, $CDCl_3$)** δ 164.98, 129.04, 128.47, 125.97, 125.83, 124.13, 68.82, 22.23.**HRMS (ESI)** m/z calcd. for $C_{22}H_{24}O_4$ ([M + H]+): 353.1753, found: 353.1749.

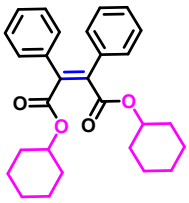

dicyclohexyl 2,3-diphenylmaleate (3d)

Purification by column chromatography (mobile phase: EtOAc/Hexane 1:20), (81mg, 75% yield) as a white solid.**^{1}H NMR (500 MHz, $CDCl_3$)** δ 7.39 – 7.34 (m, 6H), 7.32 – 7.29 (m, 4H), 5.19 – 5.13 (m, 2H), 2.13 – 2.07 (m, 4H), 1.86 (dp, *J* = 9.4, 3.2 Hz, 4H), 1.77 – 1.68 (m, 3H), 1.68 – 1.61 (m, 4H), 1.57 (dtt, *J* = 13.8, 10.4, 3.4 Hz, 5H), 1.48 – 1.39 (m, 2H).**^{13}C NMR (125 MHz, $CDCl_3$)** δ 167.56, 138.79, 135.14, 129.90, 128.08, 74.12, 31.42, 25.50, 23.77.**HRMS (ESI)** m/z calcd. for $C_{28}H_{32}O_4$ ([M + H]+): 433.2379, found: 433.2381.

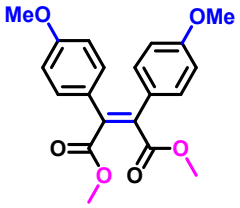

dimethyl 2,3-bis(4-methoxyphenyl)maleate (3f)

Purification by column chromatography (mobile phase: EtOAc/Hexane 1:20), (73mg, 82% yield) as a white solid.**^{1}H NMR (500 MHz, $CDCl_3$)** δ 7.02 (d, *J* = 9.0 Hz, 4H), 6.73 (d, *J* = 9.0 Hz, 4H), 3.82 (s, 6H), 3.76 (s, 6H).**^{13}C NMR (125 MHz, $CDCl_3$)** δ 168.91, 159.49, 137.38, 131.24, 129.38, 126.86, 113.75, 55.17, 52.64.**HRMS (ESI)** m/z calcd. for $C_{20}H_{20}O_6$ ([M + H]+): 357.1338, found: 357.1345

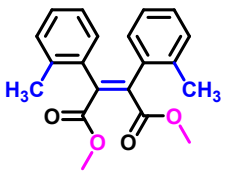

dimethyl 2,3-di-o-tolylmaleate (3g)

Purification by column chromatography (mobile phase: EtOAc/Hexane 1:20), (65.8mg, 81% yield) as a white solid.**^{1}H NMR (500 MHz, $CDCl_3$)** δ 7.10 – 7.02 (m, 4H), 6.98 – 6.93 (m, 4H), 3.80 (s, 6H), 2.22 (s, 6H).**^{13}C NMR (125 MHz, $CDCl_3$)** δ 168.25, 140.17, 136.37, 134.24, 130.22, 129.59, 128.49, 125.50, 52.77, 19.89.**HRMS (ESI)** m/z calcd. for $C_{20}H_{20}O_4$ ([M + H]+): 325.1440, found: 325.1440.

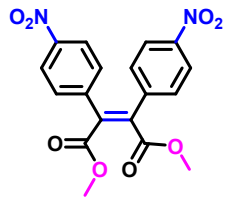

dimethyl 2,3-bis(4-nitrophenyl)maleate (3h)

Purification by column chromatography (mobile phase: EtOAc/Hexane 1:15), (76.3mg, 79% yield) as a white solid.**^{1}H NMR (500 MHz, $CDCl_3$)** δ 8.23 (d, *J* = 9.3 Hz, 4H), 7.67 (d, *J* = 9.3 Hz, 4H), 3.91 (s, 6H).**^{13}C NMR (125 MHz, $CDCl_3$)** δ 164.28, 145.25, 133.97, 124.47, 123.31, 52.57.**HRMS (ESI)** m/z calcd. for $C_{18}H_{14}N_2O_8$ ([M + H]+): 387.0828, found:387.0837

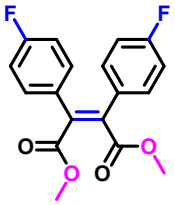

dimethyl 2,3-bis(4-fluorophenyl)maleate (3i)

Purification by column chromatography (mobile phase: EtOAc/Hexane 1:20), (69mg, 83% yield) as a white solid.**^{1}H NMR (500 MHz, $CDCl_3$)** δ 7.06 (dd, *J* = 9.0, 5.3 Hz, 4H), 6.89 (t, *J* = 8.8 Hz, 4H), 3.83 (s, 6H).**^{13}C NMR (125 MHz, $CDCl_3$)** δ 168.13, 163.66 (d, C–F), 161.68, 138.11, 131.71 (d, $^{3}J_{C–F}$ = 8.5 Hz),130.25 (d, $^{3}J_{C–F}$ = 4.0 Hz), 115.72, 52.95. **HRMS (ESI)** m/z calcd. for $C_{18}H_{14}F_2O_4$([M + H]+): 333.0938, found: 333.0940.

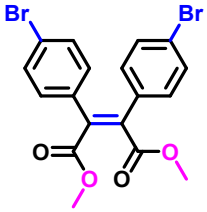

dimethyl 2,3-bis(4-bromophenyl)maleate (3j)

Purification by column chromatography (mobile phase: EtOAc/Hexane 1:20), (96.5mg, 85% yield) as a white solid.**^{1}H NMR (400 MHz, $CDCl_3$)** δ 7.28 (s, 4H), 6.89 (d, *J* = 8.6 Hz, 4H), 3.74 (s, 6H).**^{13}C NMR (100 MHz, $CDCl_3$)** δ 167.70, 133.98, 131.77, 129.65, 123.41, 52.56.**HRMS (ESI)** m/z calcd. for $C_{18}H_{14}Br_2O_4$ ([M + H]+): 453.9238, found: 453.9243.

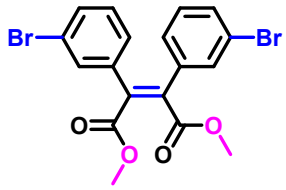

dimethyl 2,3-bis(3-bromophenyl)maleate(3k)

Purification by column chromatography (mobile phase: EtOAc/Hexane 1:20), (93.1.5mg, 82% yield) as a white solid.**^{1}H NMR (500 MHz, $CDCl_3$)** δ 7.58 (t, *J* = 1.7 Hz, 2H), 7.53 (ddd, *J* = 8.0, 2.0, 1.1 Hz, 2H), 7.34 (ddd, *J* = 7.7, 1.7, 1.1 Hz, 2H), 7.28 (d, *J* = 7.9 Hz, 2H), 3.59 (s, 6H).**^{13}C NMR (126 MHz, $CDCl_3$)** δ 167.35, 138.18, 135.82, 132.28, 131.74, 129.80, 128.28, 122.28, 52.97.

HRMS (ESI) m/z calcd. for $C_{20}H_{18}Br_2O_4$ ([M + H]+): 482.9630, found: 482.9634.

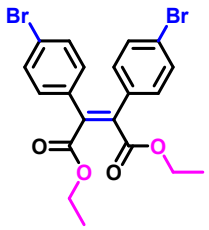

diethyl 2,3-bis(4-bromophenyl)maleate (3l)

Purification by column chromatography (mobile phase: EtOAc/Hexane 1:20), (102.5mg, 85% yield) as a white solid.**^{1}H NMR (400 MHz, $CDCl_3$)** δ 7.49 (d, *J* = 8.4 Hz, 1H), 7.28 (s, 1H), 4.00 (q, *J* = 7.1 Hz, 1H), 0.97 (t, *J* = 7.1 Hz, 2H).**^{13}C NMR (100 MHz, $CDCl_3$)** δ 167.40, 137.26, 134.31, 131.73, 129.95, 123.33, 61.82, 13.80.**HRMS (ESI)** m/z calcd. for $C_{20}H_{18}Br_2O_4$ ([M + H]+): 482.9630, found: 482.9634.

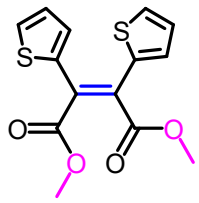

dimethyl 2,3-di(thiophen-2-yl)maleate (3p)

Purification by column chromatography (mobile phase: EtOAc/Hexane 1:20), (35.5mg, 43% yield) as a white solid.

^{1}H NMR (500 MHz, $CDCl_3$) δ 7.21 – 7.16 (m, 4H), 6.71 (dd, *J* = 4.9, 1.3 Hz, 2H), 3.84 (s, 6H).**^{13}C NMR (125 MHz, $CDCl_3$)** δ 168.04, 134.46, 132.73, 128.29, 126.86, 125.49, 52.74.

HRMS (ESI) m/z calcd. for $C_{14}H_{12}O_4S_2$ ([M + H]+): 309.0255, found: 309.0265

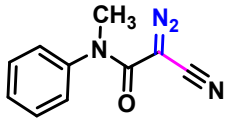

2-cyano-2-diazo-N-methyl-N-phenylacetamide (1o)

Purification by column chromatography (mobile phase: EtOAc/Hexane 2:10), **^{1}H NMR (500 MHz, $CDCl_3$)** δ 7.48 – 7.44 (m, 3H), 7.29 – 7.25 (m, 2H), 3.38 (s, 3H).**^{13}C NMR (126 MHz, $CDCl_3$)** δ 159.33, 141.30, 130.19, 129.59, 127.81, 107.28, 39.17.

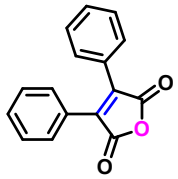

3,4-diphenylfuran-2,5-dione(4a)

Purification by column chromatography (mobile phase: EtOAc/Hexane 2:10), (67.5mg, 90% yield) as a pale yellow solid.**^{1}H NMR (500 MHz, $CDCl_3$)** δ 7.54 (dd, *J* = 8.4, 1.4 Hz, 4H), 7.49 – 7.45 (m, 2H), 7.43 – 7.38 (m, 4H).**^{13}C NMR (125 MHz, $CDCl_3$)** δ 164.95, 138.31, 131.28, 129.83, 129.07, 127.32.**HRMS (ESI)** m/z calcd. for $C_{16}H_{10}O_3$ ([M + H]+): 251.0708, found: 251.072.

Spectral data of NMR Analysis:

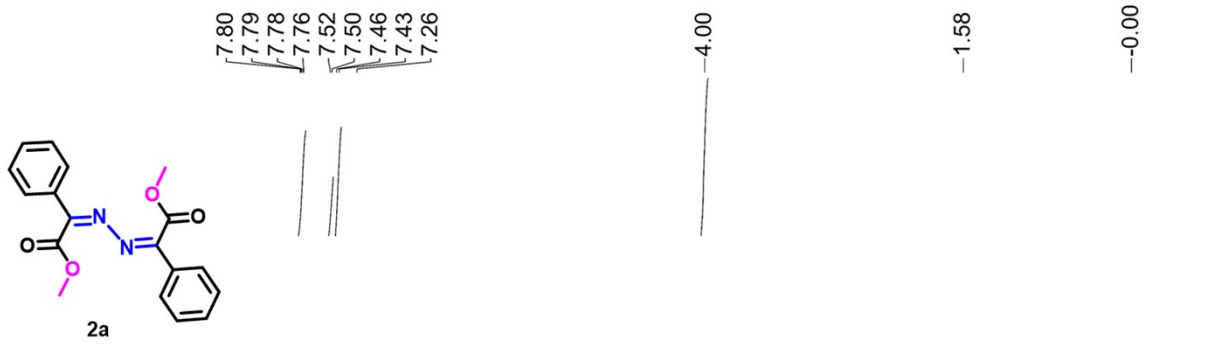

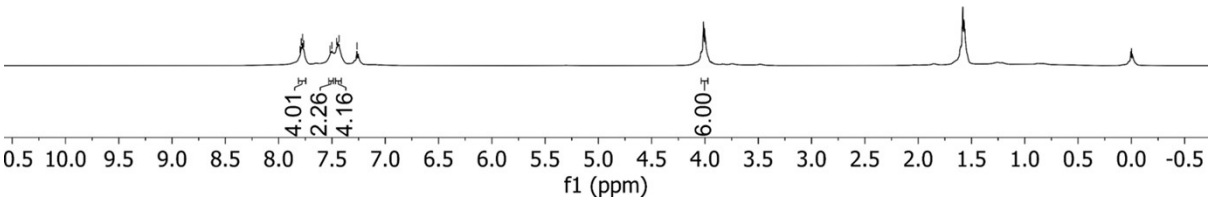

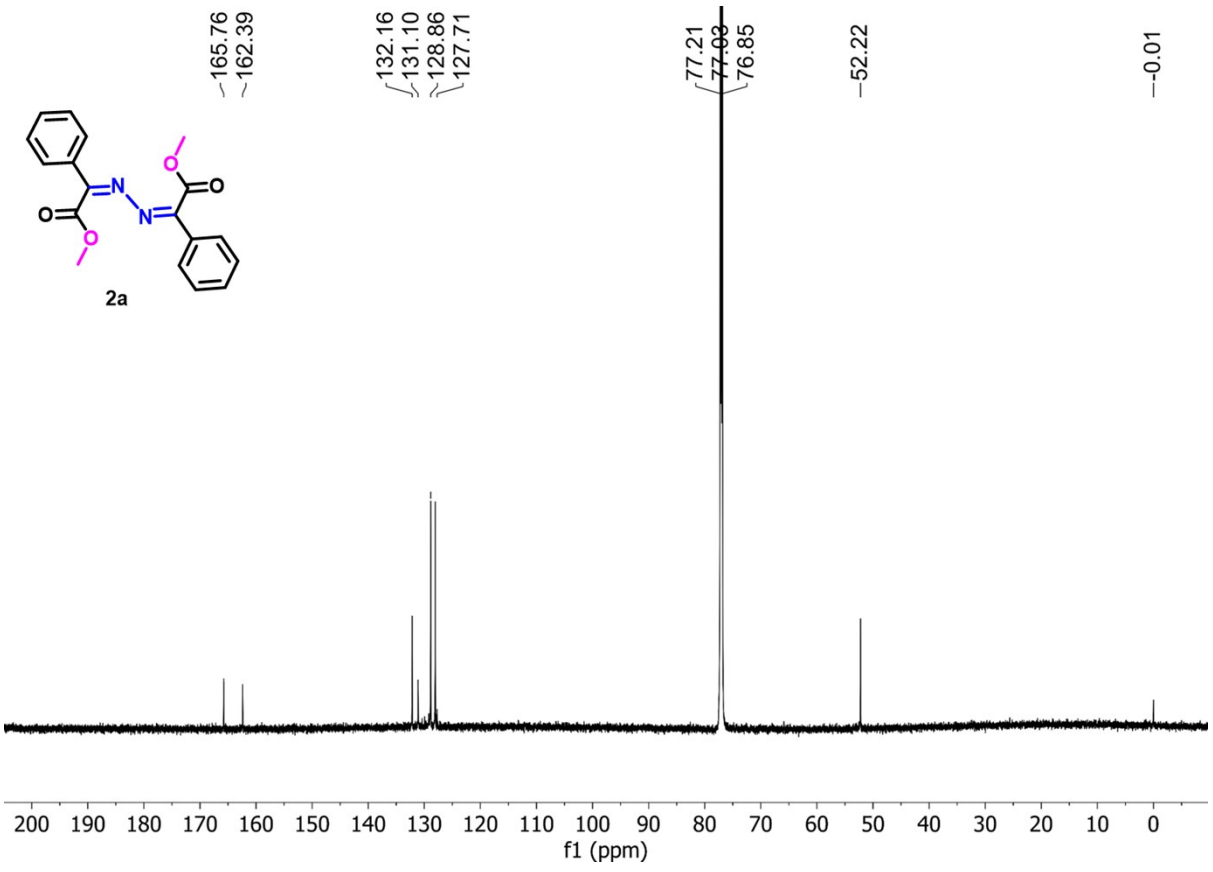

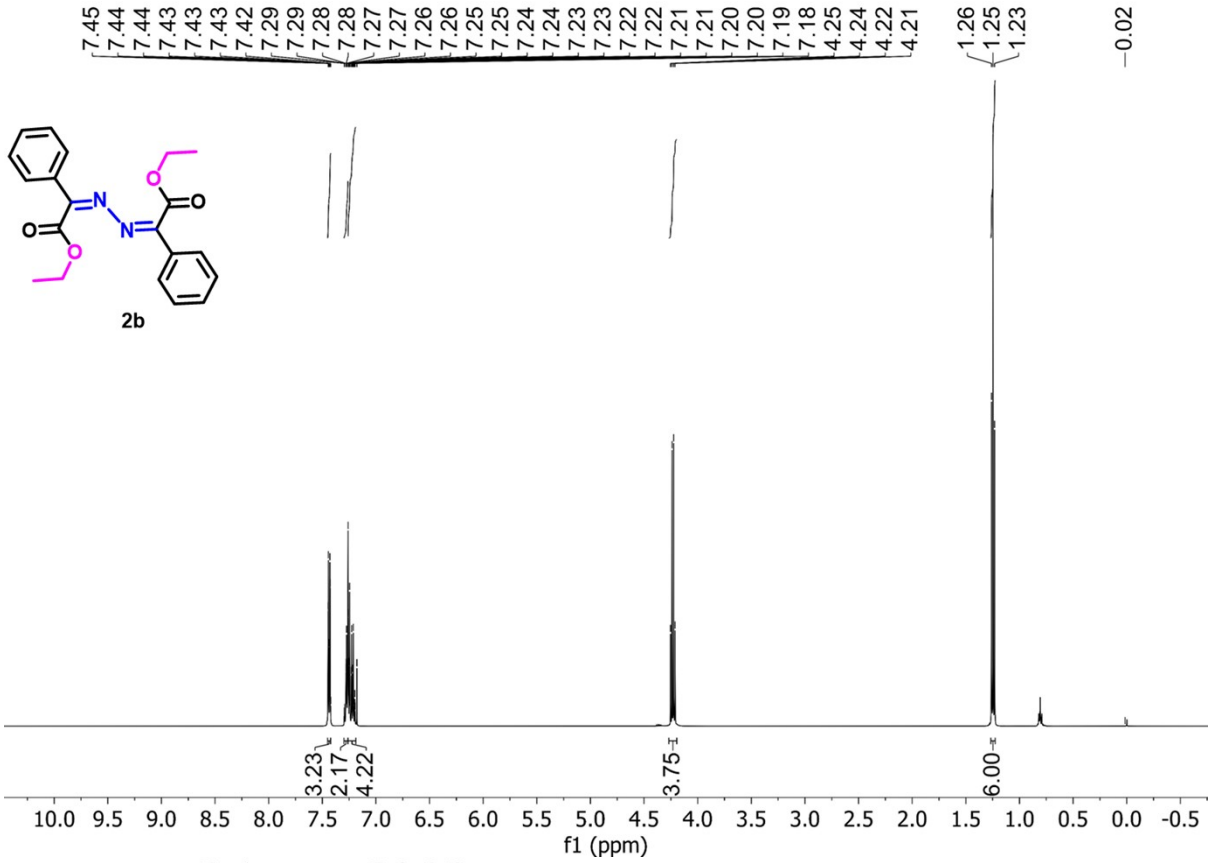
7.45 7.44 7.44 7.43 7.43 7.43 7.42 7.29 7.29 7.28 7.28 7.27 7.27 7.26 7.26 7.25 7.25 7.24 7.24 7.23 7.23 7.22 7.22 7.21 7.21 7.20 7.20 7.19 7.18 4.25 4.24 4.22 4.21
1.26 1.25 1.23
-0.02
2b
3.23 2.17 4.22 3.75 6.00
10.0 9.5 9.0 8.5 8.0 7.5 7.0 6.5 6.0 5.5 5.0 4.5 4.0 3.5 3.0 2.5 2.0 1.5 1.0 0.5 0.0 -0.5
f1 (ppm)

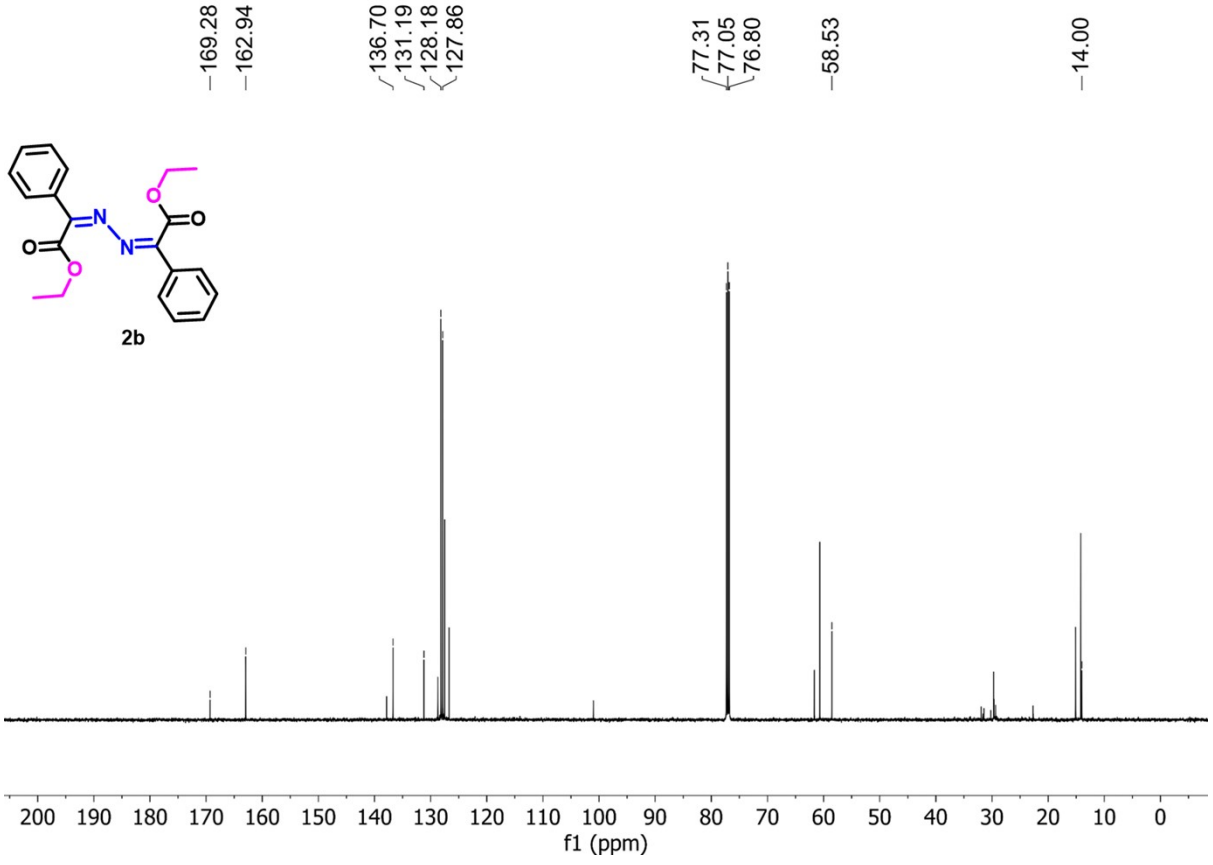
169.28 162.94 136.70 131.19 128.18 127.86 77.31 77.05 76.80 58.53 14.00
2b
200 190 180 170 160 150 140 130 120 110 100 90 80 70 60 50 40 30 20 10 0
f1 (ppm)

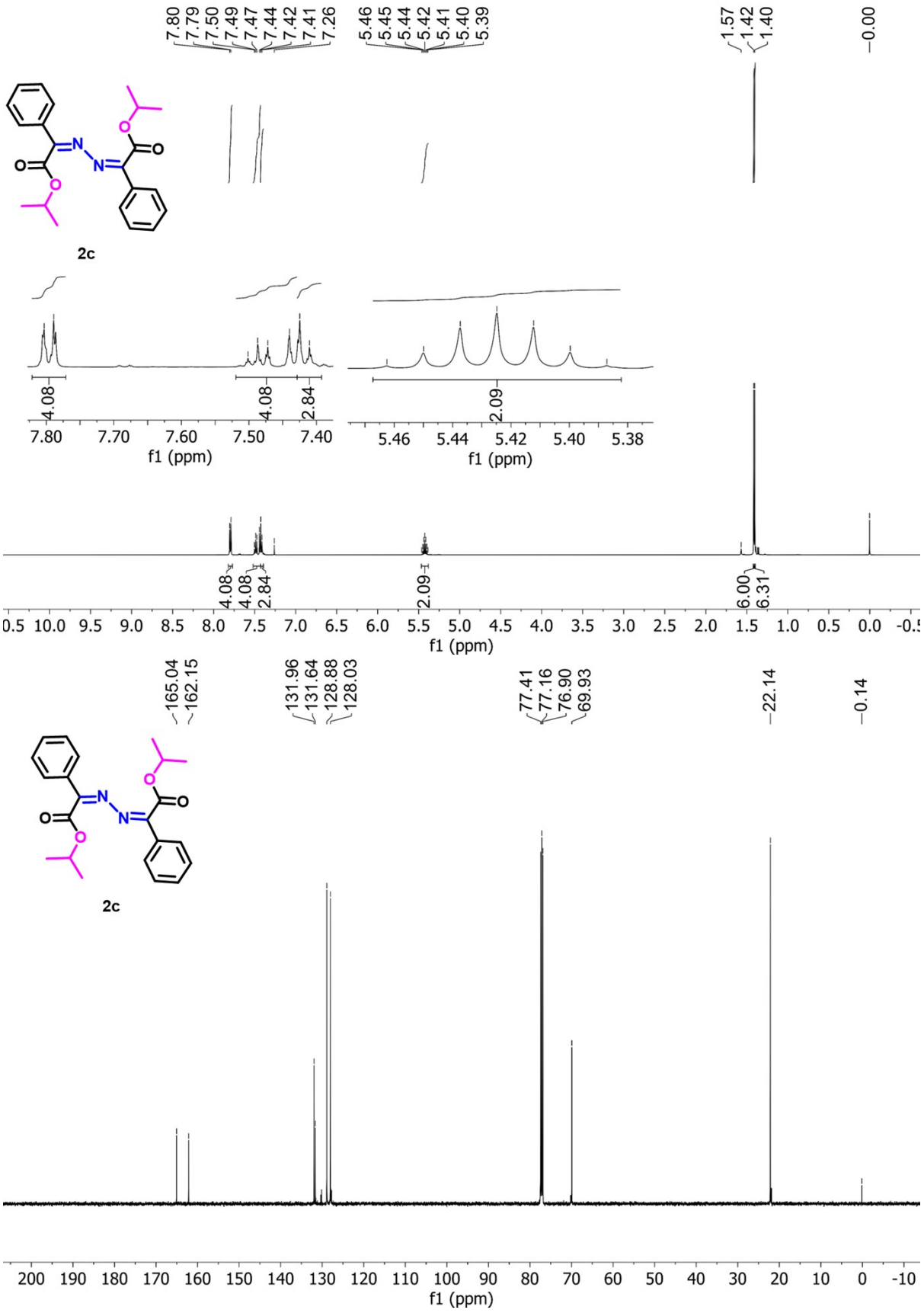
7.80
7.79
7.50
7.49
7.47
7.44
7.42
7.41
7.26
5.46
5.45
5.44
5.42
5.41
5.40
5.39
1.57
1.42
1.40
0.00
2c
4.08
4.08
2.84
2.09
f1 (ppm)
6.00
6.31
165.04
162.15
131.96
131.64
128.88
128.03
77.41
77.16
76.90
69.93
22.14
0.14

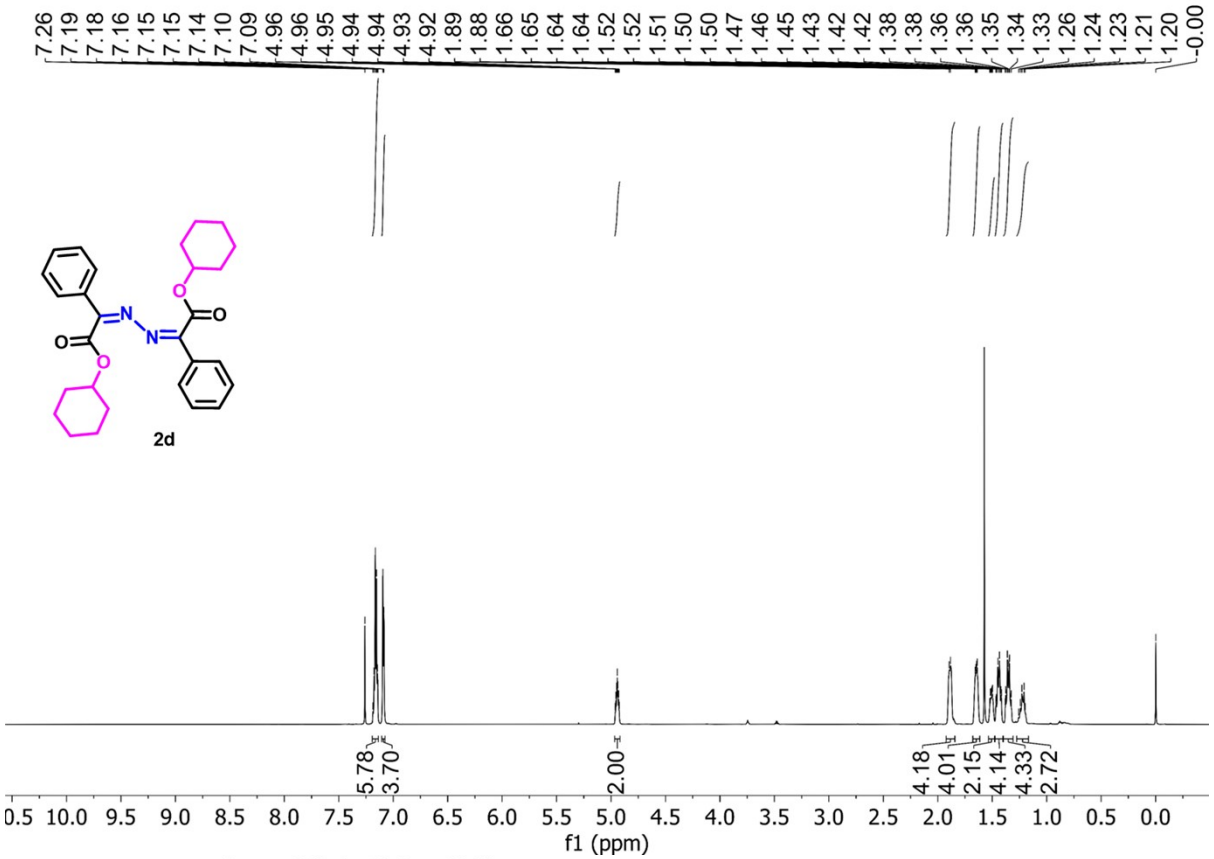
7.26
7.19
7.18
7.16
7.15
7.15
7.14
7.10
7.09
4.96
4.96
4.95
4.94
4.94
4.93
4.92
1.89
1.88
1.66
1.65
1.64
1.64
1.52
1.51
1.50
1.50
1.47
1.46
1.45
1.43
1.42
1.42
1.38
1.38
1.36
1.36
1.35
1.34
1.33
1.26
1.24
1.23
1.21
1.20
-0.00
2d
5.78
3.70
2.00
4.18
4.01
2.15
4.14
4.33
2.72
f1 (ppm)

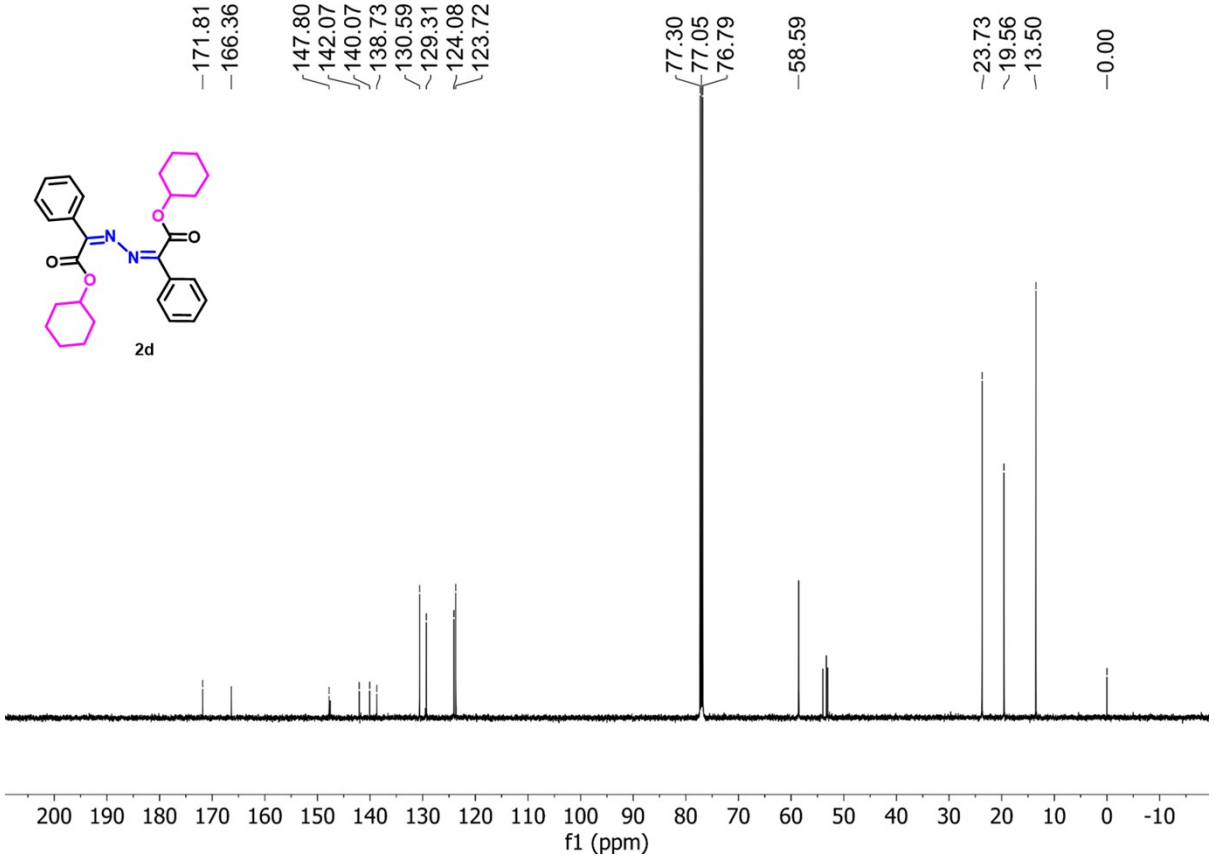
171.81
166.36
147.80
142.07
140.07
138.73
130.59
129.31
124.08
123.72
77.30
77.05
76.79
58.59
23.73
19.56
13.50
0.00
2d
f1 (ppm)

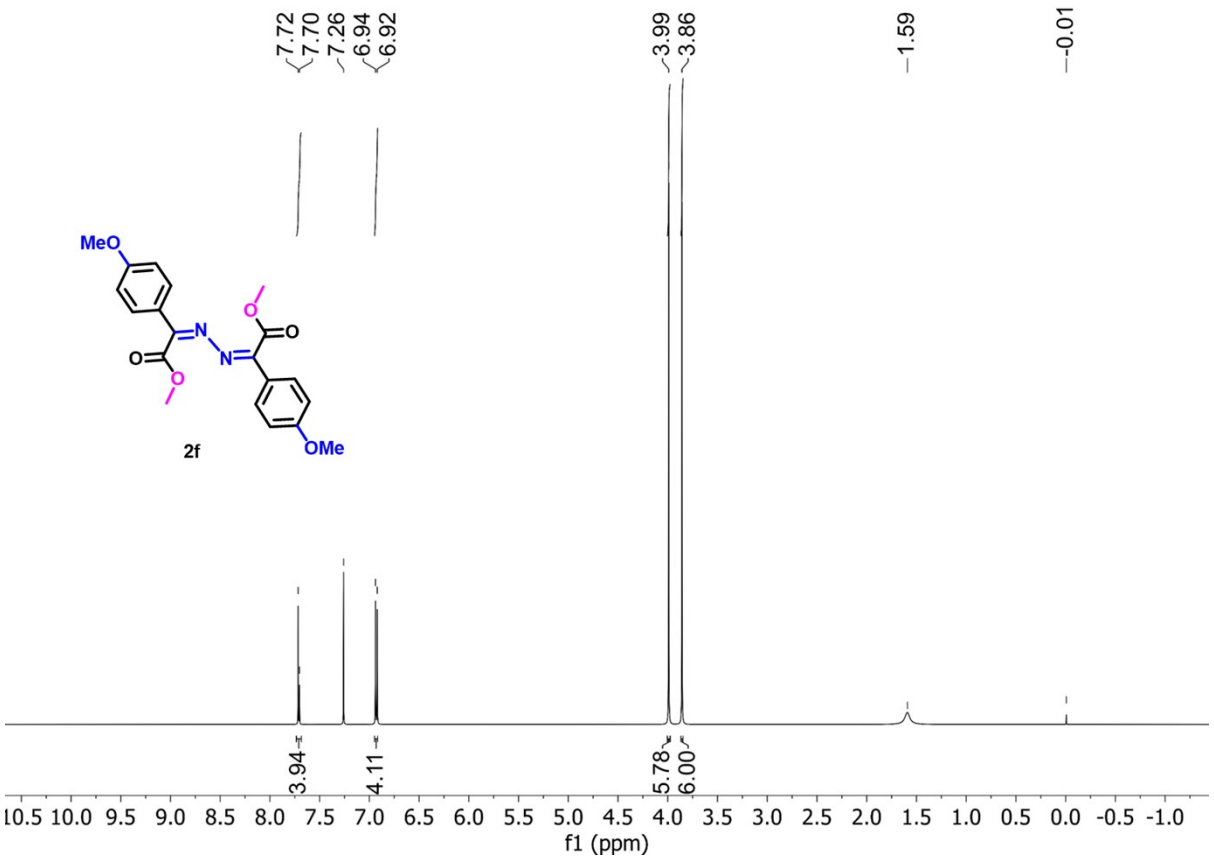
7.72
7.70
7.26
6.94
6.92
3.99
3.86
1.59
-0.01
MeO
OMe
2f
3.94
4.11
5.78
6.00
f1 (ppm)

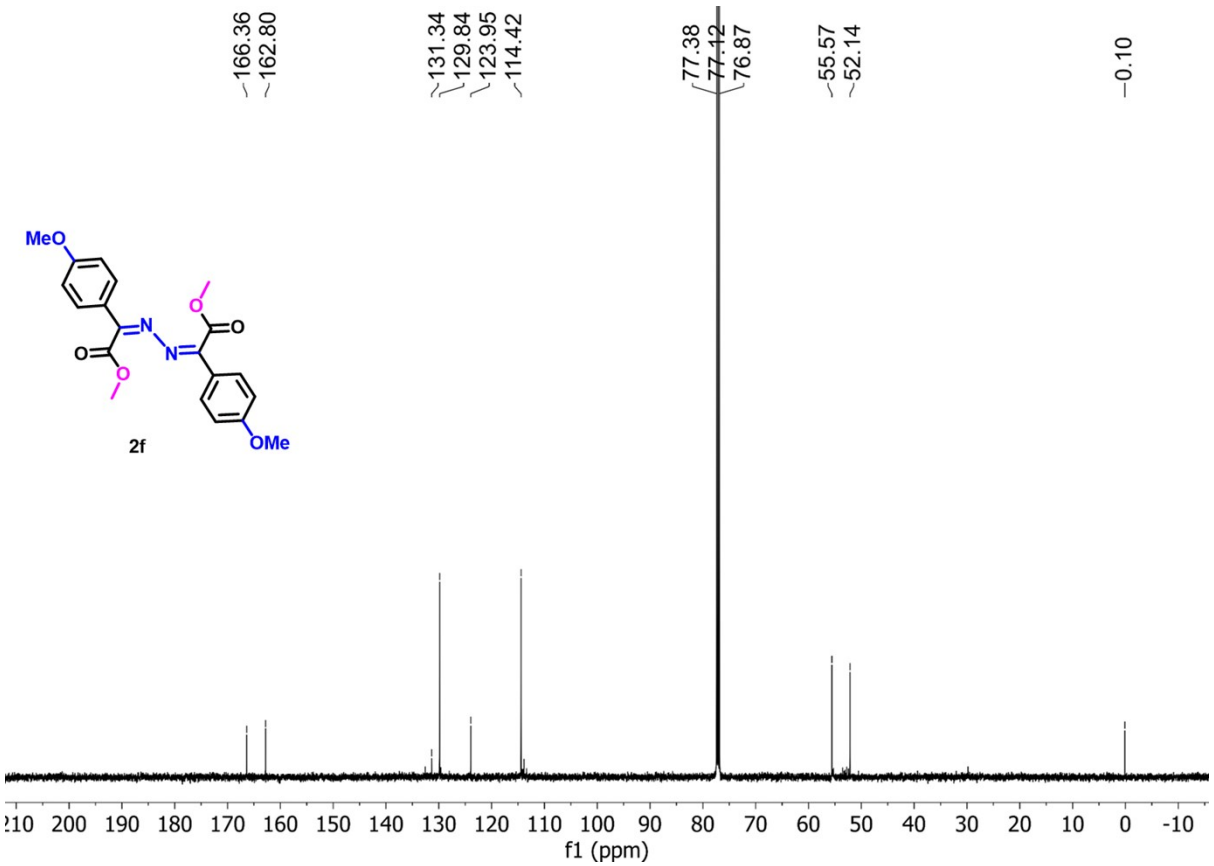
166.36
162.80
131.34
129.84
123.95
114.42
77.38
77.12
76.87
55.57
52.14
-0.10
MeO
OMe
2f
f1 (ppm)

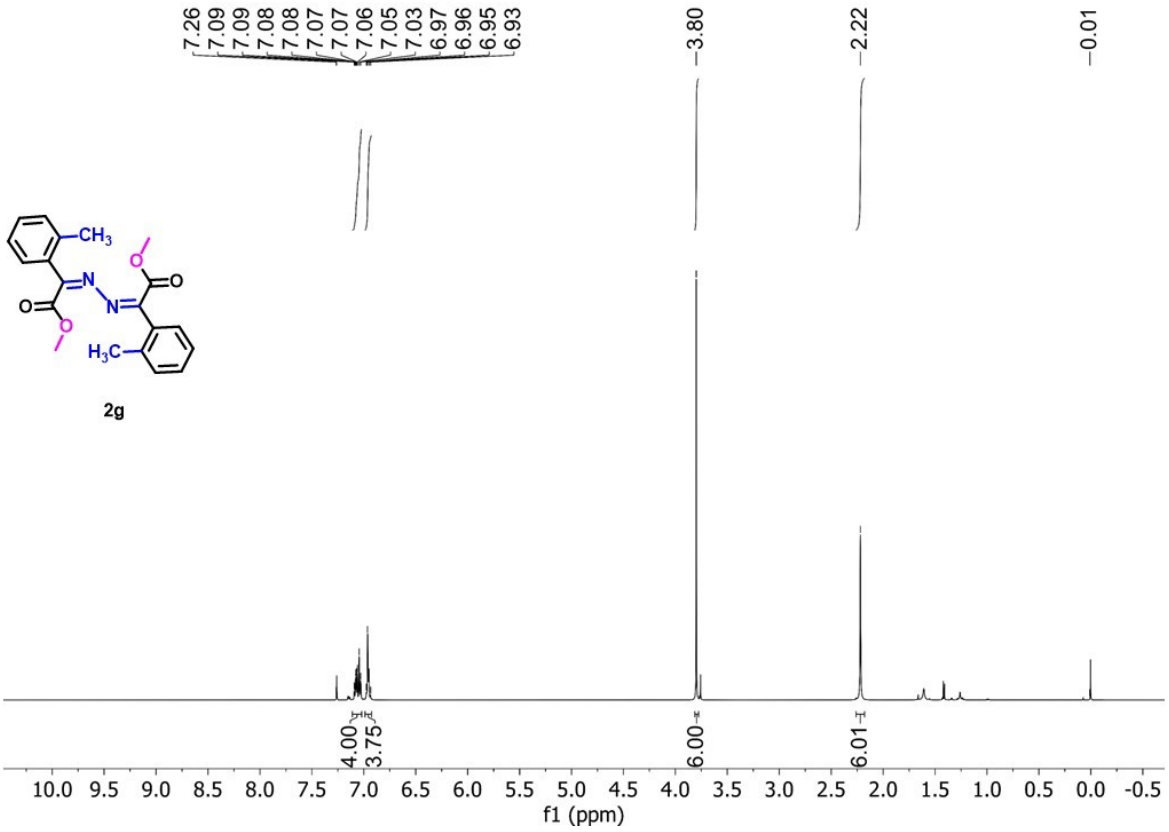
7.26
7.09
7.09
7.08
7.08
7.07
7.07
7.06
7.05
7.03
6.97
6.96
6.95
6.93
3.80
2.22
0.01
CH3
O
O
N
N
O
O
H3C
2g
4.00
3.75
6.00
6.01
10.0 9.5 9.0 8.5 8.0 7.5 7.0 6.5 6.0 5.5 5.0 4.5 4.0 3.5 3.0 2.5 2.0 1.5 1.0 0.5 0.0 -0.5
f1 (ppm)

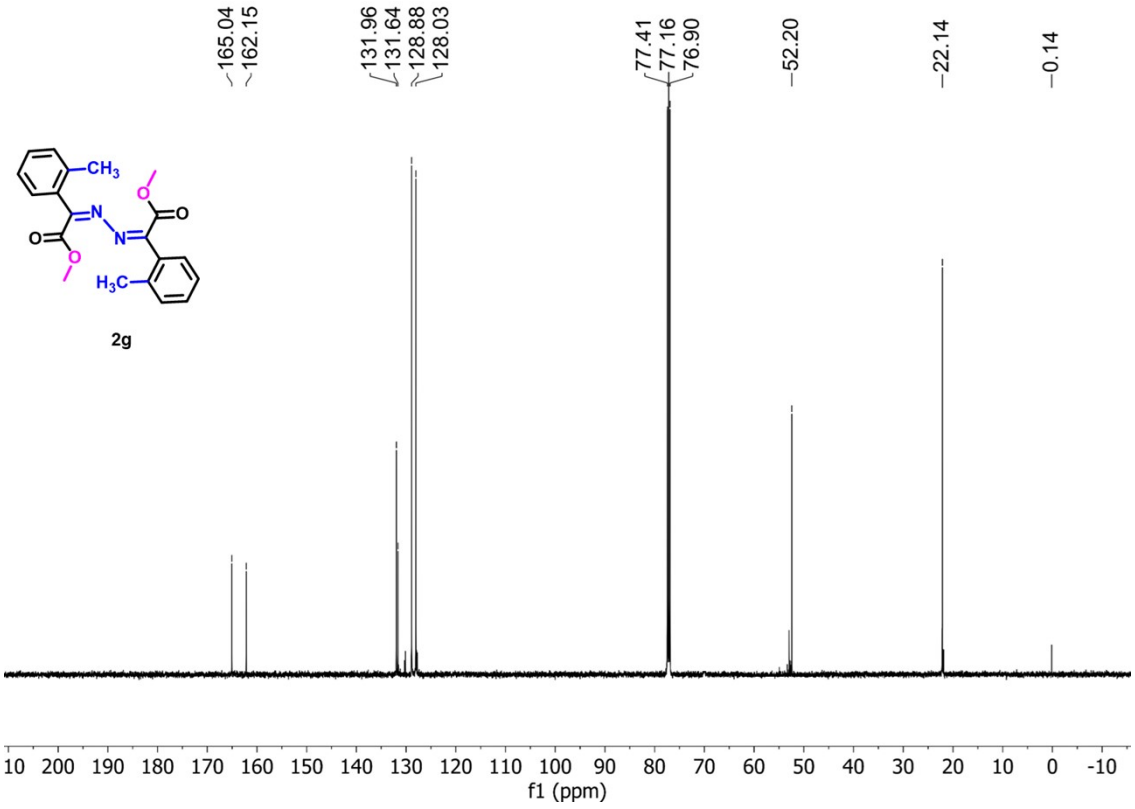
165.04
162.15
131.96
131.64
128.88
128.03
77.41
77.16
76.90
52.20
22.14
0.14
CH3
O
O
N
N
O
O
H3C
2g
10 200 190 180 170 160 150 140 130 120 110 100 90 80 70 60 50 40 30 20 10 0 -10
f1 (ppm)

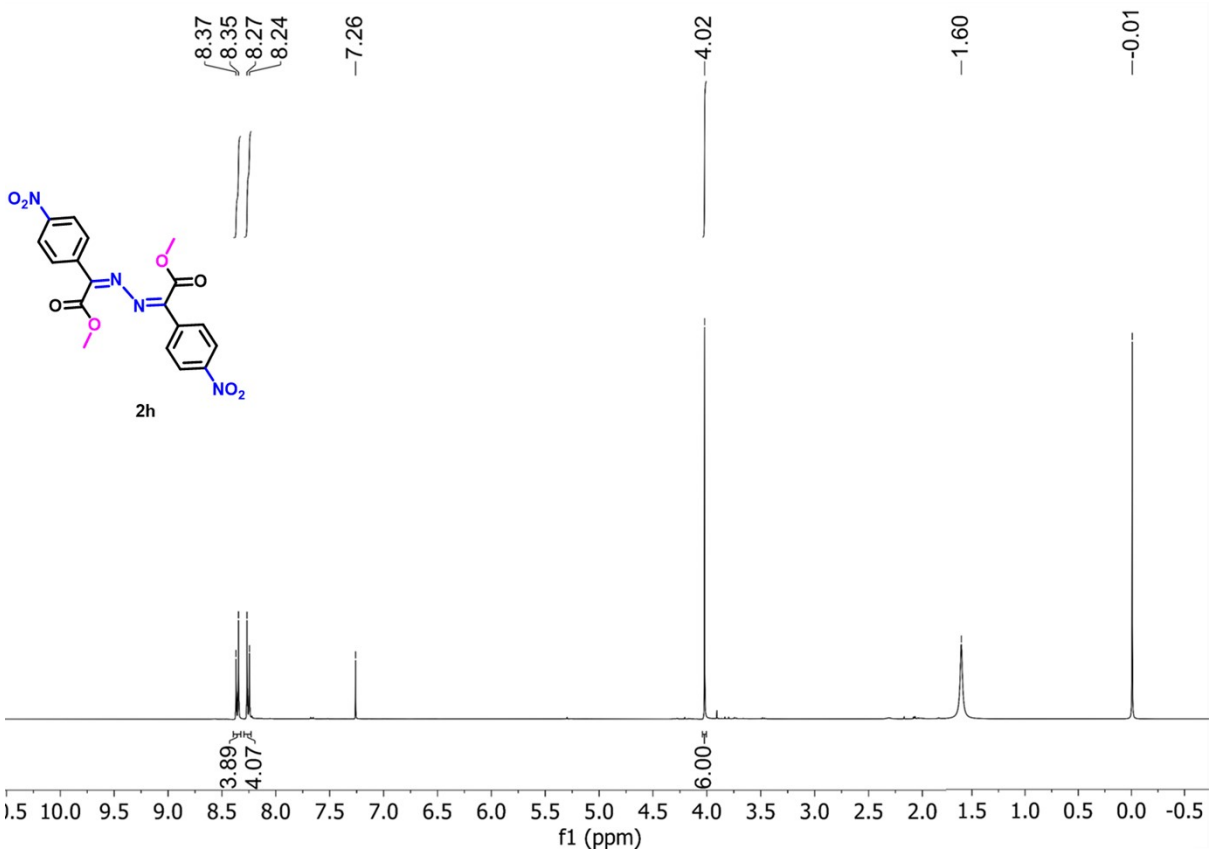
8.37
8.35
8.27
8.24
7.26
4.02
1.60
0.01
2h
3.89
4.07
6.00
f1 (ppm)

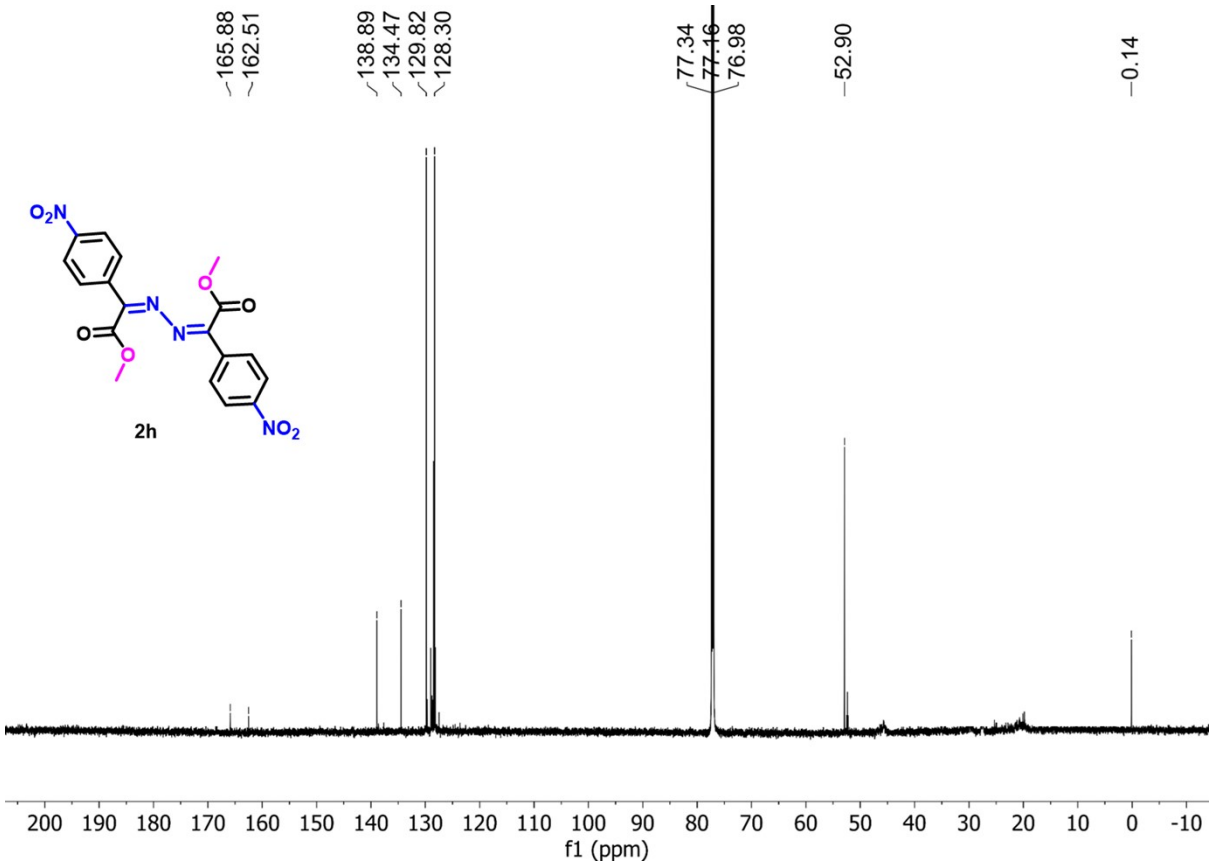
165.88
162.51
138.89
134.47
129.82
128.30
77.34
77.16
76.98
52.90
0.14
2h
f1 (ppm)

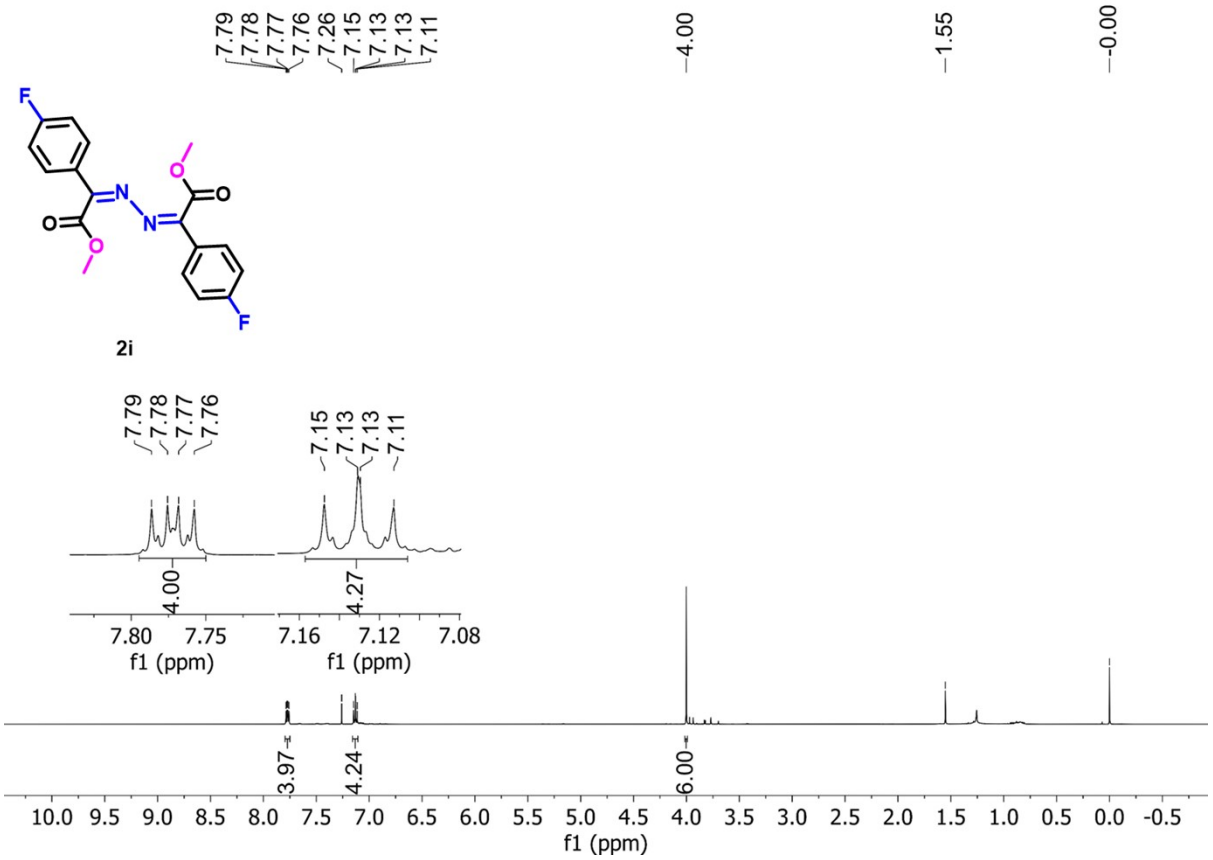
7.79
7.78
7.77
7.76
7.26
7.15
7.13
7.13
7.11
4.00
1.55
0.00
F
O
N
N
O
O
O
F
2i
7.79
7.78
7.77
7.76
7.15
7.13
7.13
7.11
4.00
4.27
7.80
7.75
f1 (ppm)
7.16
7.12
7.08
f1 (ppm)
3.97
4.24
6.00
10.0 9.5 9.0 8.5 8.0 7.5 7.0 6.5 6.0 5.5 5.0 4.5 4.0 3.5 3.0 2.5 2.0 1.5 1.0 0.5 0.0 -0.5
f1 (ppm)

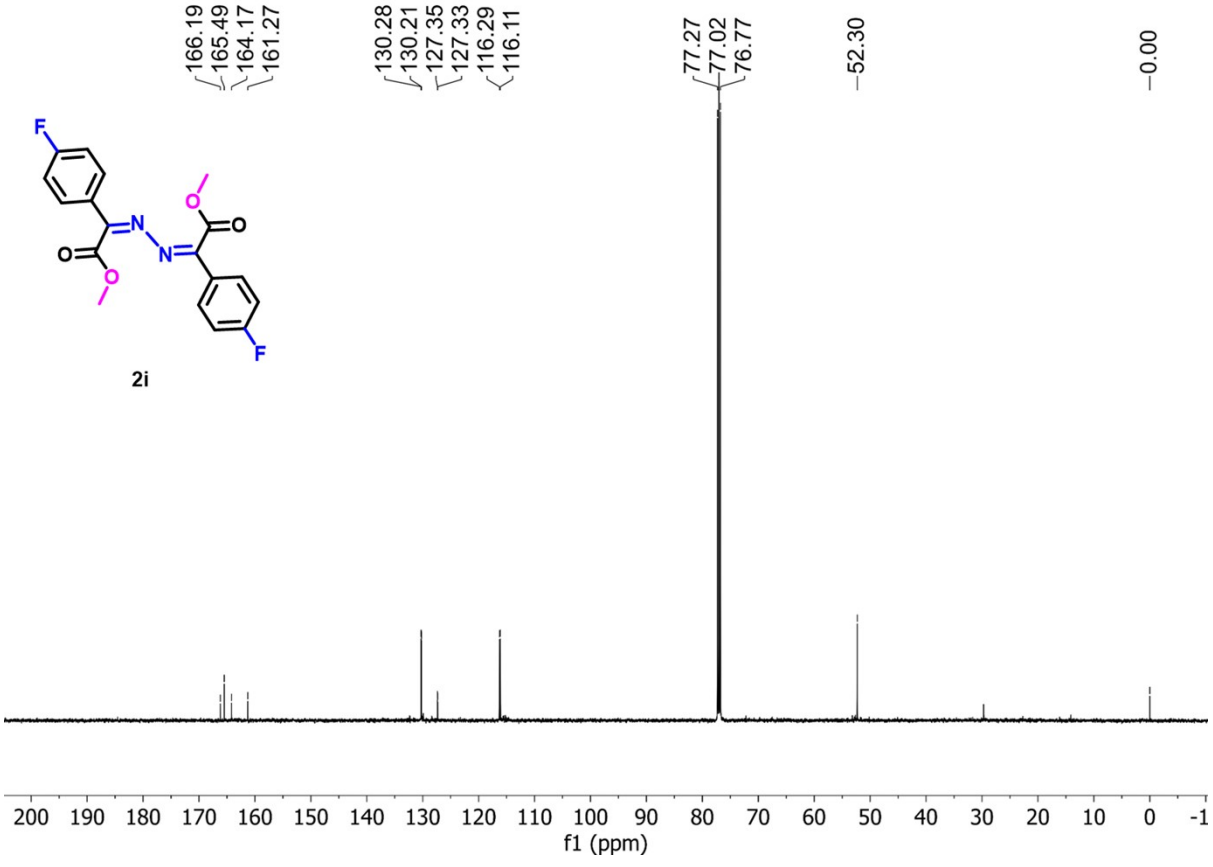
166.19
165.49
164.17
161.27
130.28
130.21
127.35
127.33
116.29
116.11
77.27
77.02
76.77
52.30
0.00
F
O
N
N
O
O
O
F
2i
200 190 180 170 160 150 140 130 120 110 100 90 80 70 60 50 40 30 20 10 0 -1
f1 (ppm)

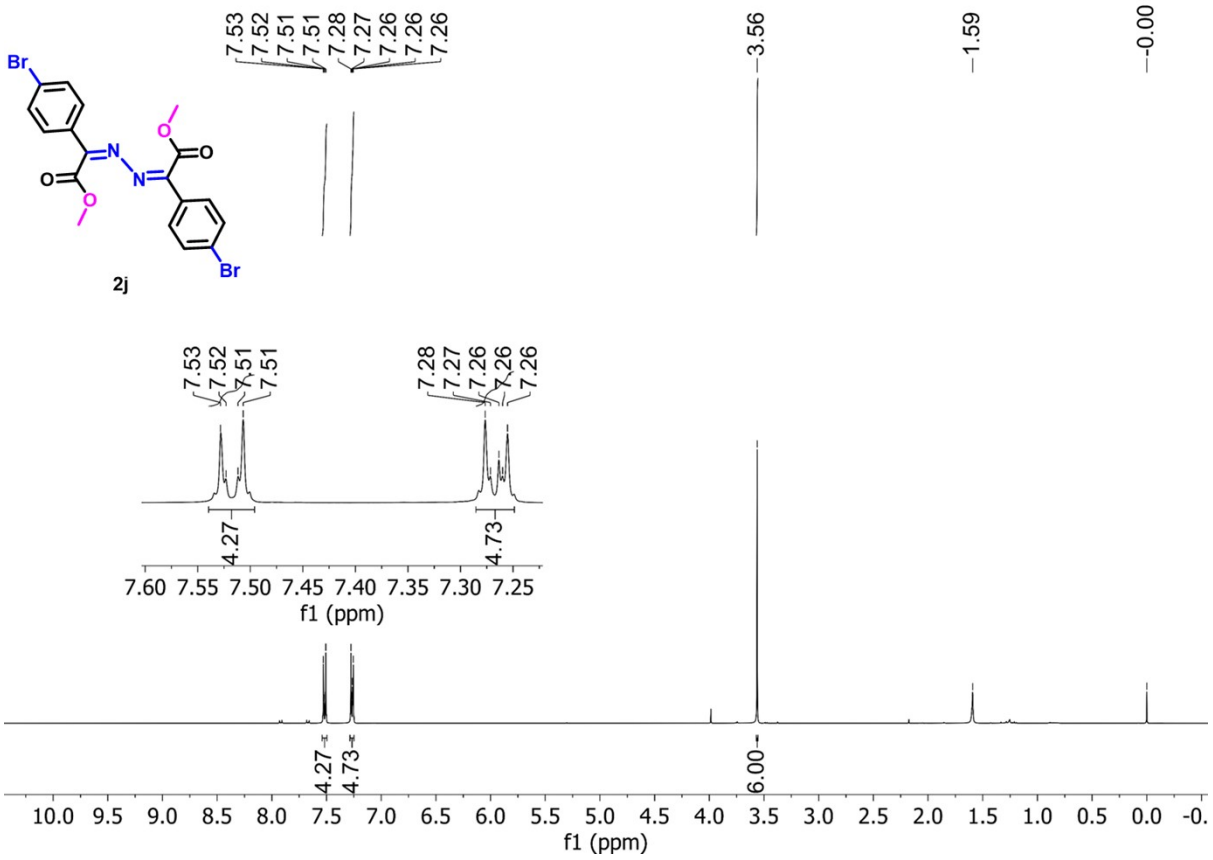
7.53
7.52
7.51
7.51
7.28
7.27
7.26
7.26
7.26
3.56
1.59
0.00
Br
O
O
N
N
O
O
Br
2j
4.27
4.73
7.60 7.55 7.50 7.45 7.40 7.35 7.30 7.25
f1 (ppm)
4.27
4.73
6.00
10.0 9.5 9.0 8.5 8.0 7.5 7.0 6.5 6.0 5.5 5.0 4.5 4.0 3.5 3.0 2.5 2.0 1.5 1.0 0.5 0.0 -0.
f1 (ppm)

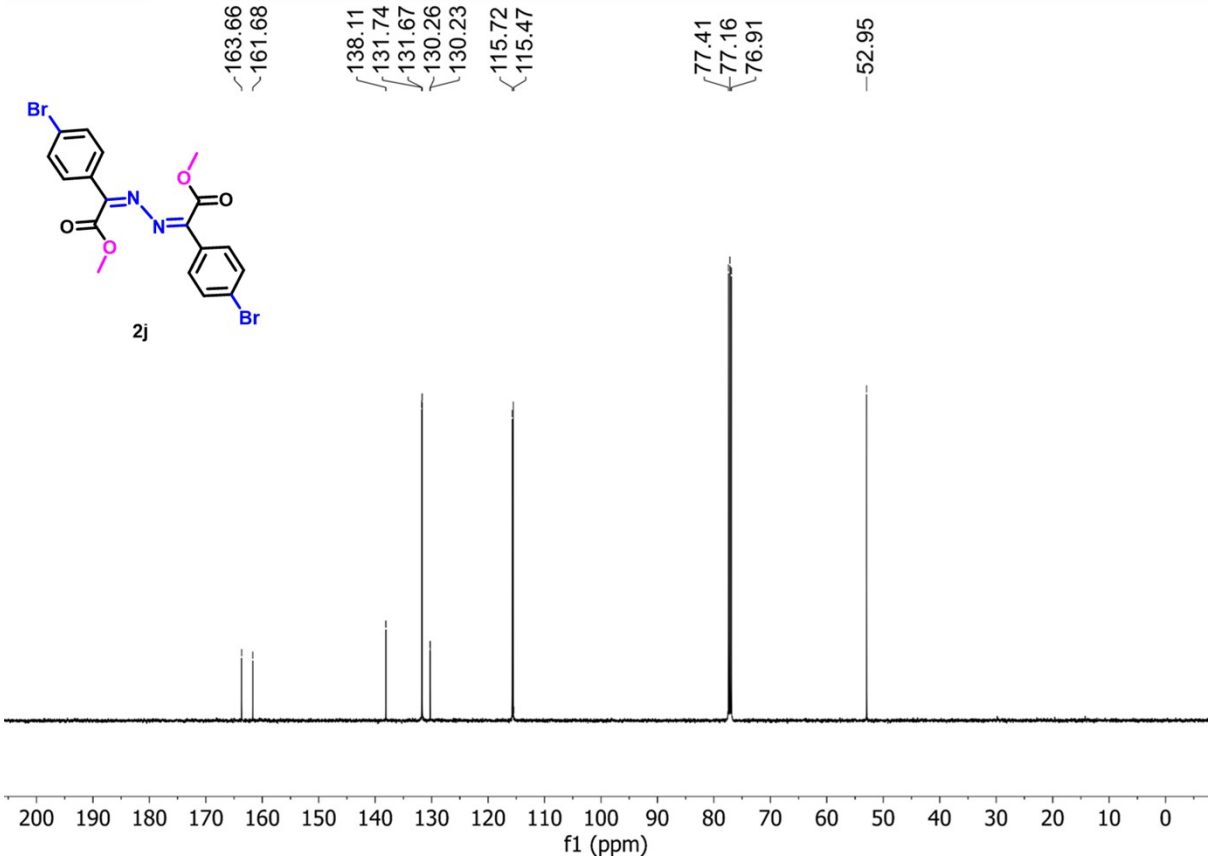
163.66
161.68
138.11
131.74
131.67
130.26
130.23
115.72
115.47
77.41
77.16
76.91
52.95
Br
O
O
N
N
O
O
Br
2j
200 190 180 170 160 150 140 130 120 110 100 90 80 70 60 50 40 30 20 10 0
f1 (ppm)

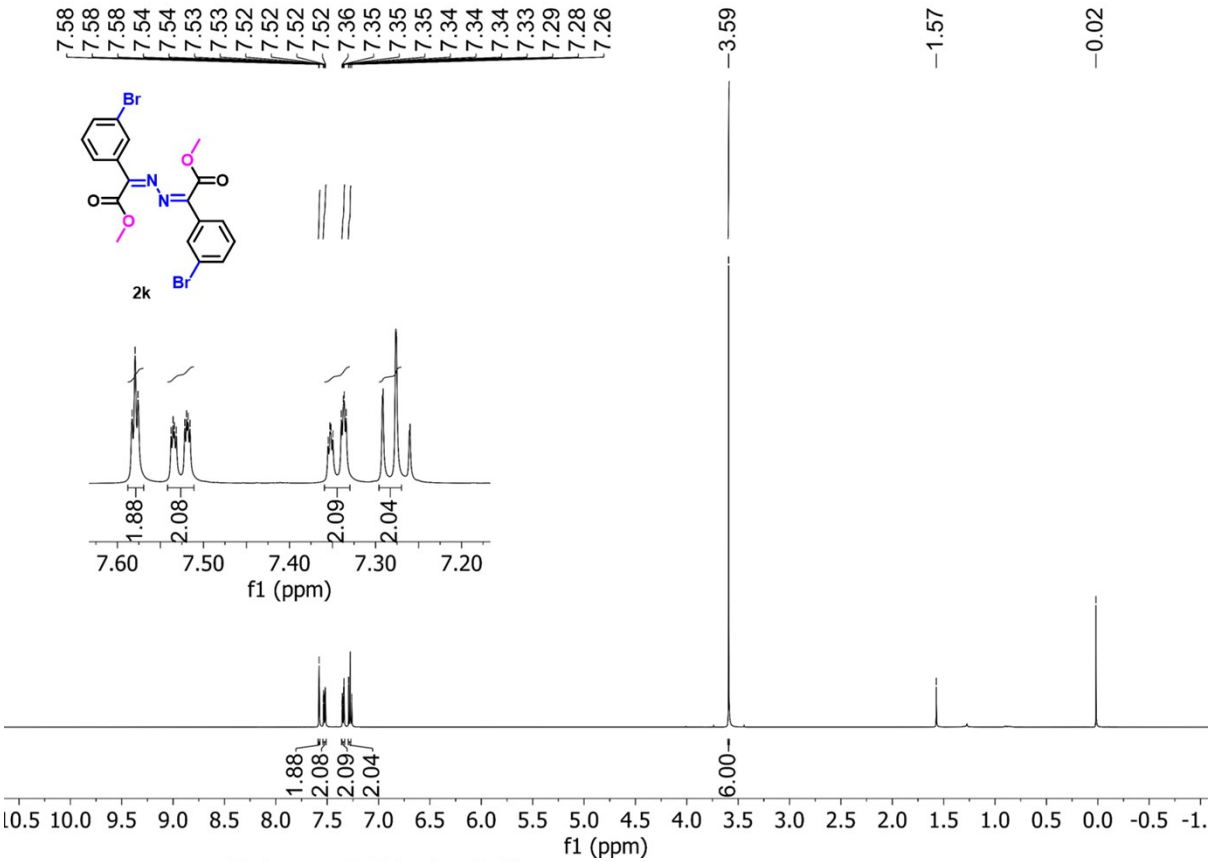
7.58
7.58
7.58
7.54
7.54
7.53
7.53
7.52
7.52
7.52
7.52
7.36
7.35
7.35
7.35
7.34
7.34
7.34
7.33
7.29
7.28
7.26
3.59
1.57
0.02
Br
O
O
N
N
O
O
Br
2k
1.88
2.08
2.09
2.04
7.60
7.50
7.40
7.30
7.20
f1 (ppm)
1.88
2.08
2.09
2.04
6.00
10.5 10.0 9.5 9.0 8.5 8.0 7.5 7.0 6.5 6.0 5.5 5.0 4.5 4.0 3.5 3.0 2.5 2.0 1.5 1.0 0.5 0.0 -0.5 -1.
f1 (ppm)

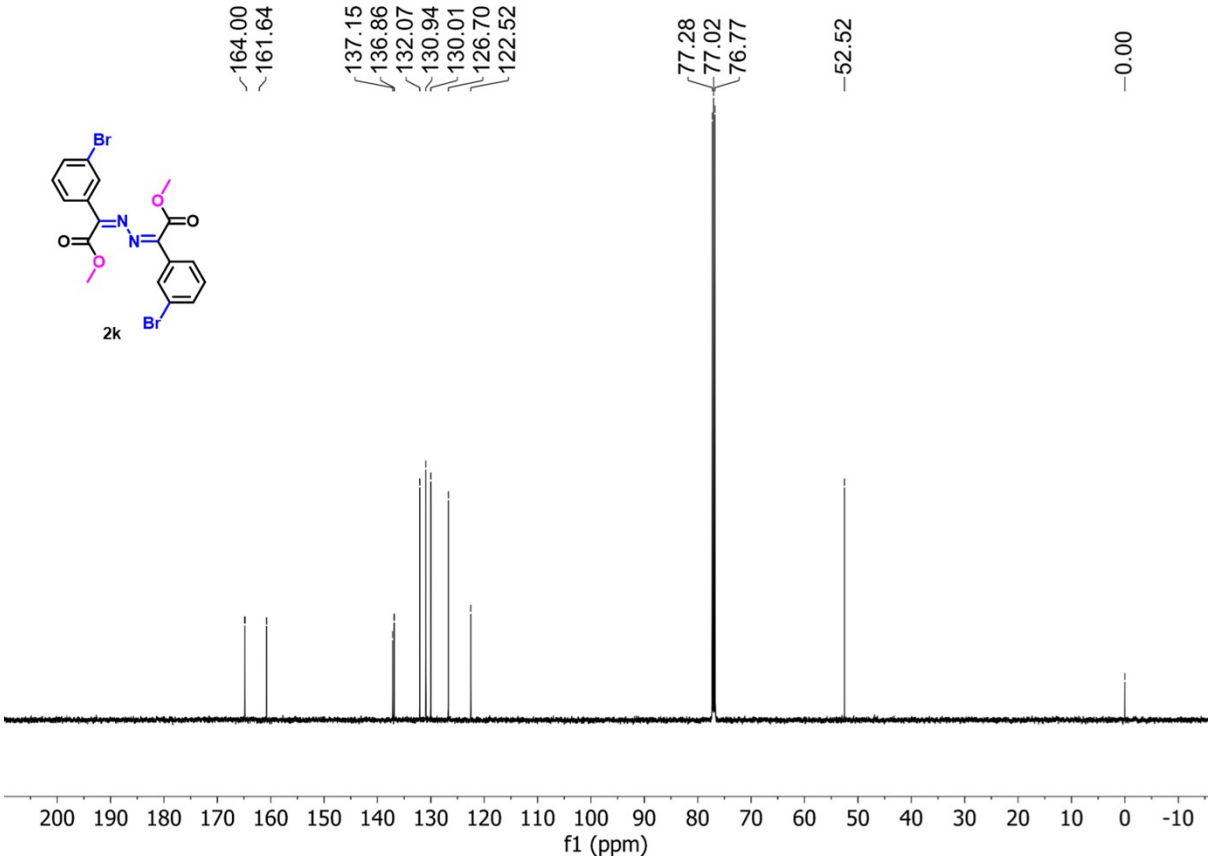
164.00
161.64
137.15
136.86
132.07
130.94
130.01
126.70
122.52
77.28
77.02
76.77
52.52
0.00
Br
O
O
N
N
O
O
Br
2k
200 190 180 170 160 150 140 130 120 110 100 90 80 70 60 50 40 30 20 10 0 -10
f1 (ppm)

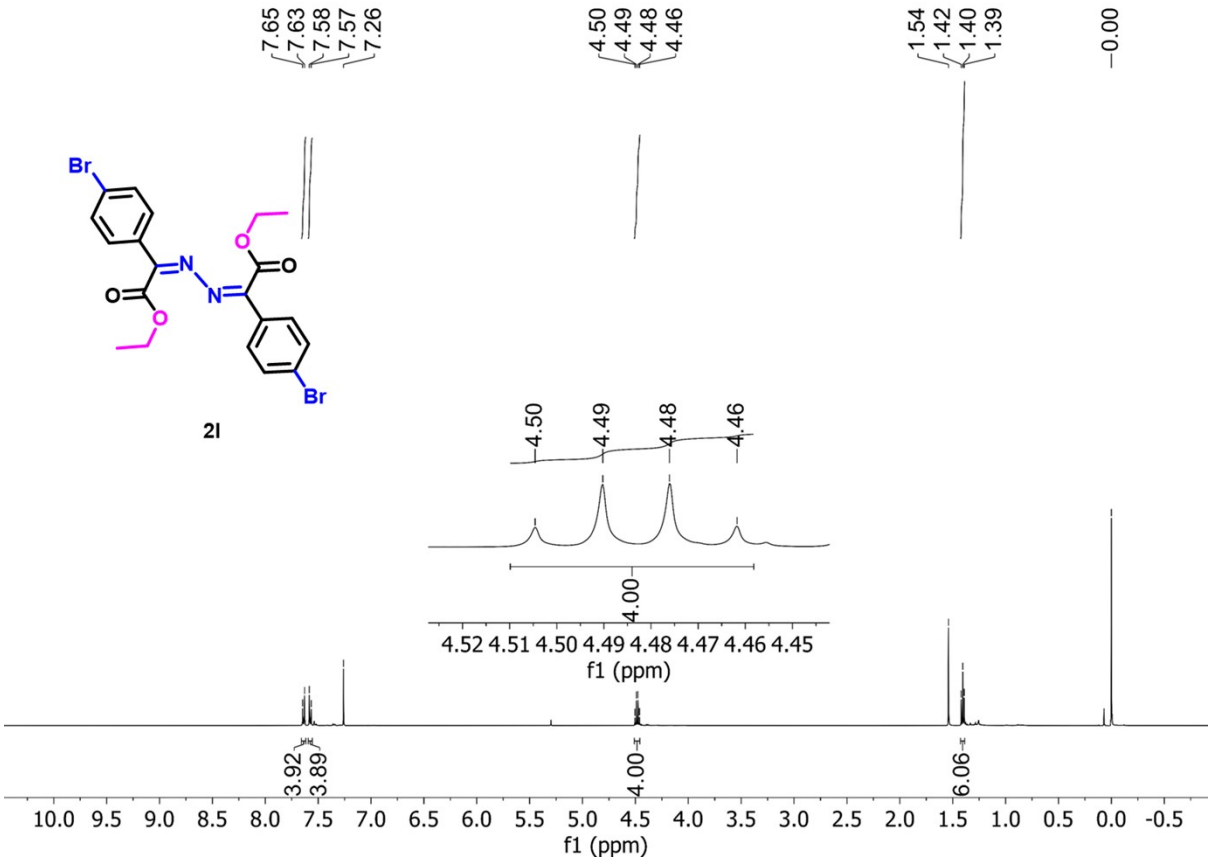
7.65
7.63
7.58
7.57
7.26
4.50
4.49
4.48
4.46
1.54
1.42
1.40
1.39
0.00
Br
N
N
O
O
O
O
Br
2l
4.00
4.52 4.51 4.50 4.49 4.48 4.47 4.46 4.45
f1 (ppm)
3.92
3.89
4.00
6.06
10.0 9.5 9.0 8.5 8.0 7.5 7.0 6.5 6.0 5.5 5.0 4.5 4.0 3.5 3.0 2.5 2.0 1.5 1.0 0.5 0.0 -0.5
f1 (ppm)

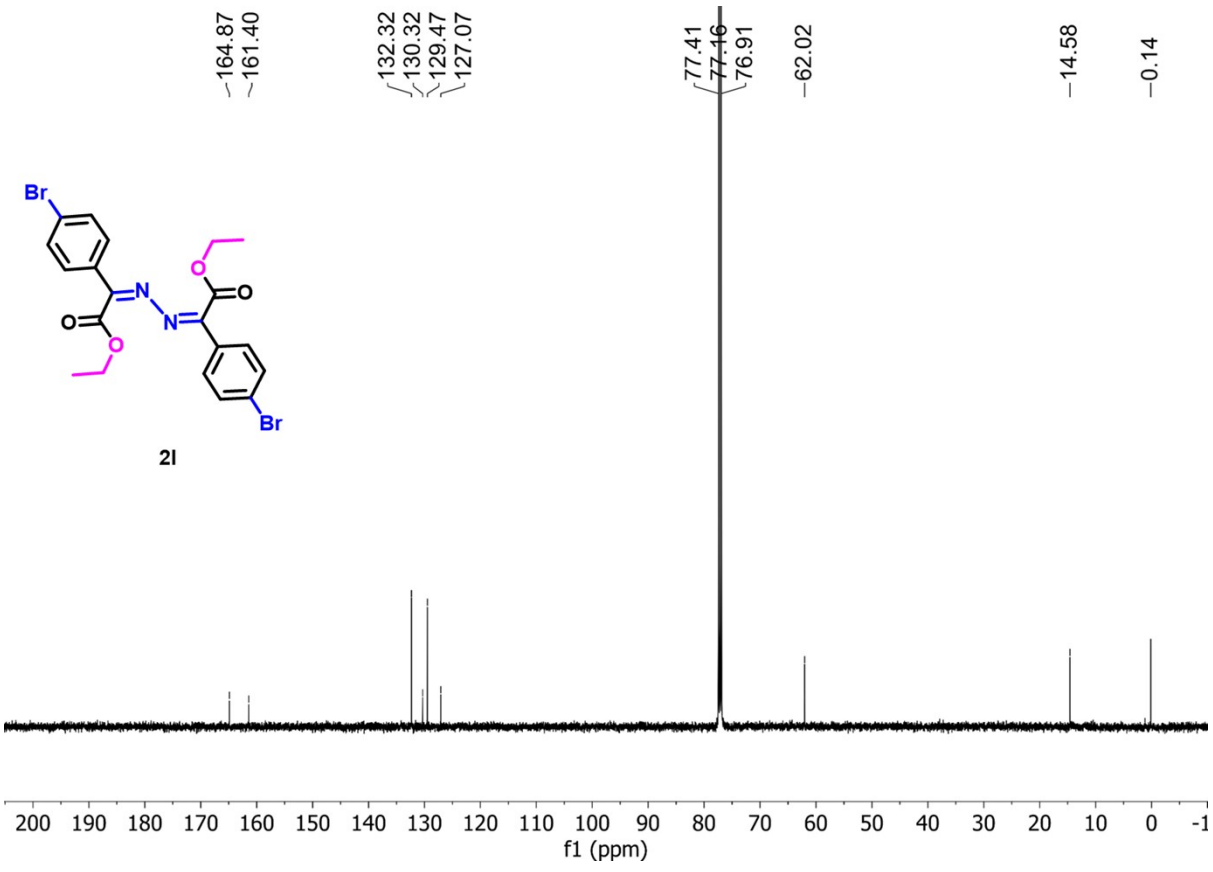
164.87
161.40
132.32
130.32
129.47
127.07
77.41
77.16
76.91
62.02
14.58
0.14
Br
N
N
O
O
O
O
Br
2l
200 190 180 170 160 150 140 130 120 110 100 90 80 70 60 50 40 30 20 10 0 -1
f1 (ppm)

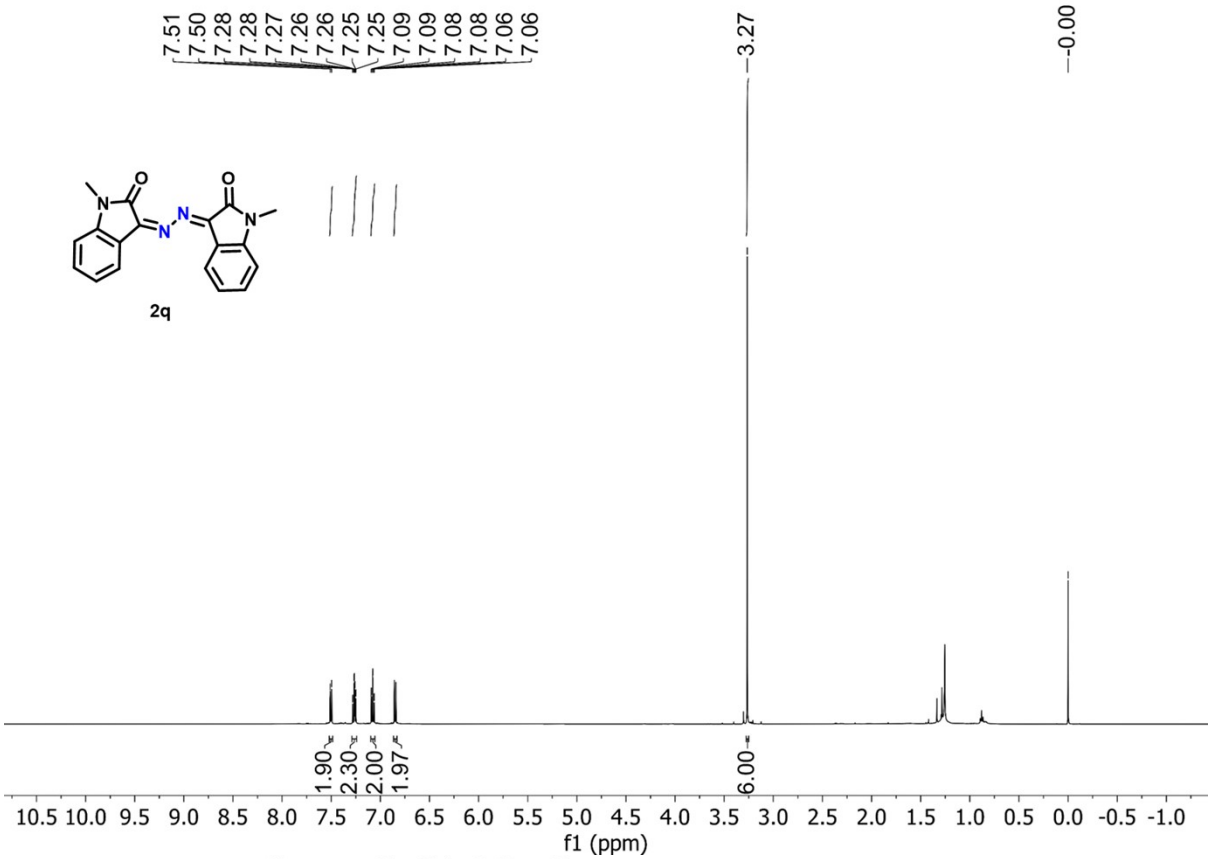
7.51
7.50
7.28
7.28
7.27
7.26
7.26
7.25
7.25
7.09
7.09
7.08
7.08
7.06
7.06
3.27
0.00
1.90
2.30
2.00
1.97
6.00
f1 (ppm)

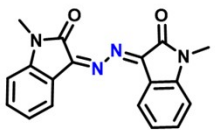

2q

161.82
141.02
128.82
127.97
122.50
121.43
118.54
108.22
77.29
77.04
76.78
25.31
0.00
f1 (ppm)

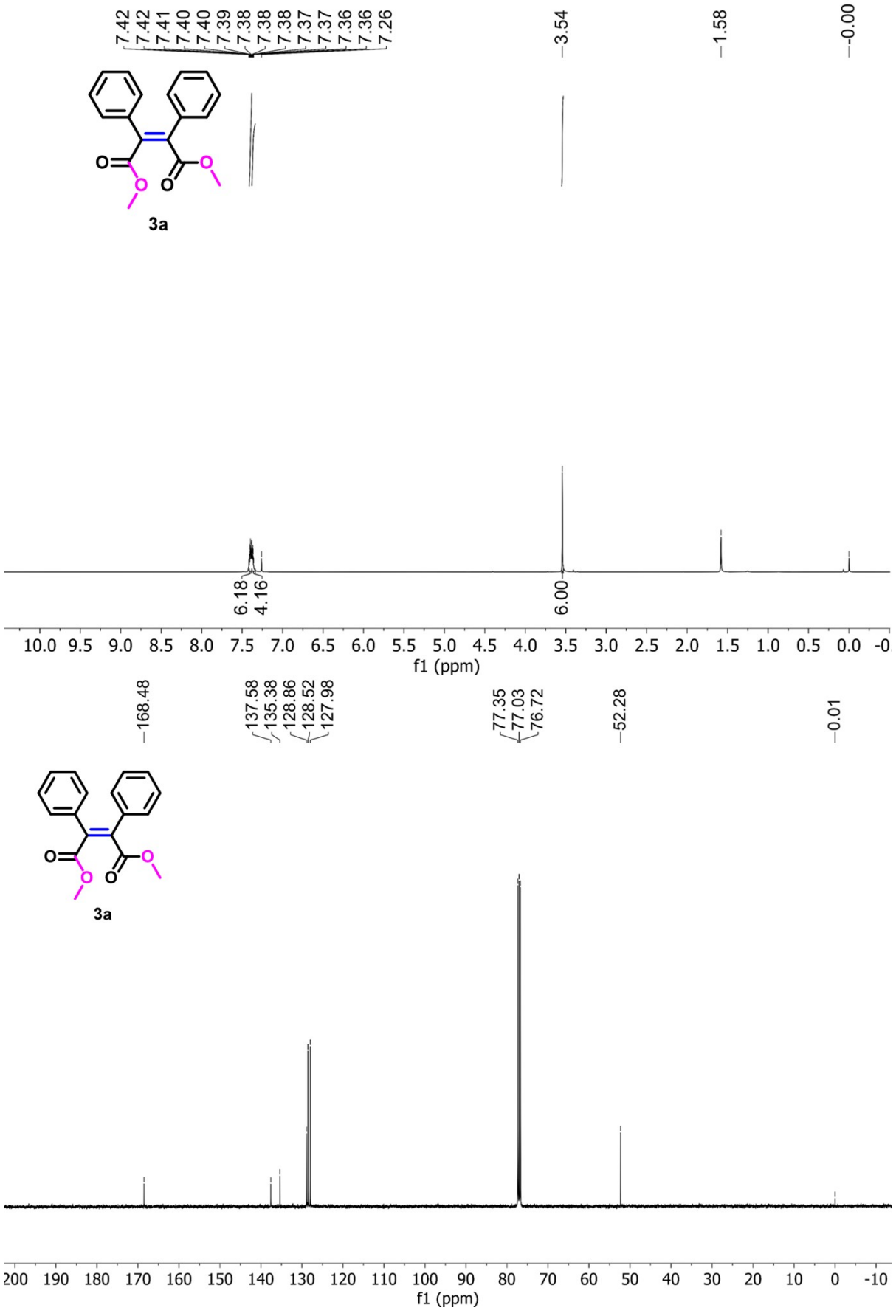
7.42
7.42
7.41
7.40
7.40
7.39
7.38
7.38
7.38
7.37
7.37
7.36
7.36
7.26
3.54
1.58
0.00
3a
6.18
4.16
6.00
f1 (ppm)
168.48
137.58
135.38
128.86
128.52
127.98
77.35
77.03
76.72
52.28
0.01
3a
f1 (ppm)

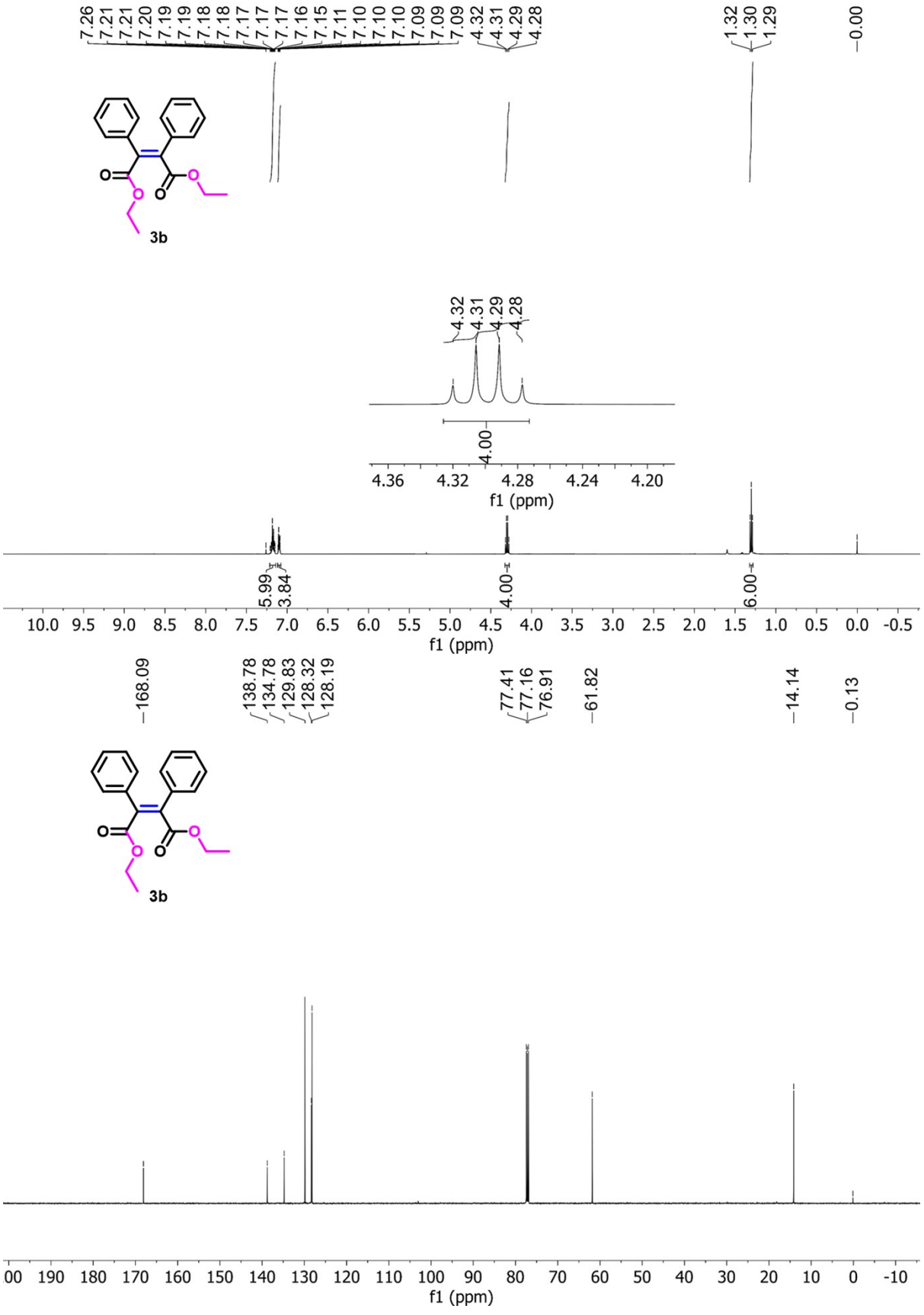
7.26
7.21
7.21
7.20
7.19
7.19
7.18
7.18
7.17
7.17
7.17
7.16
7.15
7.11
7.10
7.10
7.10
7.09
7.09
7.09
4.32
4.31
4.29
4.28
1.32
1.30
1.29
0.00
3b
4.32
4.31
4.29
4.28
4.00
4.36
4.32
4.28
4.24
4.20
f1 (ppm)
5.99
3.84
4.00
6.00
10.0 9.5 9.0 8.5 8.0 7.5 7.0 6.5 6.0 5.5 5.0 4.5 4.0 3.5 3.0 2.5 2.0 1.5 1.0 0.5 0.0 -0.5
f1 (ppm)
168.09
138.78
134.78
129.83
128.32
128.19
77.41
77.16
76.91
61.82
14.14
0.13
3b
00 190 180 170 160 150 140 130 120 110 100 90 80 70 60 50 40 30 20 10 0 -10
f1 (ppm)

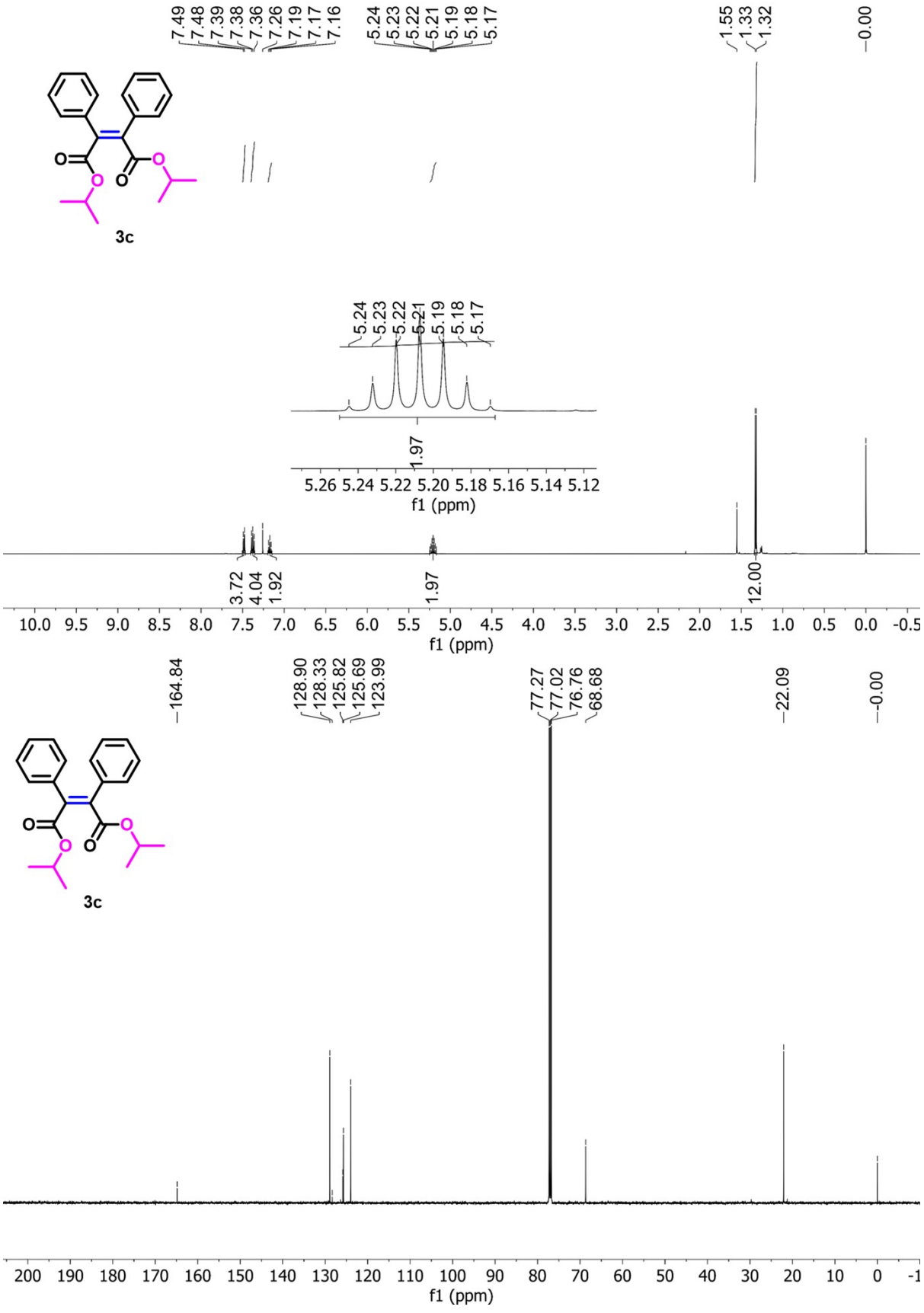
7.49
7.48
7.39
7.38
7.36
7.26
7.19
7.17
7.16
5.24
5.23
5.22
5.21
5.19
5.18
5.17
1.55
1.33
1.32
0.00
3c
1.97
5.26 5.24 5.22 5.20 5.18 5.16 5.14 5.12
f1 (ppm)
3.72
4.04
1.92
1.97
12.00
10.0 9.5 9.0 8.5 8.0 7.5 7.0 6.5 6.0 5.5 5.0 4.5 4.0 3.5 3.0 2.5 2.0 1.5 1.0 0.5 0.0 -0.5
f1 (ppm)
164.84
128.90
128.33
125.82
125.69
123.99
77.27
77.02
76.76
68.68
22.09
0.00
3c
200 190 180 170 160 150 140 130 120 110 100 90 80 70 60 50 40 30 20 10 0 -1
f1 (ppm)

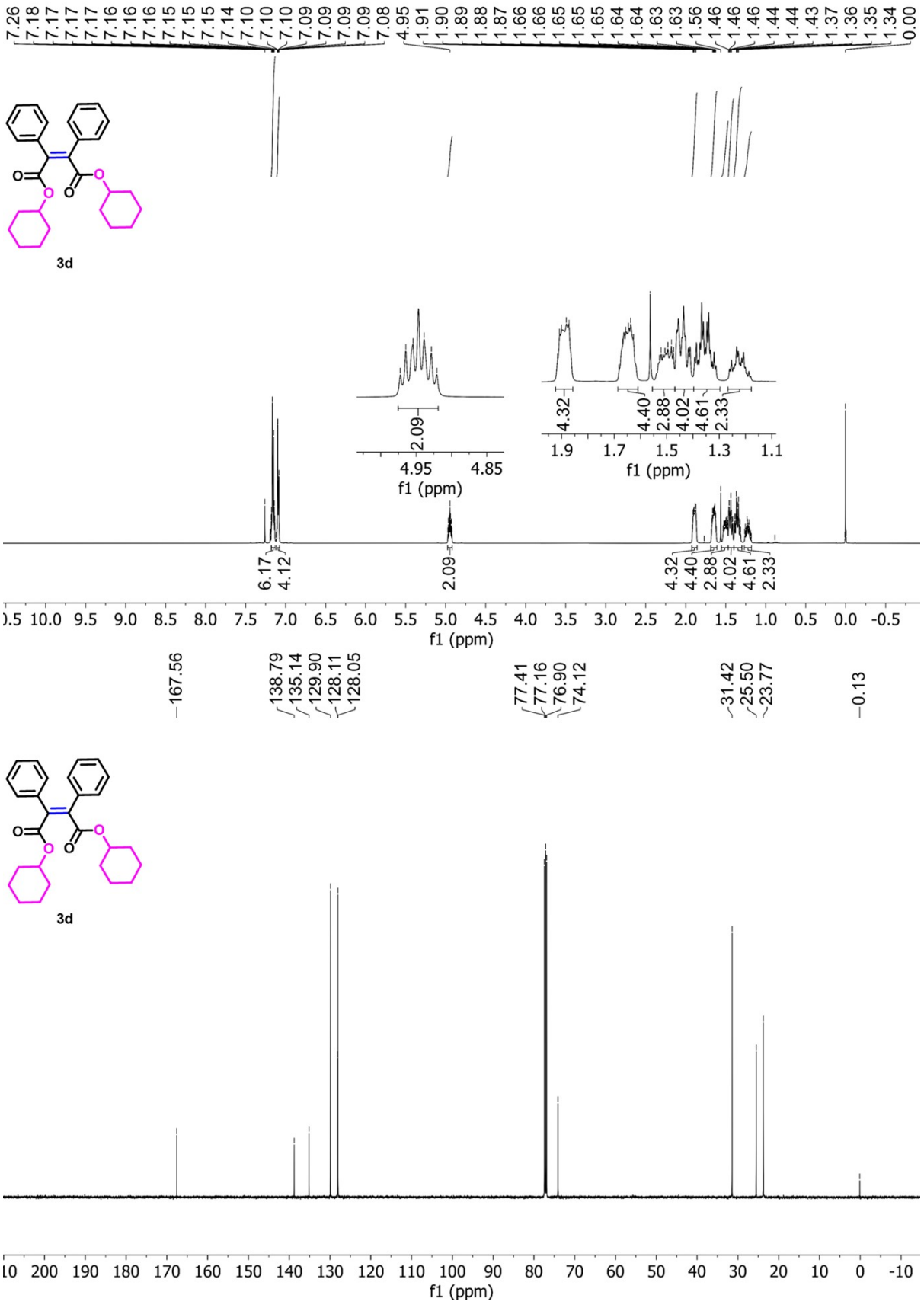
7.26 7.18 7.17 7.17 7.17 7.16 7.16 7.16 7.15 7.15 7.15 7.14 7.10 7.10 7.09 7.09 7.09 7.09 7.08 4.95 1.91 1.90 1.89 1.88 1.87 1.66 1.66 1.65 1.65 1.65 1.64 1.64 1.63 1.63 1.56 1.46 1.46 1.44 1.44 1.43 1.37 1.36 1.35 1.34 0.00
3d
2.09
4.95 4.85
f1 (ppm)
4.32 4.40 2.88 4.02 4.61 2.33
1.9 1.7 1.5 1.3 1.1
f1 (ppm)
6.17 4.12 2.09 4.32 4.40 2.88 4.02 4.61 2.33
f1 (ppm)
167.56 138.79 135.14 129.90 128.11 128.05 77.41 77.16 76.90 74.12 31.42 25.50 23.77 0.13
3d
f1 (ppm)

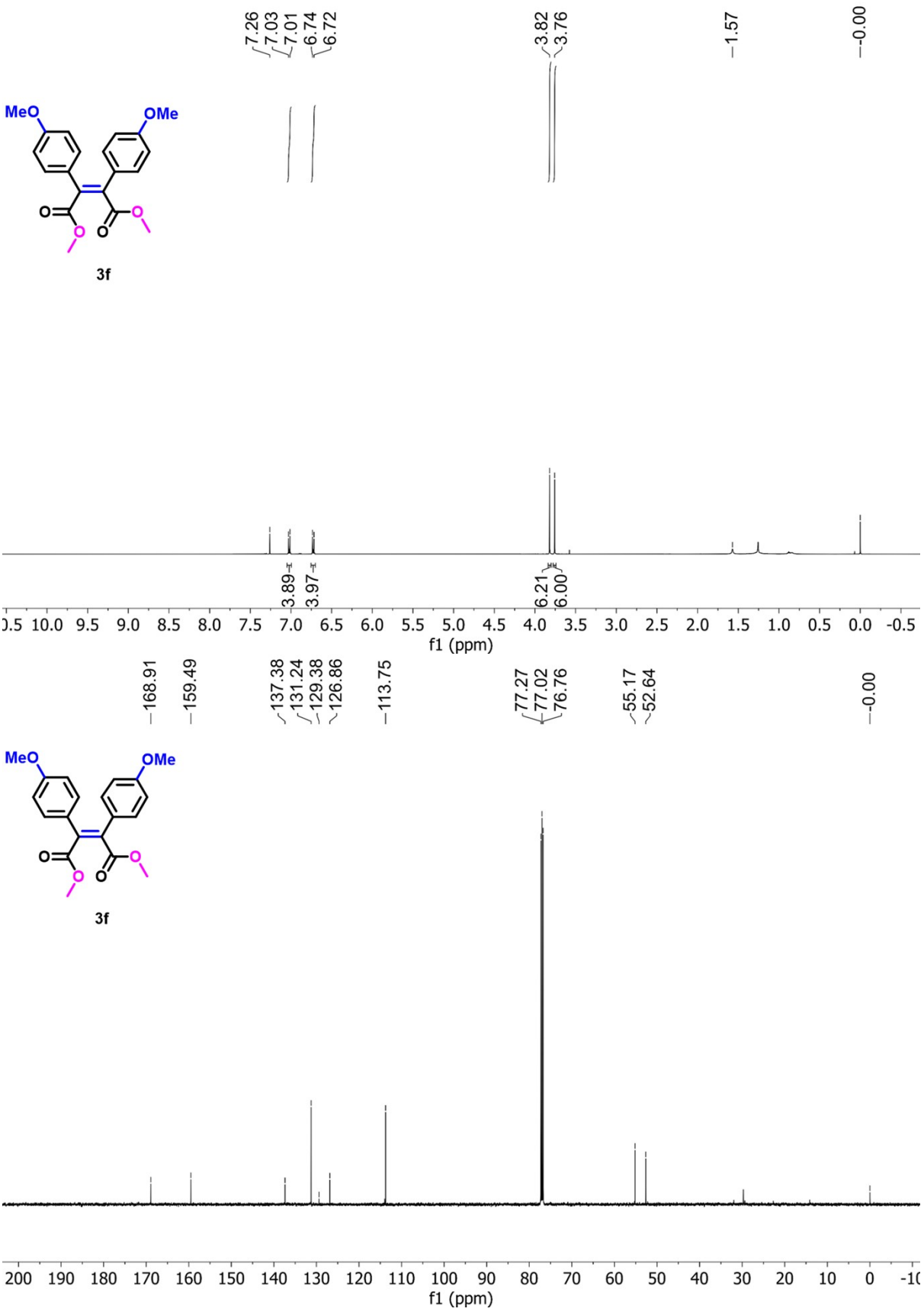
7.26
7.03
7.01
6.74
6.72
3.82
3.76
1.57
0.00
MeO
OMe
3f
3.89
3.97
6.21
6.00
f1 (ppm)
168.91
159.49
137.38
131.24
129.38
126.86
113.75
77.27
77.02
76.76
55.17
52.64
0.00
MeO
OMe
3f
f1 (ppm)

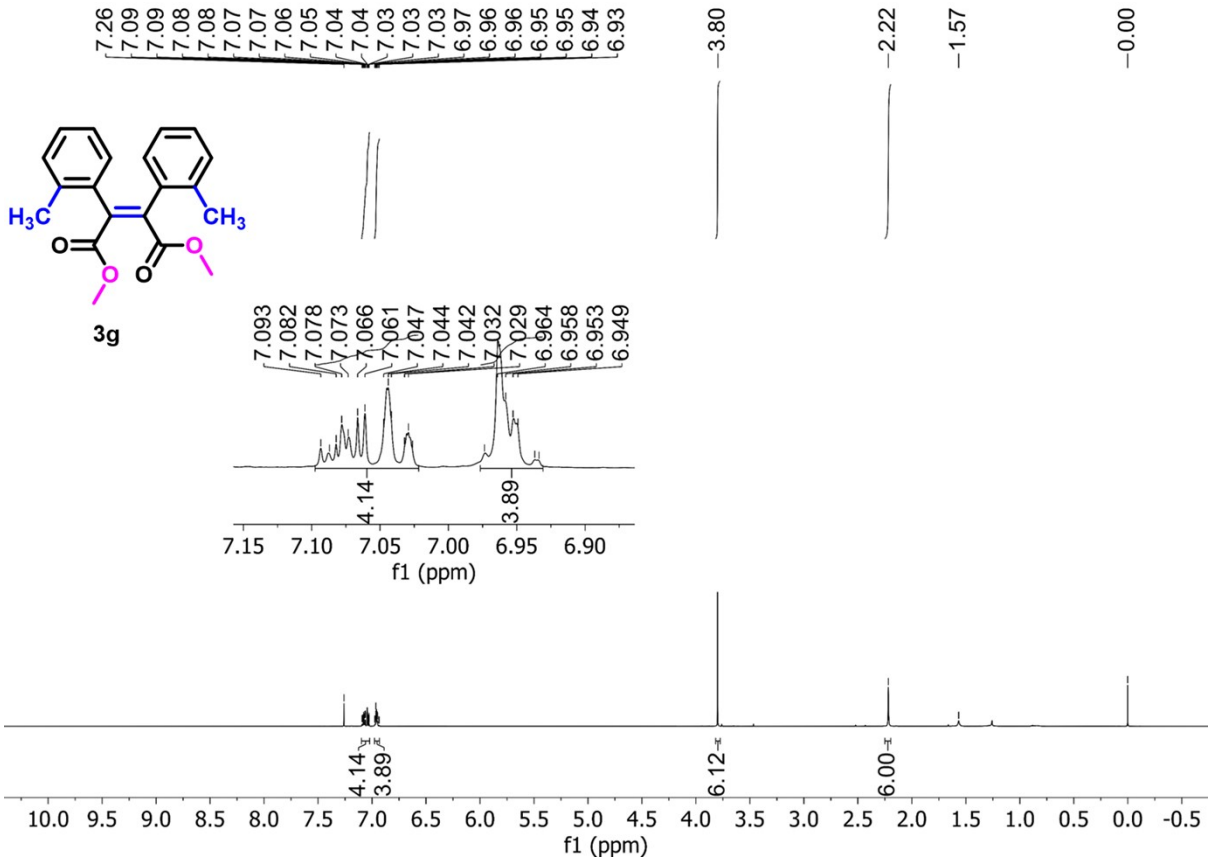
7.26
7.09
7.09
7.08
7.08
7.07
7.07
7.06
7.05
7.04
7.04
7.03
7.03
7.03
6.97
6.96
6.96
6.95
6.95
6.94
6.93
3.80
2.22
1.57
0.00
H3C
CH3
O
O
O
O
3g
7.093
7.082
7.078
7.073
7.066
7.061
7.047
7.044
7.042
7.032
7.029
6.964
6.958
6.953
6.949
4.14
3.89
7.15 7.10 7.05 7.00 6.95 6.90
f1 (ppm)
4.14
3.89
6.12
6.00
10.0 9.5 9.0 8.5 8.0 7.5 7.0 6.5 6.0 5.5 5.0 4.5 4.0 3.5 3.0 2.5 2.0 1.5 1.0 0.5 0.0 -0.5
f1 (ppm)

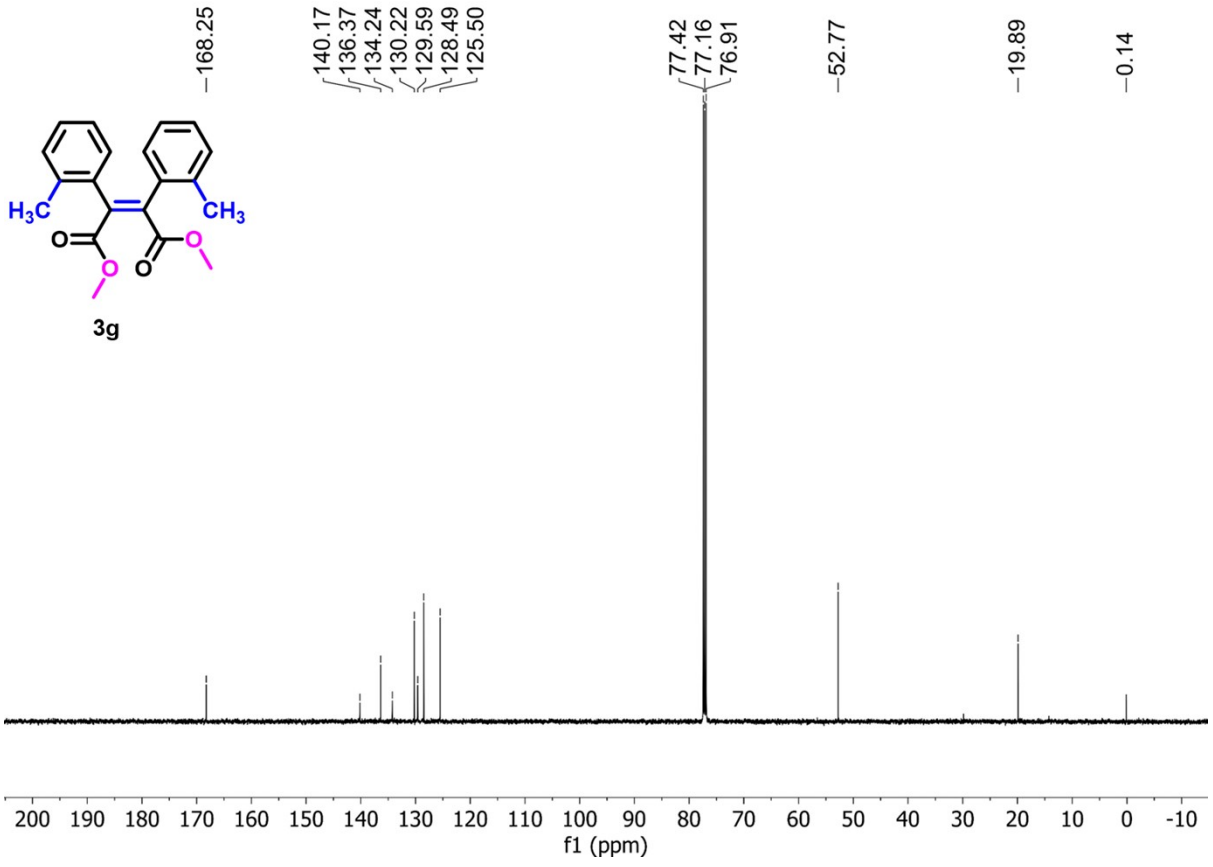
168.25
140.17
136.37
134.24
130.22
129.59
128.49
125.50
77.42
77.16
76.91
52.77
19.89
0.14
H3C
CH3
O
O
O
O
3g
200 190 180 170 160 150 140 130 120 110 100 90 80 70 60 50 40 30 20 10 0 -10
f1 (ppm)

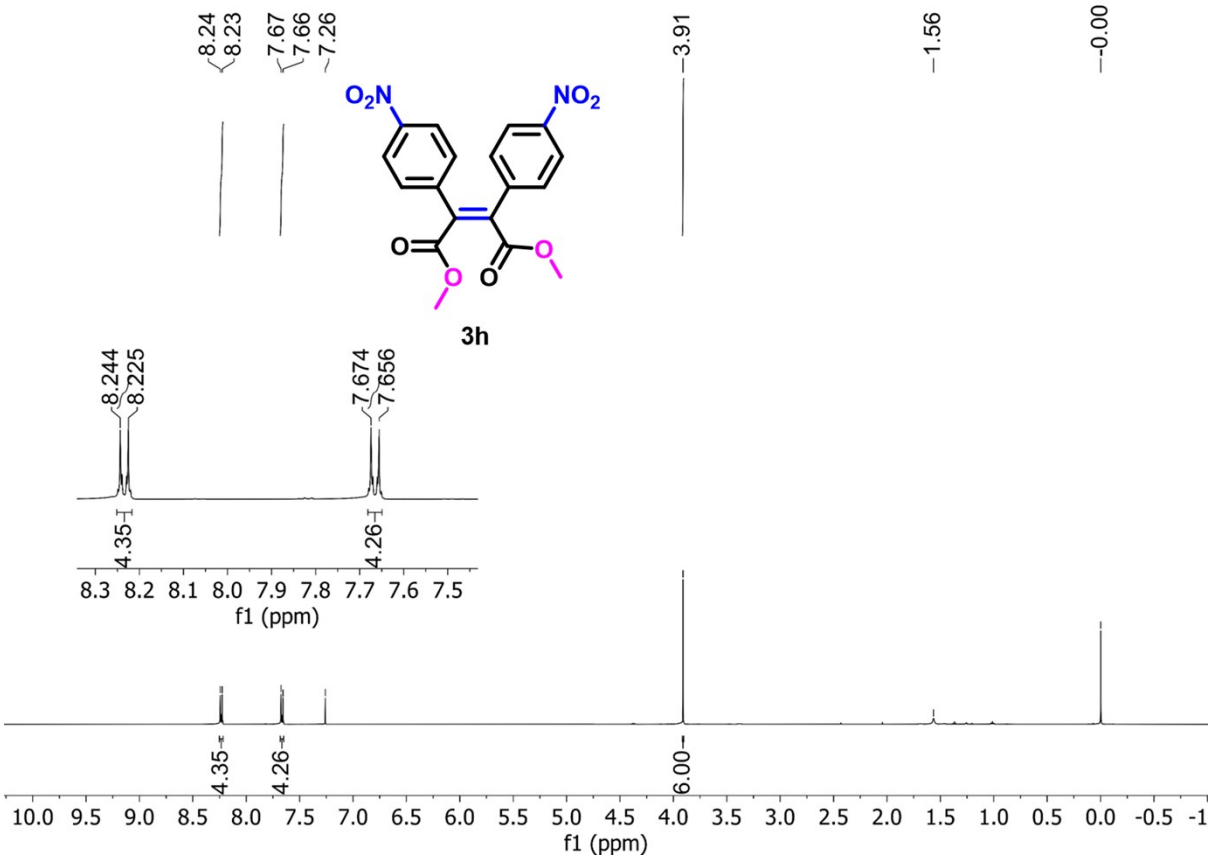
8.24
8.23
7.67
7.66
7.26
3.91
1.56
0.00
O2N
NO2
3h
8.244
8.225
7.674
7.656
4.35
4.26
8.3 8.2 8.1 8.0 7.9 7.8 7.7 7.6 7.5
f1 (ppm)
4.35
4.26
6.00
10.0 9.5 9.0 8.5 8.0 7.5 7.0 6.5 6.0 5.5 5.0 4.5 4.0 3.5 3.0 2.5 2.0 1.5 1.0 0.5 0.0 -0.5 -1
f1 (ppm)

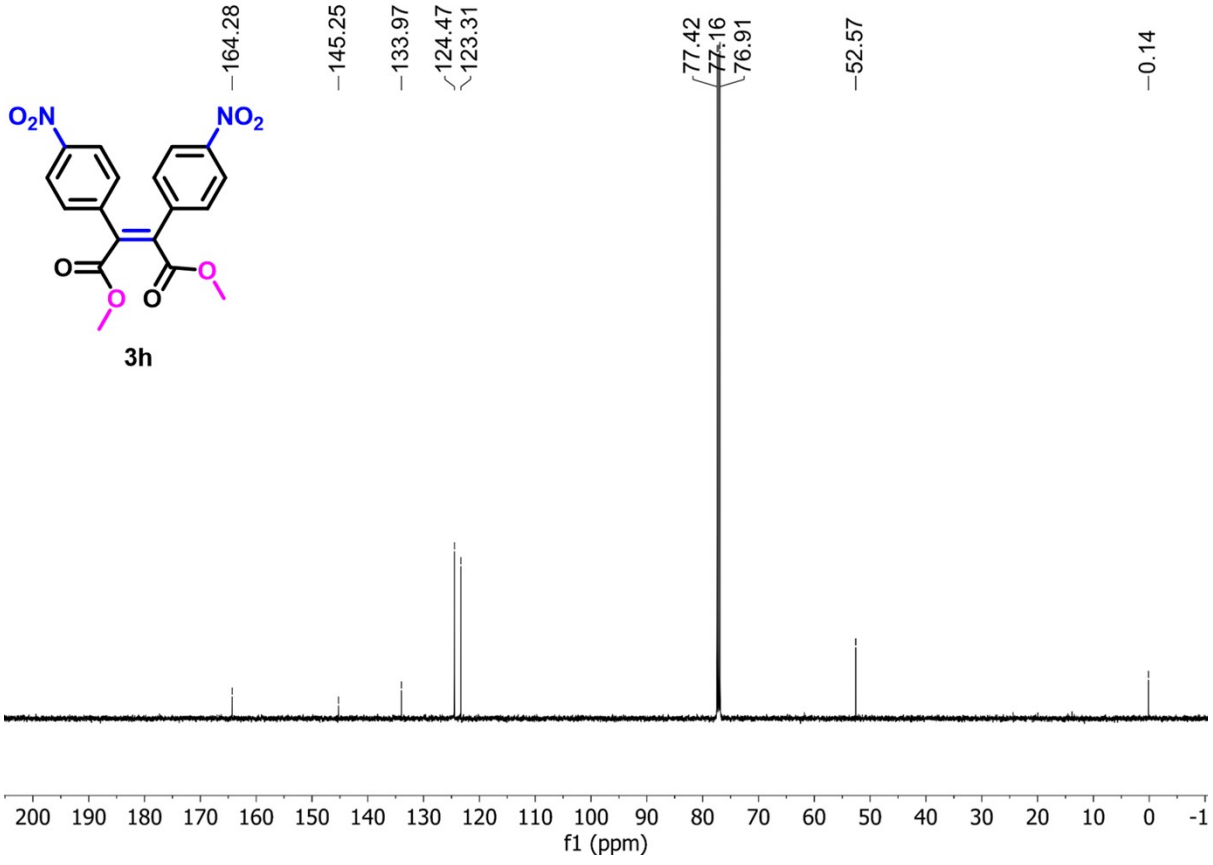
164.28
145.25
133.97
124.47
123.31
77.42
77.16
76.91
52.57
0.14
O2N
NO2
3h
200 190 180 170 160 150 140 130 120 110 100 90 80 70 60 50 40 30 20 10 0 -1
f1 (ppm)

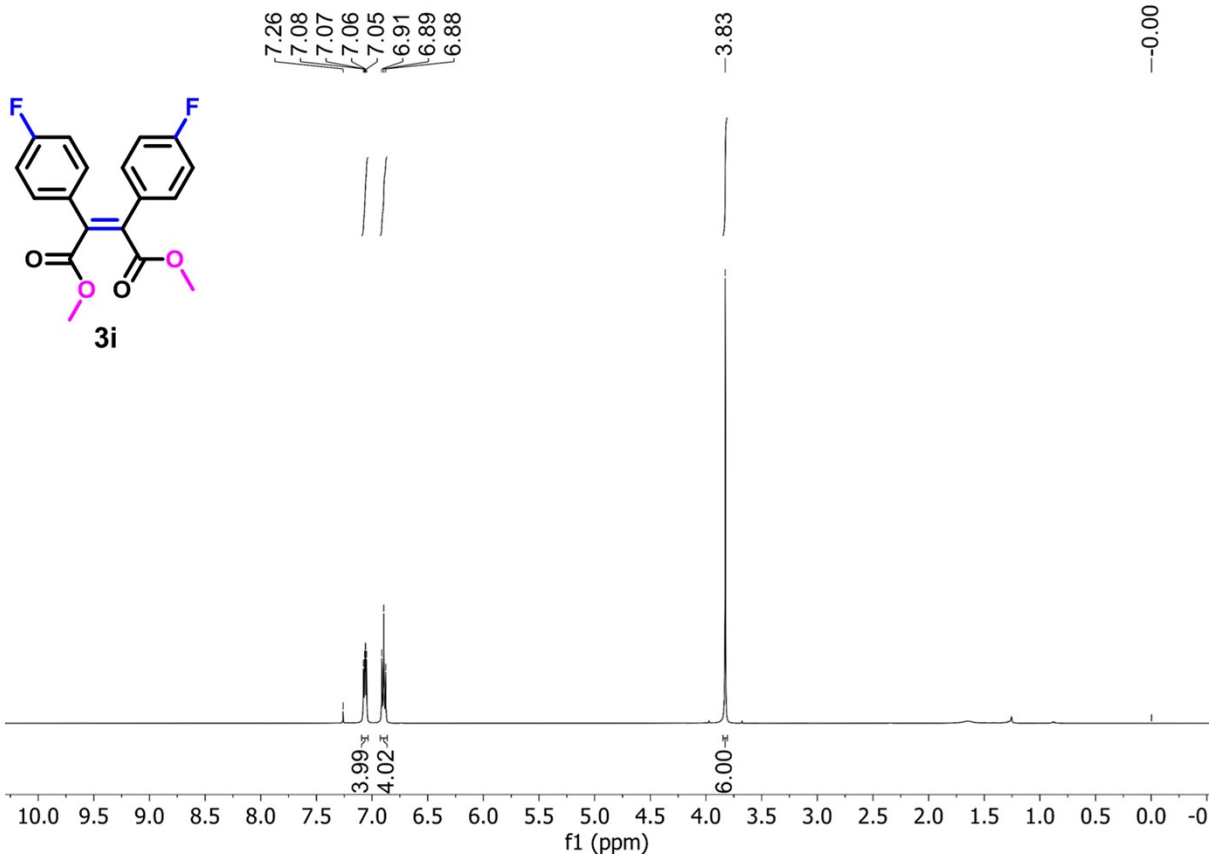
7.26
7.08
7.07
7.06
7.05
6.91
6.89
6.88
3.83
0.00
3.99
4.02
6.00
f1 (ppm)

3i

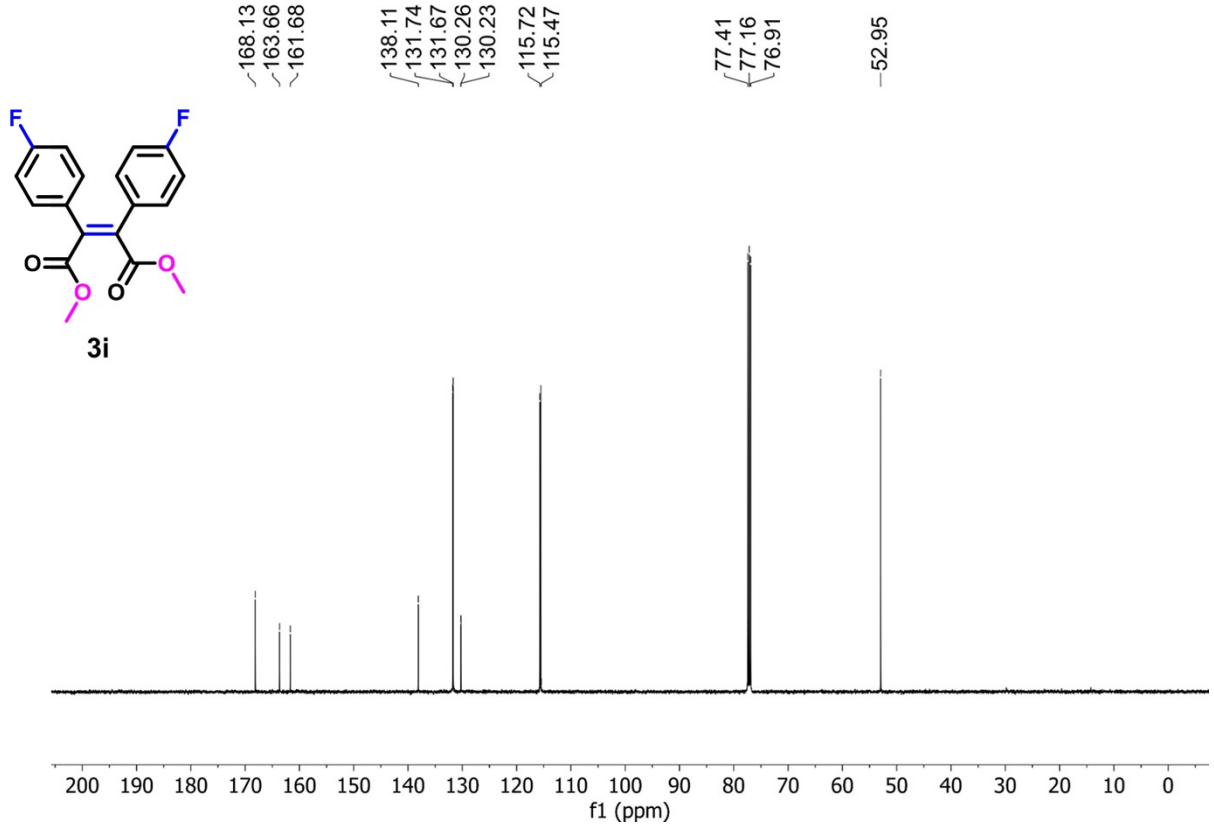
168.13
163.66
161.68
138.11
131.74
131.67
130.26
130.23
115.72
115.47
77.41
77.16
76.91
52.95
f1 (ppm)

3i

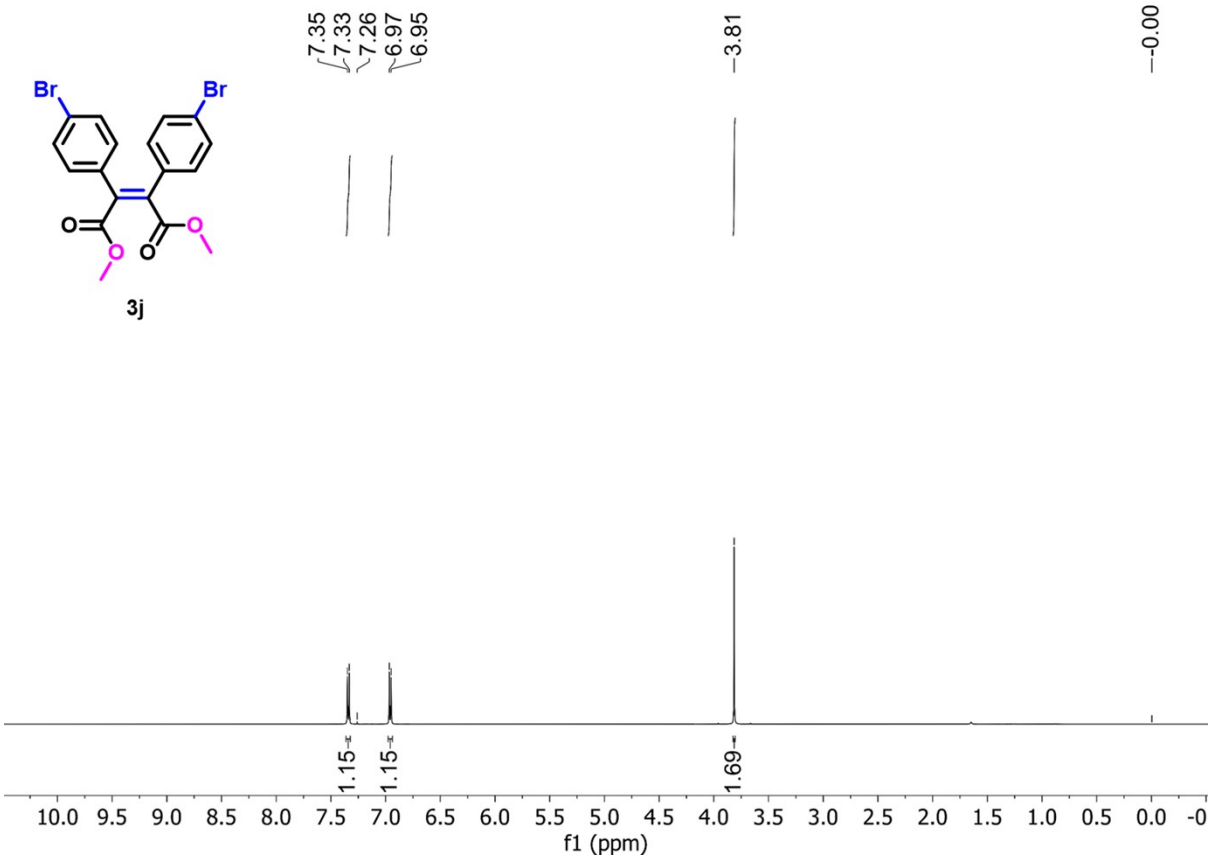
7.35
7.33
7.26
6.97
6.95
3.81
0.00
Br
Br
O
O
O
O
3j
1.15
1.15
1.69
10.0 9.5 9.0 8.5 8.0 7.5 7.0 6.5 6.0 5.5 5.0 4.5 4.0 3.5 3.0 2.5 2.0 1.5 1.0 0.5 0.0 -0
f1 (ppm)

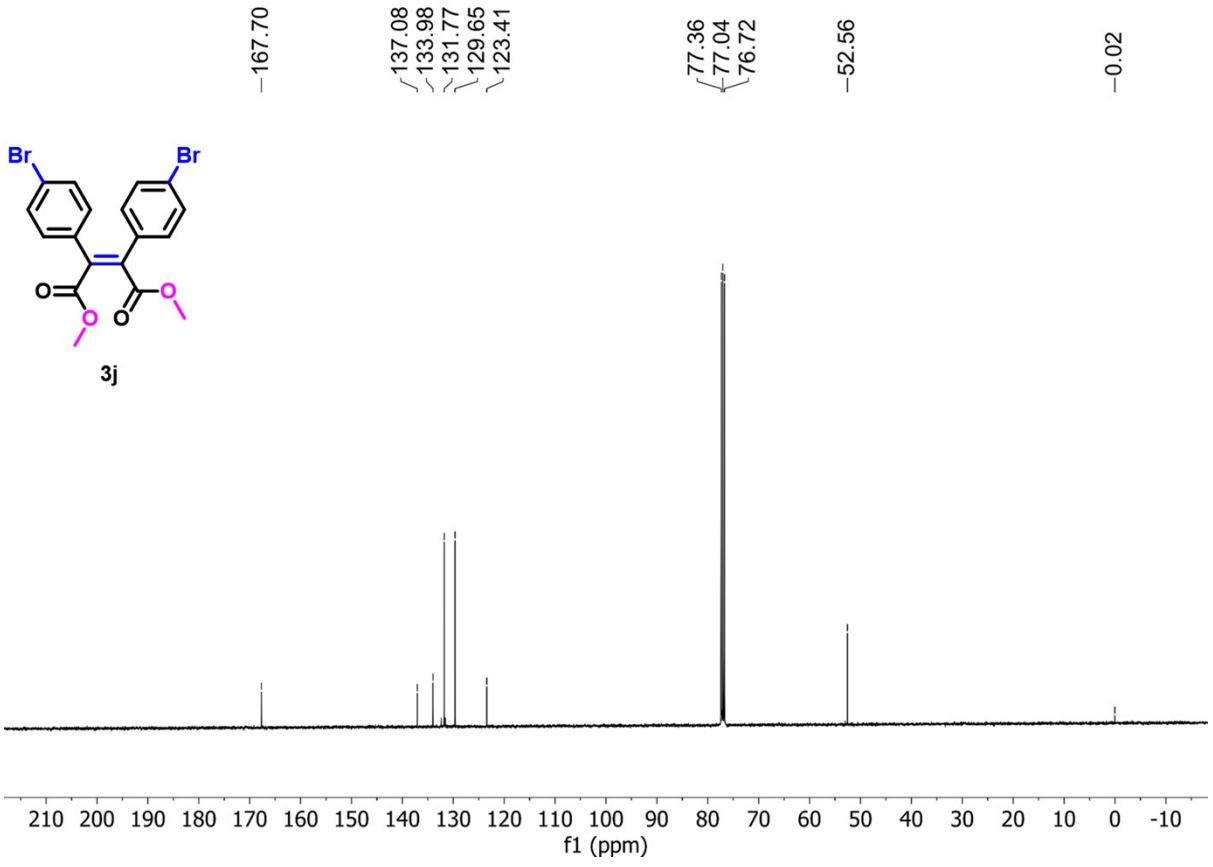
167.70
137.08
133.98
131.77
129.65
123.41
77.36
77.04
76.72
52.56
0.02
Br
Br
O
O
O
O
3j
210 200 190 180 170 160 150 140 130 120 110 100 90 80 70 60 50 40 30 20 10 0 -10
f1 (ppm)

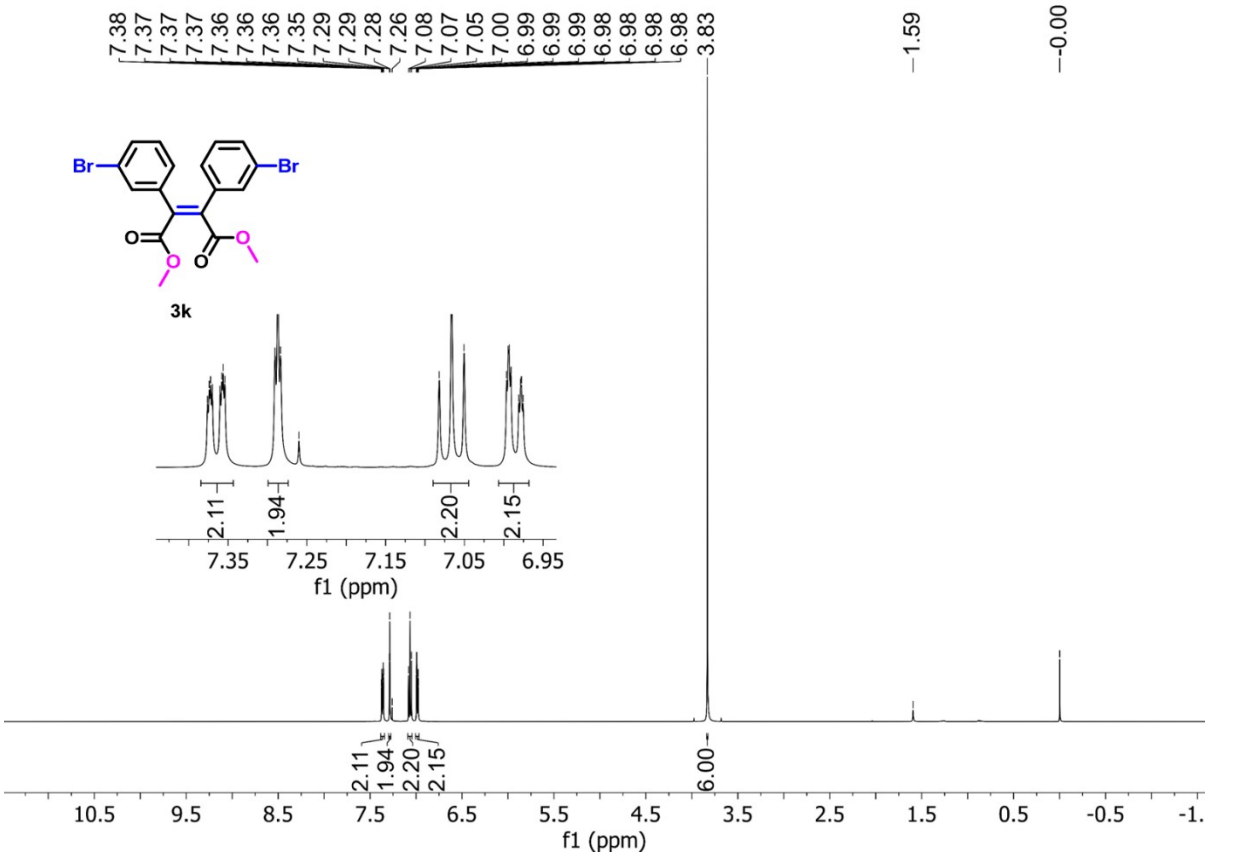
7.38
7.37
7.37
7.37
7.36
7.36
7.36
7.35
7.29
7.29
7.28
7.26
7.08
7.07
7.05
7.00
6.99
6.99
6.99
6.98
6.98
6.98
3.83
1.59
0.00
Br
Br
O
O
O
O
3k
2.11
1.94
2.20
2.15
7.35
7.25
7.15
7.05
6.95
f1 (ppm)
2.11
1.94
2.20
2.15
6.00
10.5
9.5
8.5
7.5
6.5
5.5
4.5
3.5
2.5
1.5
0.5
-0.5
f1 (ppm)

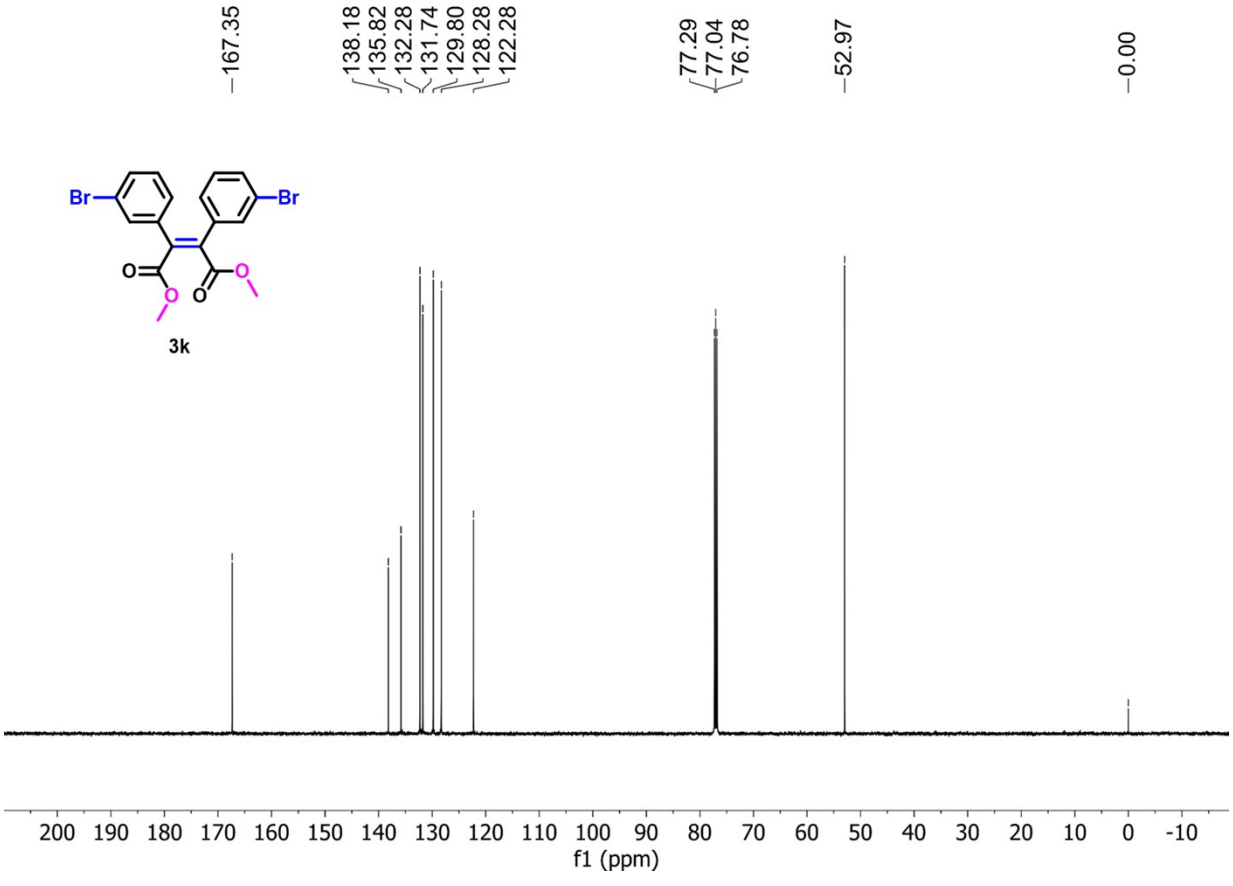
167.35
138.18
135.82
132.28
131.74
129.80
128.28
122.28
77.29
77.04
76.78
52.97
0.00
Br
Br
O
O
O
O
3k
200
190
180
170
160
150
140
130
120
110
100
90
80
70
60
50
40
30
20
10
0
-10
f1 (ppm)

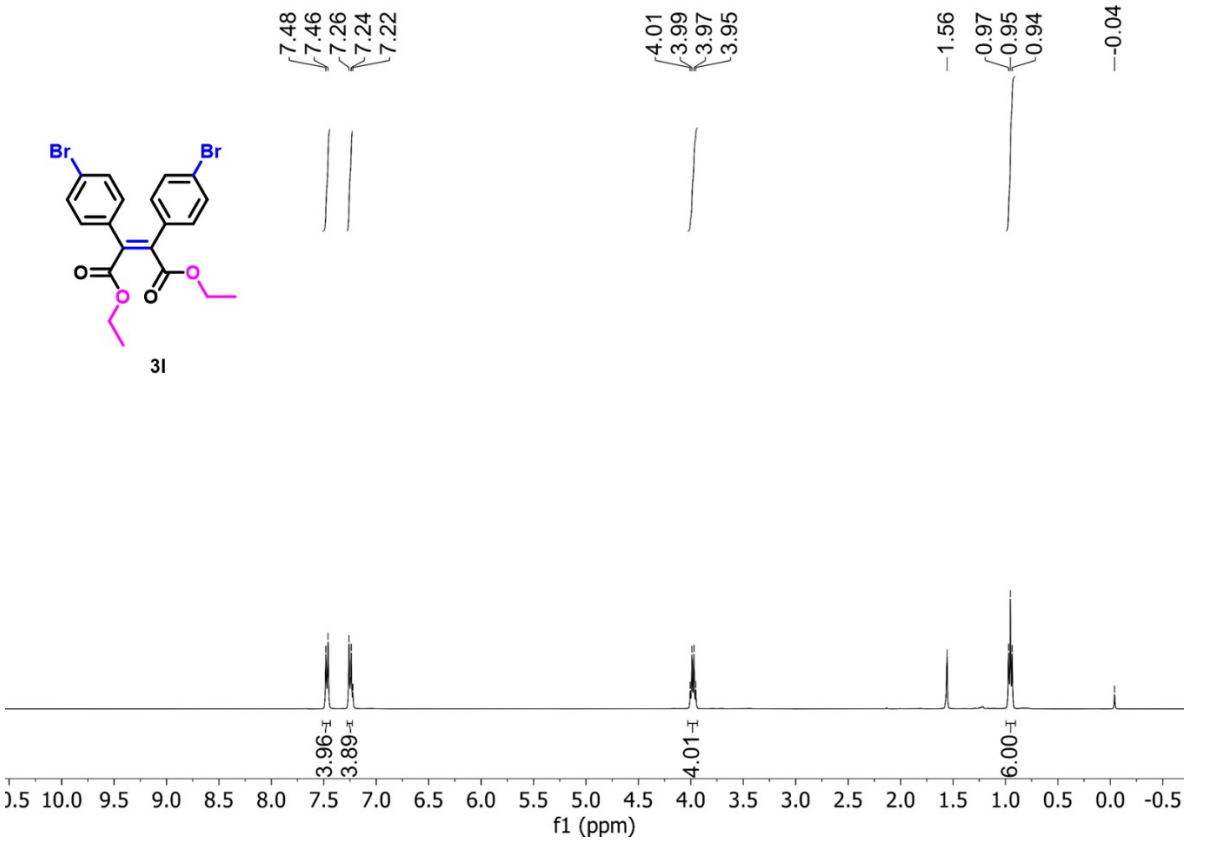
7.48
7.46
7.26
7.24
7.22
4.01
3.99
3.97
3.95
1.56
0.97
0.95
0.94
-0.04
Br
Br
O
O
O
O
3l
3.96
3.89
4.01
6.00
f1 (ppm)

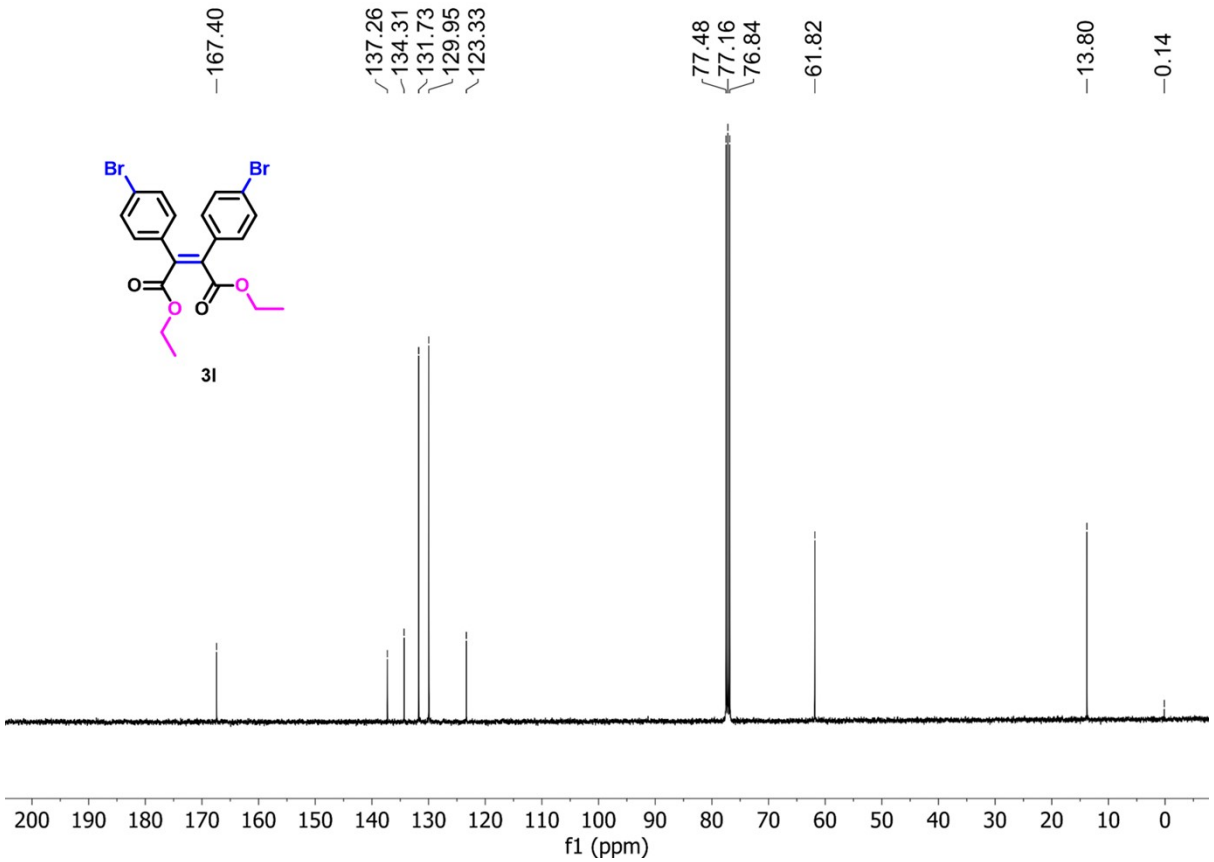
167.40
137.26
134.31
131.73
129.95
123.33
77.48
77.16
76.84
61.82
13.80
0.14
Br
Br
O
O
O
O
3l
f1 (ppm)

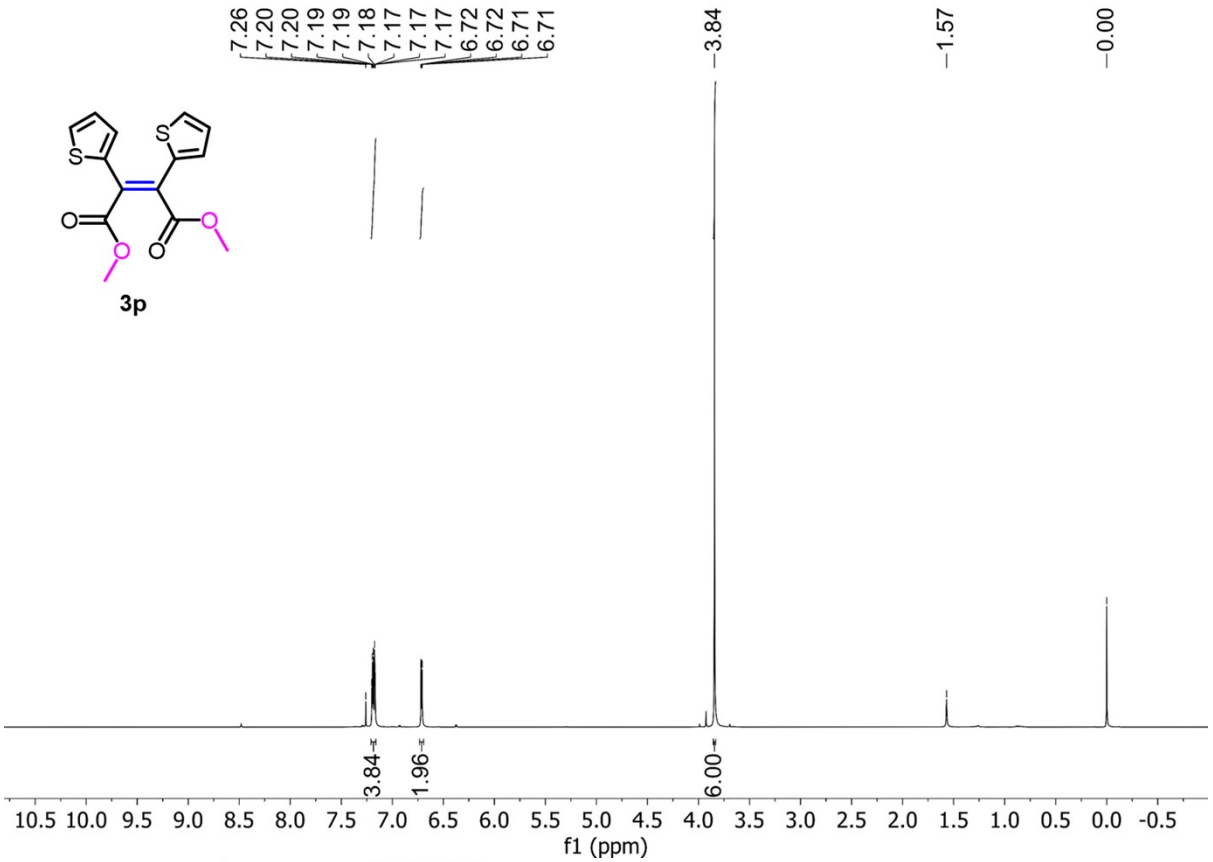
7.26
7.20
7.20
7.19
7.19
7.18
7.17
7.17
7.17
6.72
6.72
6.71
6.71
3.84
1.57
0.00
3p
3.84
1.96
6.00
f1 (ppm)

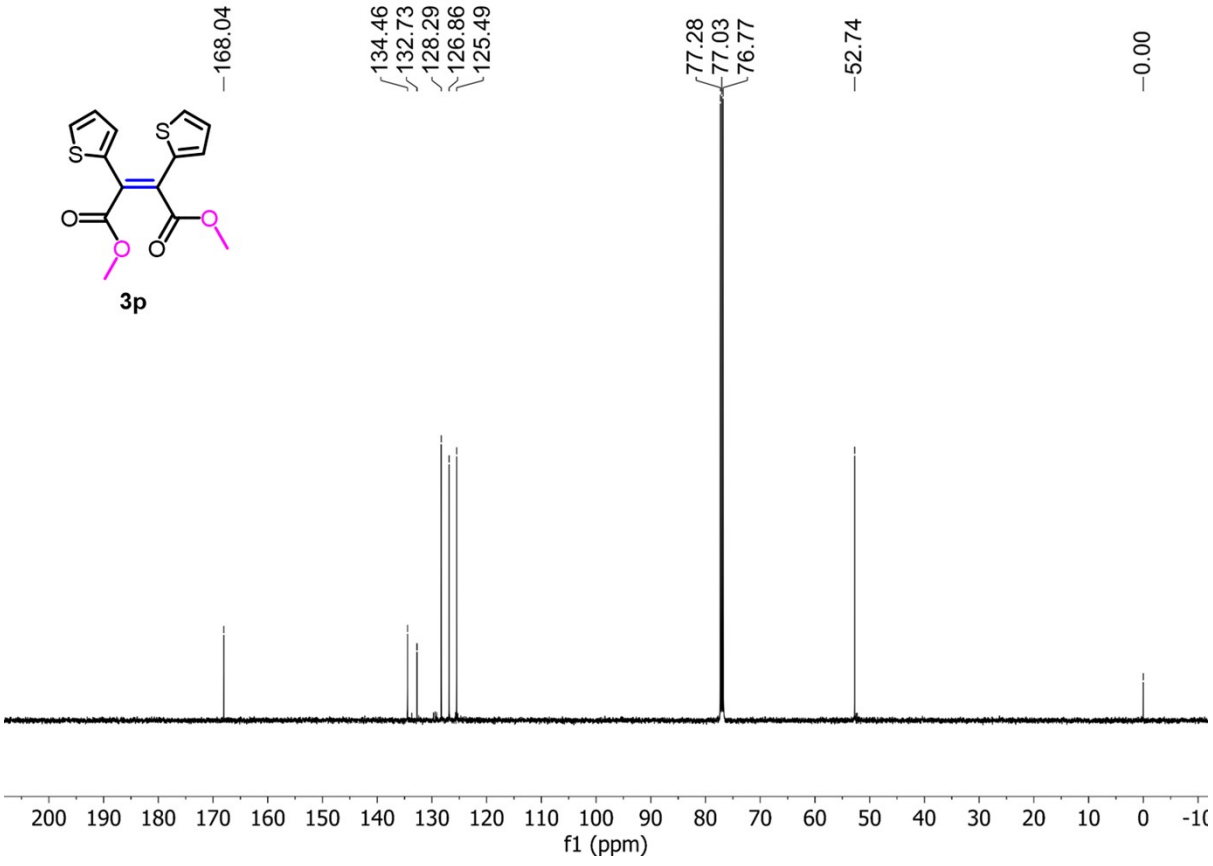
168.04
134.46
132.73
128.29
126.86
125.49
77.28
77.03
76.77
52.74
0.00
3p
f1 (ppm)

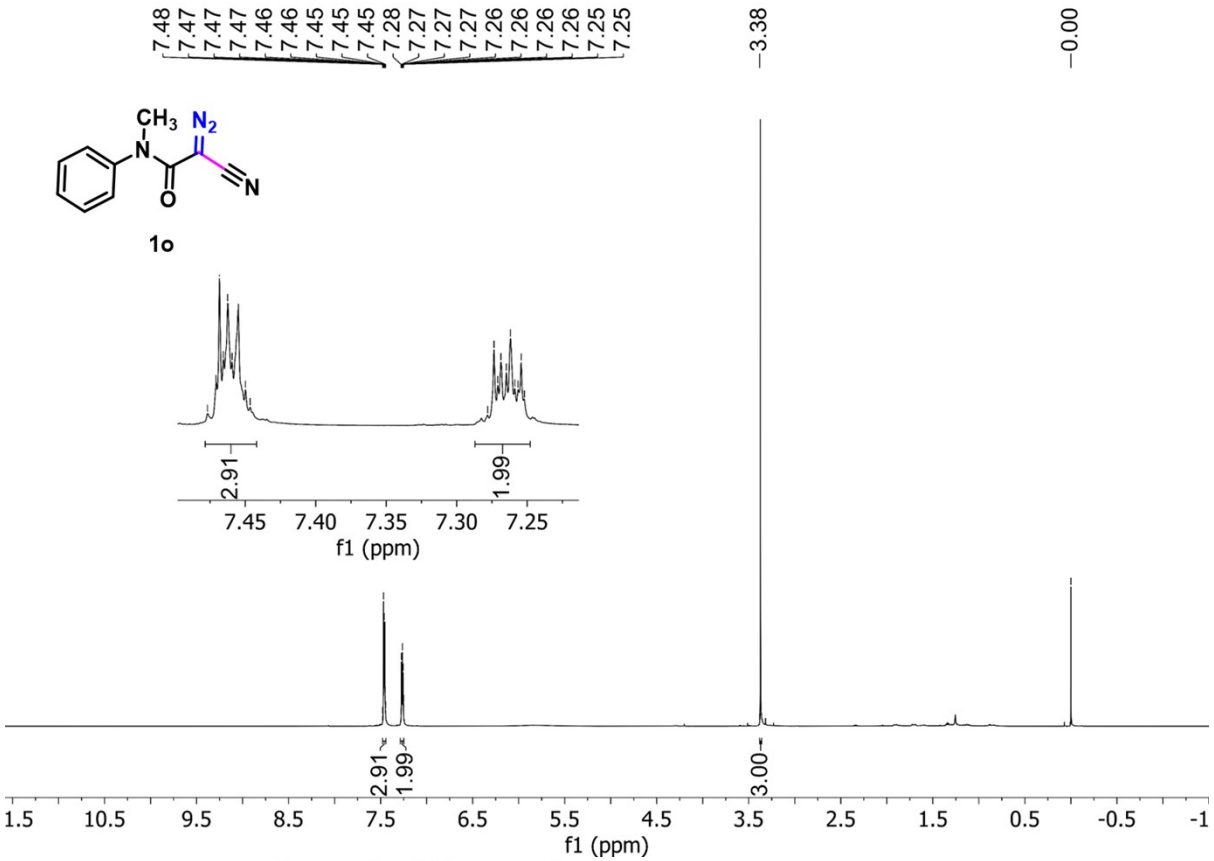
7.48
7.47
7.47
7.47
7.46
7.46
7.45
7.45
7.45
7.28
7.27
7.27
7.27
7.26
7.26
7.26
7.26
7.25
7.25
3.38
0.00
CH3
N2
N
O
N
1o
2.91
1.99
7.45
7.40
7.35
7.30
7.25
f1 (ppm)
2.91
1.99
3.00
1.5
10.5
9.5
8.5
7.5
6.5
5.5
4.5
3.5
2.5
1.5
0.5
-0.5
-1
f1 (ppm)

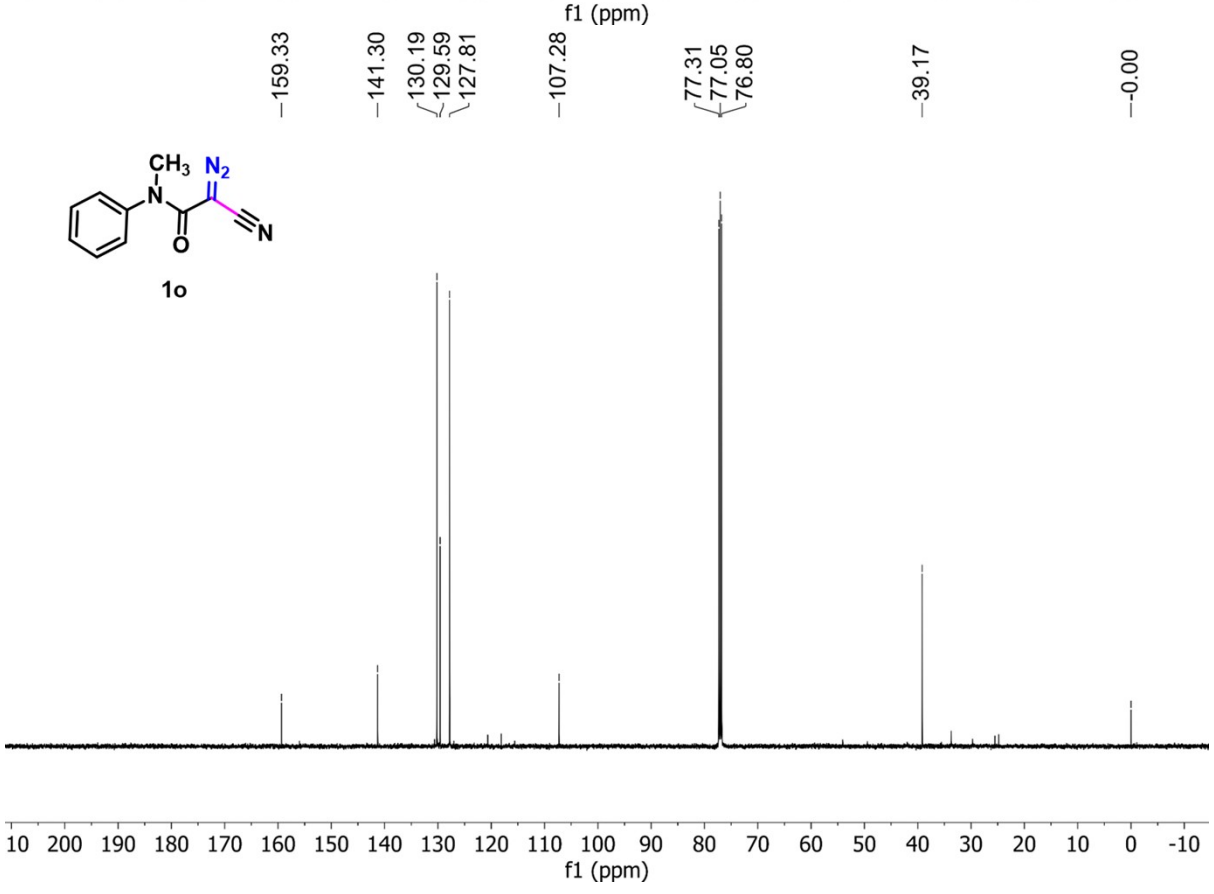
159.33
141.30
130.19
129.59
127.81
107.28
77.31
77.05
76.80
39.17
0.00
CH3
N2
N
O
N
1o
10
200
190
180
170
160
150
140
130
120
110
100
90
80
70
60
50
40
30
20
10
0
-10
f1 (ppm)

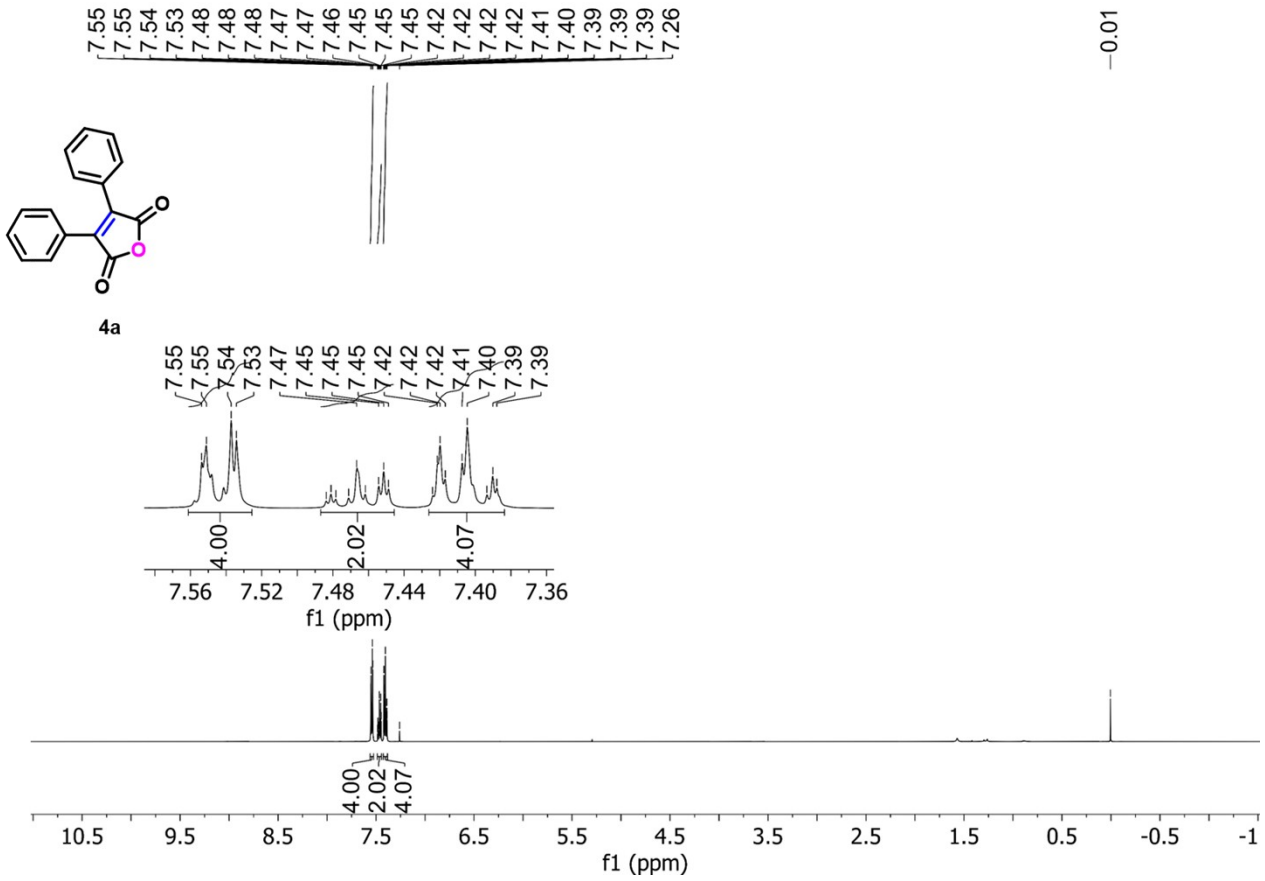
7.55
7.55
7.54
7.53
7.48
7.48
7.48
7.47
7.47
7.46
7.45
7.45
7.45
7.42
7.42
7.42
7.42
7.41
7.40
7.39
7.39
7.39
7.26
-0.01
4a
4.00
2.02
4.07
7.56
7.52
7.48
7.44
7.40
7.36
f1 (ppm)
10.5
9.5
8.5
7.5
6.5
5.5
4.5
3.5
2.5
1.5
0.5
-0.5
-1
f1 (ppm)

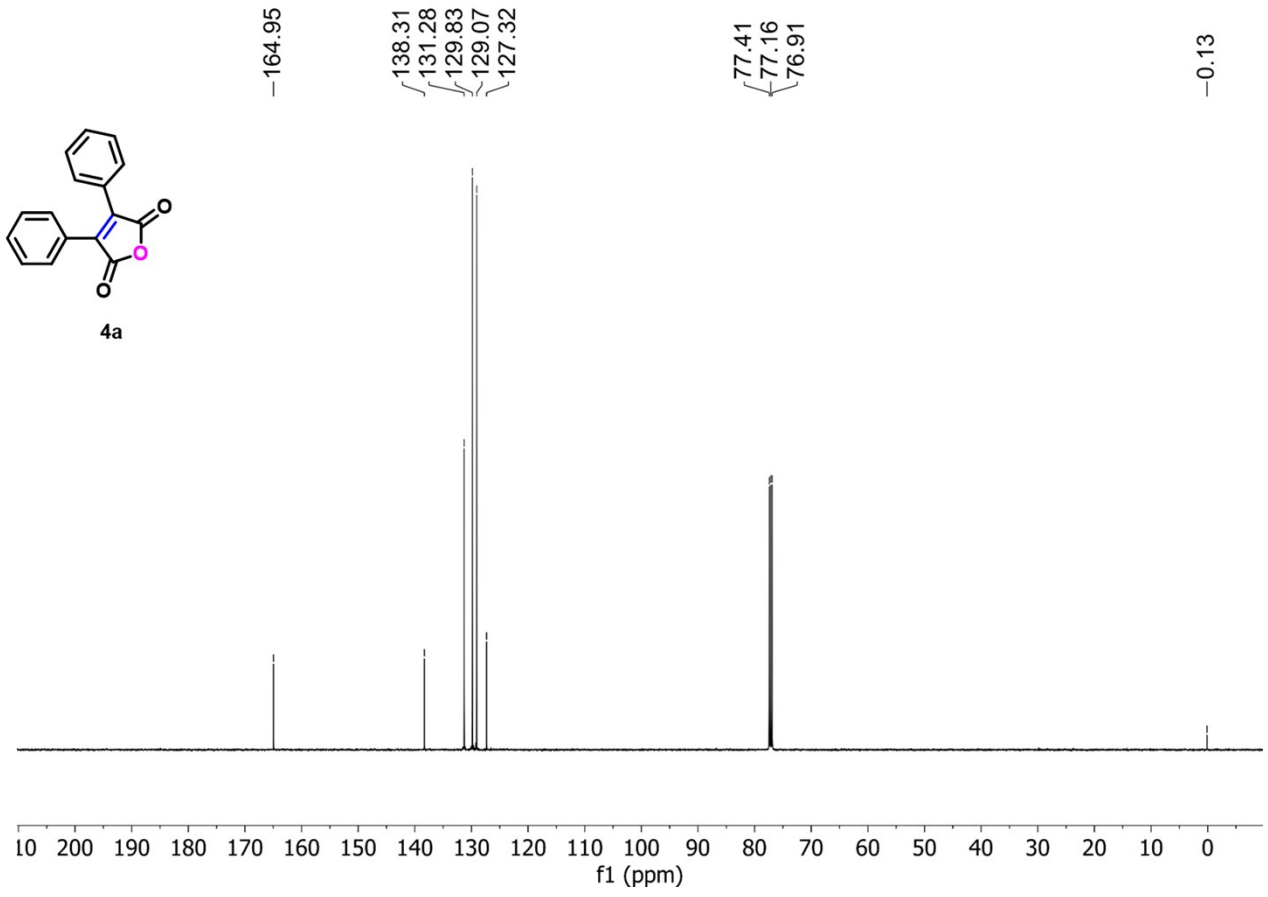
164.95
138.31
131.28
129.83
129.07
127.32
77.41
77.16
76.91
-0.13
4a
210
200
190
180
170
160
150
140
130
120
110
100
90
80
70
60
50
40
30
20
10
0
f1 (ppm)